AD NUMBER
AD859704
LIMITATION CHANGES
TO: **Approved for public release; distribution is unlimited.**
FROM: **Distribution authorized to U.S. Gov't. agencies and their contractors; Critical Technology; OCT 1968. Other requests shall be referred to Air Force Technical Applications Center, Washington, DC. This document contains export-controlled technical data.**
AUTHORITY
usaf ltr jan 1972

Wash D.C. 20330

AFTAC Project No. VELA T/7704
ARPA Order No. 624
ARPA Program Code No. 7F10

SIGNAL AND NOISE ANALYSIS REPORT
ALEUTIAN ISLANDS EXPERIMENT
OCEAN-BOTTOM SEISMOGRAPHIC EXPERIMENTS

Prepared by

A. Frank Linville R. Fred Howard Gary D. McNeely

Terence W. Harley, Program Manager
Telephone: 1-214-238-3473

TEXAS INSTRUMENTS INCORPORATED
Science Services Division
P.O. Box 5621
Dallas, Texas 75222

Effective Date of Contract: 5 April 1967
Contract Expiration Date: 31 October 1968
Amount of Contract: $1,054,991

670215

ACKNOWLEDGMENT

This research was supported by the
ADVANCED RESEARCH PROJECTS AGENCY
Nuclear Test Detection Office
under Project VELA UNIFORM
and accomplished under the technical direction of the
AIR FORCE TECHNICAL APPLICATIONS CENTER
Contract No. F33657-67-C-1341

31 October 1968

BLANK PAGE

AFTAC Project No. VELA T/7704
ARPA Order No. 624
ARPA Program Code No. 7F10

SIGNAL AND NOISE ANALYSIS REPORT
ALEUTIAN ISLANDS EXPERIMENT
OCEAN-BOTTOM SEISMOGRAPHIC EXPERIMENTS

Prepared by

A. Frank Linville R. Fred Howard Gary D. McNeely

Terence W. Harley, Program Manager
Telephone: 1-214-238-3473

TEXAS INSTRUMENTS INCORPORATED
Science Services Division
P.O. Box 5621
Dallas, Texas 75222

Effective Date of Contract: 5 April 1967
Contract Expiration Date: 31 October 1968
Amount of Contract: $1,054,991

ACKNOWLEDGMENT

This research was supported by the
ADVANCED RESEARCH PROJECTS AGENCY
Nuclear Test Detection Office
under Project VELA UNIFORM
and accomplished under the technical direction of the
AIR FORCE TECHNICAL APPLICATIONS CENTER
Contract No. F33657-67-C-1341

31 October 1968

ABSTRACT

Aleutian Islands signal and noise data were analyzed to determine the teleseismic recording capability of the Ocean-Bottom Seismograph (OBS). From this analysis it was concluded that both noise and signal levels vary with OBS location, and the lowest noise sites are in deep water far from land. The noise spectrum is sharply peaked at 1 Hz; as the frequency increases to 2 Hz, the levels are down 10 to 20 db. Thus, ocean-bottom seismographs can perceive higher-frequency events up to a full magnitude better than they can perceive 1-Hz events (important in detecting explosive events at teleseismic distances). OBS perceptibility is quite variable at 1 Hz because of the variability of signal level with location and noise level with location and time. It appears that events of magnitude 5.0 or greater can be detected by at least some of the OBS stations, provided that the events are 40° or less from the array. Events of magnitude 6.0 or greater usually can be detected at all epicentral distances. The noise field determines the type of processing which can be used.

TABLE OF CONTENTS

APPENDIXES

ILLUSTRATIONS

ILLUSTRATIONS (CONTD)

ILLUSTRATIONS (CONTD)

TABLES

SECTION I
SUMMARY

Presented in this report are results of an analysis of the Aleutian Islands signal and noise data which was conducted to determine the teleseismic recording capability of the Ocean-Bottom Seismograph (OBS). Data used in the analysis were collected during the 3-phase 1967 Aleutian Islands Ocean-Bottom Seismographic Experiment. A total of 349 noise samples taken from all three phases were used in the noise analysis; eight teleseisms recorded during Phase I were used in the signal studies. Signal information contained in the OBS Preliminary Analysis Report was also used.[1]

Average noise levels at 1 Hz ranged from 90 mμ to 1μ; the lower noise levels were observed at deep stations far from land. Except for the shallow-water near-shore sites where significant high-frequency power was observed, the noise spectrum peaked sharply at 1 Hz; as the frequency increased to 2 Hz, levels were down 10 to 20 db from the peak. Noise levels at a site varied with time due to the effects of surface weather conditions. The maximum variation was 18 db, with typical variations of 12 db. Thus, the detection level at a given site varied as a function of time up to 0.9 magnitude units. High-frequency energy observed at shallow-water near-shore sites appeared to be related to tidal effects. Coherence between both the pressure and vertical traces and the vertical and horizontal traces was low over the entire frequency band, indicating that the noise field was isotropic and composed of several modes.

Teleseismic signal strength varied as much as 12 db (0.6 magnitude units) across the 200-km Phase I array, with 6-db variation being typical. Some sites had consistently high signal amplitudes; however, variations appeared to depend partially on the location of the event as well.

Comparison of average OBS and USC&GS magnitudes for five events showed that signal amplitudes on the ocean bottom were slightly higher (0.2 magnitude units) than on land. The average period of the teleseismic arrivals observed (20° to 70° range) was 0.6 sec (1.67 Hz), which is somewhat higher than normal. Because noise levels generally decrease rapidly above 1 Hz, higher-frequency events are significantly better perceived by the OBS, as probably reflected by the sample of events used. Fourteen of 15 events with a reported magnitude of 5.0 or better occurring between 10° and 40° from from the OBS stations were recorded by at least one OBS. Beyond 40°, some events were recorded, generally those which exhibited higher frequency energy.

Because the noise field was incoherent, signal enhancement techniques were limited to summing and differencing the pressure and vertical traces and to bandpass filtering. About 3-db signal-to-noise improvement could be obtained using the sum-and-difference techniques, providing the signal-to-noise ratios on the pressure and vertical traces were similar. For the higher-frequency arrivals, bandpass filtering improved the signal-to-RMS-noise ratio and thus enhanced identification of the arrivals.

The following major conclusions can be drawn.

- Both noise and signal levels vary with OBS location. The lowest noise sites are in deep water far from land, where noise levels of 100 to 200 μ at 1 Hz are typical. Signal variations appear to be caused by a combination of site- and source-location effects and are typically 6 db across a 200-km array.

- The noise spectrum is sharply peaked at 1 Hz; as the frequency increases to 2 Hz, the levels are down 10 to 20 db. Thus, ocean-bottom seismographs can perceive higher-frequency events up to a full magnitude better than they can perceive 1-Hz events. Because explosive sources are generally relatively rich in high-frequency energy, the OBS would be able to detect magnitude 4.8 to 5.0 explosive events at teleseismic distances.

- Due to the variability in both signal and noise levels with location (and with time for the noise), the OBS perceptibility is quite variable at 1 Hz. On the average, it appears that events of magnitude 5.0 or greater can be detected by at least some of the OBS-array stations, provided that the events are 40° or less from the array. Events of magnitude 6.0 or greater usually can be detected at all epicentral distances.
- The type of processing which can be used depends on the noise field. In the worst case (incoherent noise), a signal-to-noise improvement of 3 db can often be achieved.

BLANK PAGE

SECTION II

ALEUTIAN ISLANDS NOISE ANALYSIS

A detailed noise analysis of 1967 Aleutian Islands OBS data was conducted to

- Define the ambient noise field characteristics (frequency, power, coherence, etc.) within the Aleutian OBS array
- Relate the noise field to the environment (water depth, geographic location, weather, and tides)

A total of 349 3-min noise samples, representing 19 OBS stations and approximately 1900 km of inline array, was digitized for this study (Figures II-1 and II-2). Of these, 209 were taken daily at 2300 GCT [1200 Bering Daylight Savings Time (BDST)] and represent simultaneous recordings during each phase of the operation (Table II-1, Figure II-3). The remaining 140 samples were simultaneous recordings from stations S2 and S10 taken at 2-hr intervals beginning at 1225 GCT on 3 September and continuing through 0625 GCT on 9 September 1967.

A. DESCRIPTION OF THE DATA

Figure II-4 outlines the order of processing and analysis followed for this study. The data ensemble was selected after reviewing existing film transcriptions of the field data. The 0.0075-ips recorded data were then digitally sampled at 16 samples/sec (0.0625 sec/sample), resulting in an 8-Hz folding frequency. Antialias filters using a 6-Hz corner frequency and a 35-db/octave rolloff rate were applied prior to digitization.

Processing of these data included

- Computation of power-density spectra
- Computation of root-mean-square (RMS) values
- Visual period-amplitude measurements from film playbacks with subsequent conversion to ground motion

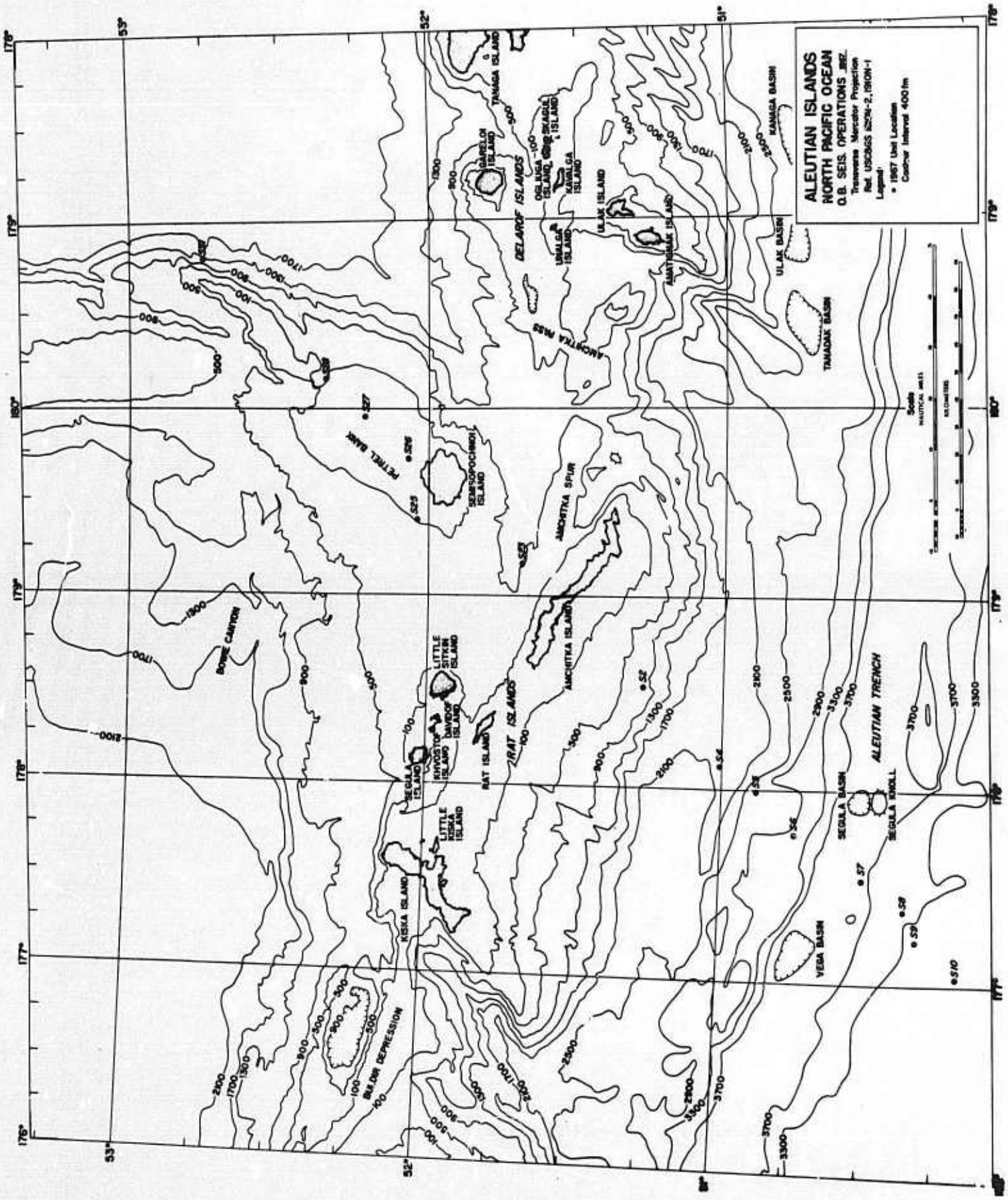

Figure II-1. Phase I and Phase III Station Locations

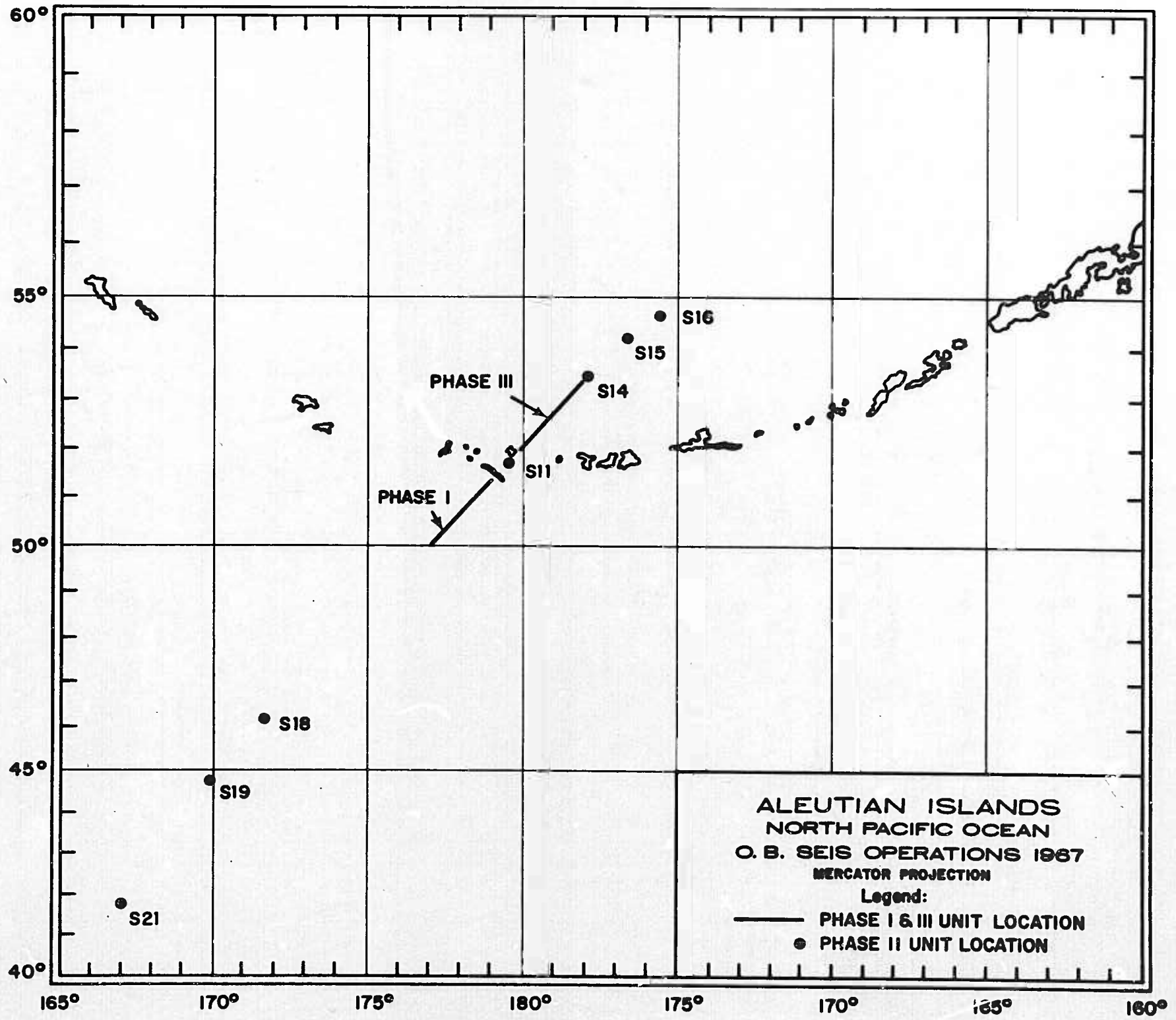

Figure II-2. Phase II Station Locations

Table II-1

ALEUTIAN NOISE DATA ENSEMBLE

	Time Interval	Sample Time (GCT)	Station	Location		Distance to Land (km)	Water Depth (fm)
				Latitude	Longitude		
Phase I	Sept 3 - Sept 9	2300	S2	51°16'24"N	178°32'00"E	42.3	785
	Sept 3 - Sept 9	2300	S4	51°01'00"N	178°06'48"E	83.3	1784
	Sept 3 - Sept 9	2300	S5	50°53'15"N	177°59'42"E	99.4	2580
	Sept 3 - Sept 9	2300	S6	50°45'00"N	177°46'00"E	121.6	2980
	Sept 3 - Sept 9	2300	S7	50°36'20"N	177°37'00"E	140.6	3840
	Sept 3 - Sept 9	2300	S8	50°26'12"N	177°22'42"E	165.9	3150
	Sept 3 - Sept 9	2300	S9	50°20'42"N	177°13'12"E	181.0	2850
	Sept 3 - Sept 9	2300	S10	50°11'48"N	177°02'12"E	202.0	2690
Phase II	July 26 - Aug 16	2300	S11	51°50'00"N	179°21'30"E	8.0	320
	July 26 - Aug 16	2300	S14	53°32'00"N	178°00'00"W	253.0	2030
	July 26 - Aug 16	2300	S15	54°10'06"N	176°58'00"W	350.0	2025
	July 26 - Aug 16	2300	S16	54°47'48"N	175°50'30"W	451.0	2000
	Aug 5 - Aug 12	2300	S18	45°59'00"N	172°02'48"E	799.8	3020
	Aug 5 - Aug 12	2300	S19	44°30'30"N	170°26'54"E	1006.1	720
	Aug 8 - Aug 14	2300	S21	41°34'36"N	167°42'12"E	1401.0	2840
Phase III	July 12 - July 19	2300	S23	51°41'00"N	179°09'30"E	17.0	460
	July 12 - July 19	2300	S25	52°02'50"N	179°23'54"E	9.0	101
	July 12 - July 19	2300	S26	52°05'06"N	179°44'24"E	6.0	32
	July 12 - July 19	2300	S27	52°13'00"N	179°56'00"E	29.0	36
	July 12 - July 19	2300	S28	52°21'00"N	179°50'40"W	48.0	95
	July 12 - July 19	2300	S31	52°46'30"N	179°12'24"W	110.0	862

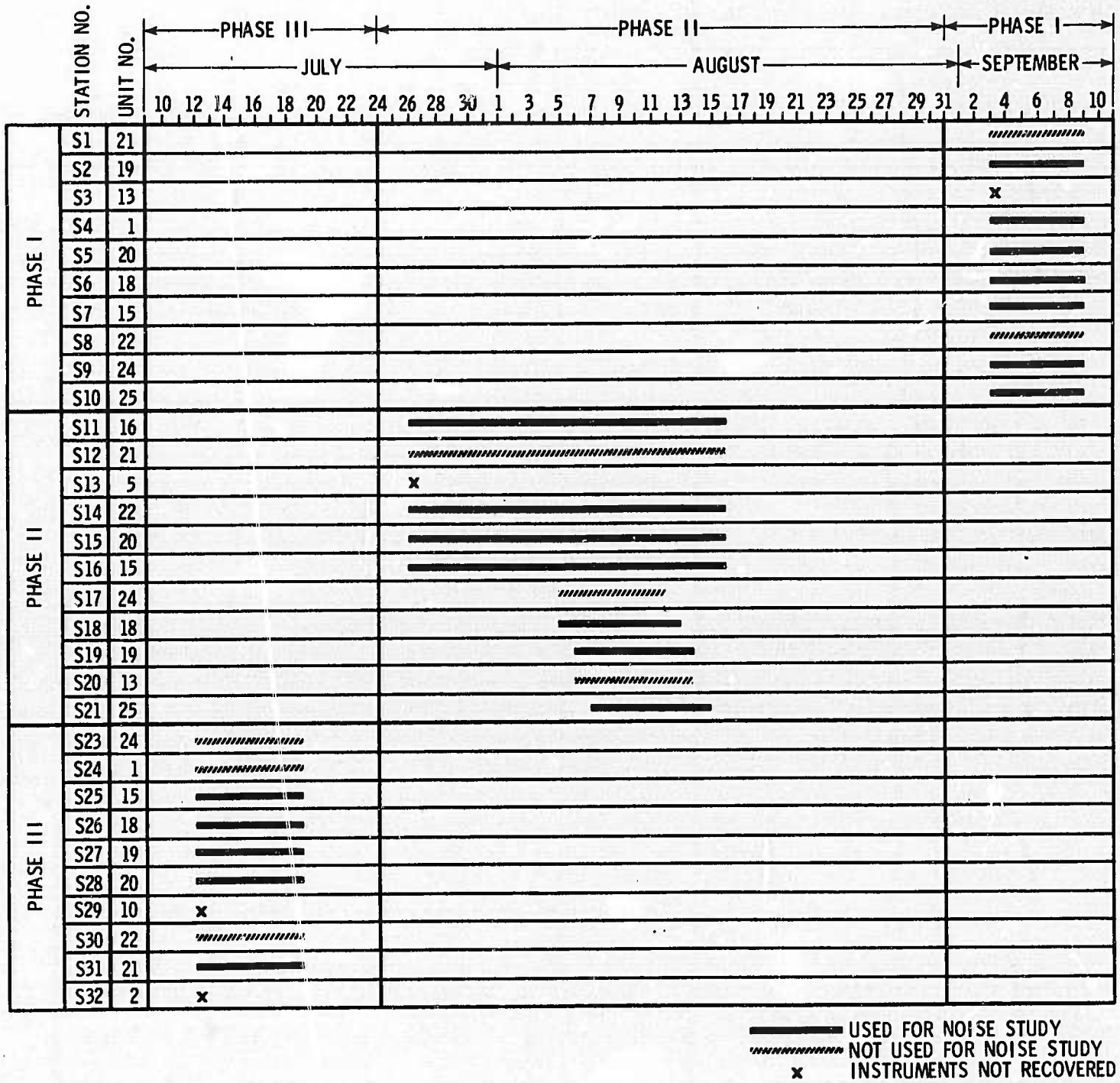

Figure II-3. Ocean-Bottom Seismograph Noise Study Periods

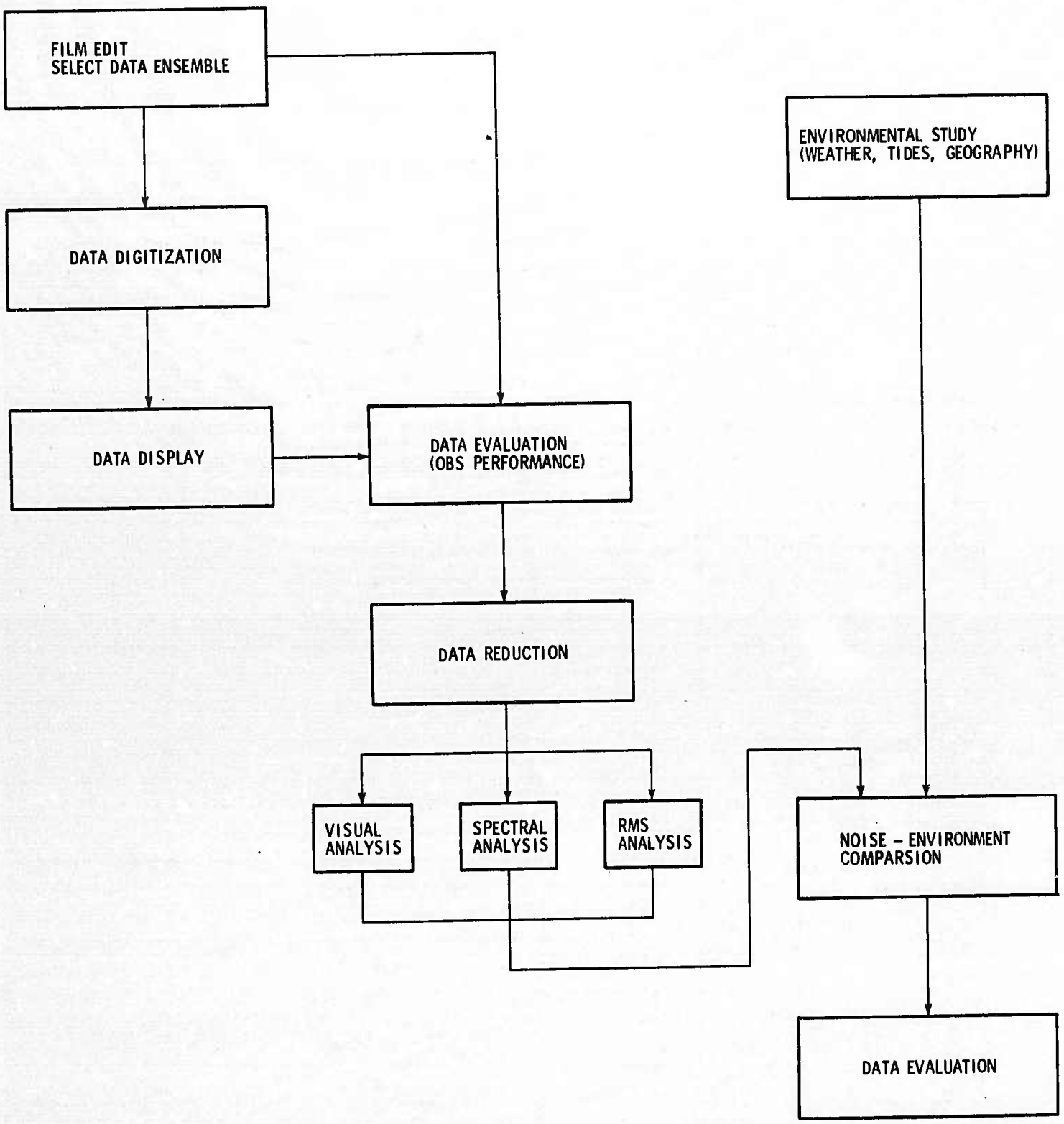

Figure II-4. Data Processing and Analysis Flow Chart

Power-density spectra were computed for the vertical data traces (x1 and x10) on each of the daily samples. The spectra were computed from slightly more than 3 min of data and have a frequency resolution of about 0.05 Hz. To estimate the playback and total system noise, spectra also were computed on open-input recordings during transcription to digital format and on low-level or inoperable component traces from the field data.[2] Figure II-5 shows that these noise levels are substantially below seismic noise levels (shown later).

RMS computations (σ) were obtained for both the daily and 2-hr samples by using

$$\sigma = \left[\frac{1}{N} \sum_{i=1}^{N} X_i^2 \right]^{\frac{1}{2}}$$

where N is the number of digitial samples. These values were used to compare the total noise power at each station as a function of water depth, weather, location, etc.

Visual period-amplitude measurements from film seismograms of selected daily samples were converted to millimicrons of ground motion. Peak amplitudes were measured at 1 Hz because the noise peaked at this frequency at nearly all stations.

B. SUPPLEMENTARY INFORMATION

Daily weather maps of the North Pacific area were obtained through the Naval Weather Service at Adak, Alaska. Barometric pressures at Amchitka Island (recorded at 0100 local time) were derived from these charts and used as weather indicators for the OBS arrays.

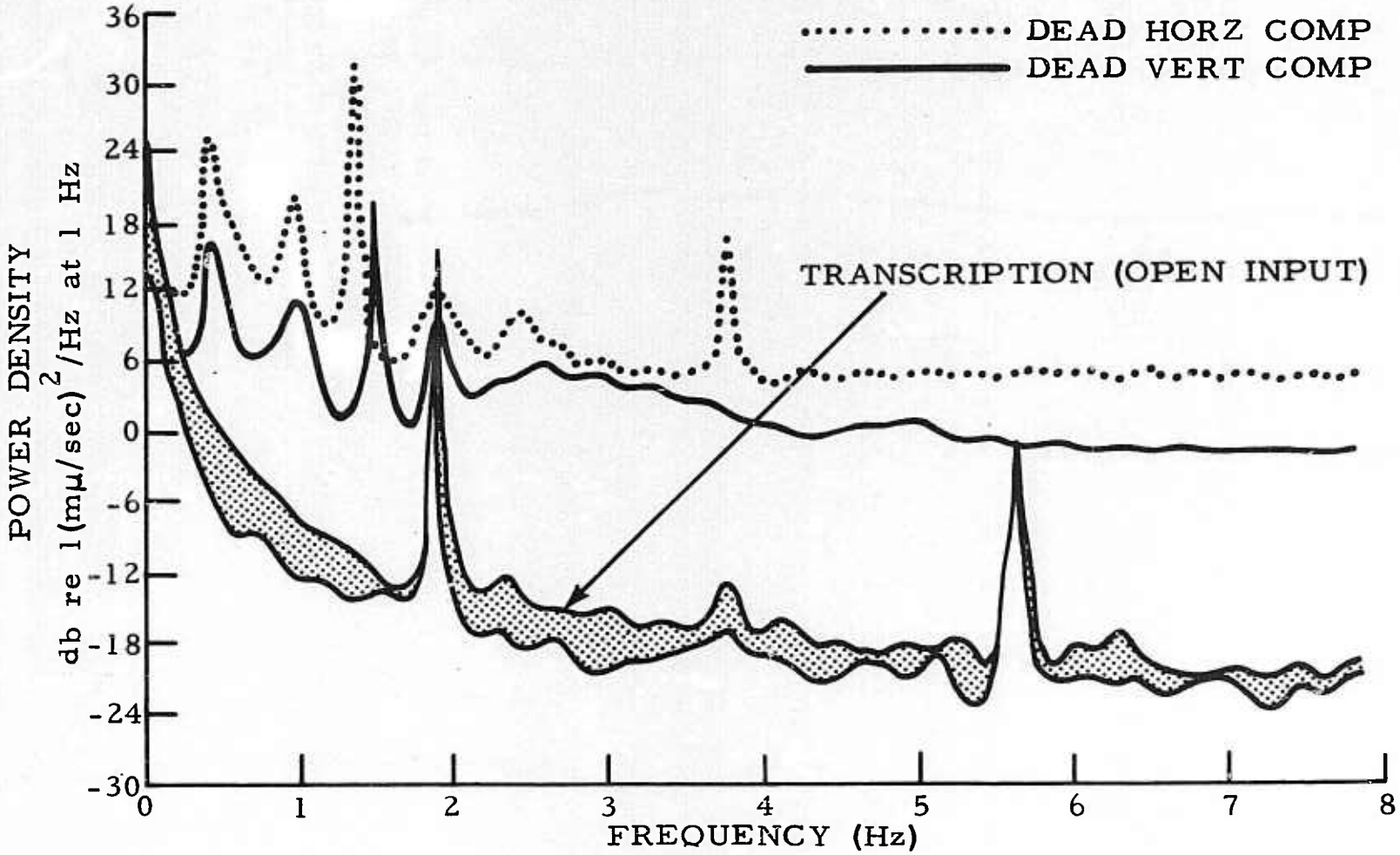

Figure II-5. Power-Density Spectra of Total System Noise

The weather maps also provided Adak tidal information (time and level for high and low tide) used in this study because previous work[3] attributes significant microseismic activity to tidal phenomenon. Tidal characteristics at Adak (Figure II-6) were assumed representative for the mid-Aleutian area.

The weather and tide data were combined with existing OBS station information (water depth and proximity to land) to determine the factors which influence the ocean-bottom noise levels.

C. DATA ANALYSIS

The 19 OBS stations used vary in water depth from 32 to 3840 fm (0.06 to 7.02 km) and in distance from land from 6.0 to 1401 km. Water depth and distance from land were the main parameters considered in correlating absolute noise amplitudes with the ocean-bottom environment.

Noise spectra at most sites were sharply peaked at about 1 Hz (Figures II-7 and II-8). Although these spectra have been normalized to $1(m\mu/sec)^2/Hz$ at 1 Hz, they have not been corrected for system response, so they represent the frequency content seen on the output records. At 2 Hz, the noise levels are 10 to 20 db lower.

Considerable high-frequency energy existed at five sites (S11, S19, S25, S26, and S27) on half of the samples (Figure II-9). Figure II-10 shows the unprocessed data at S11 during periods of "normal" and high-frequency background noise. These five stations were located in less than 750 fm of water and, except for S19, were less than 30 km from land (Table II-1). Noise level at S19 was lower than at the other sites, but a distinct high-frequency peak was still evident. Station S19 was located on top of a submarine mountain where the line of OBS stations crossed the Emperor Seamounts. Gains at station S27 (Figure II-9) were anomalously low, which accounts for the apparently low noise levels at that shallow-water near-shore site.

PHASE I

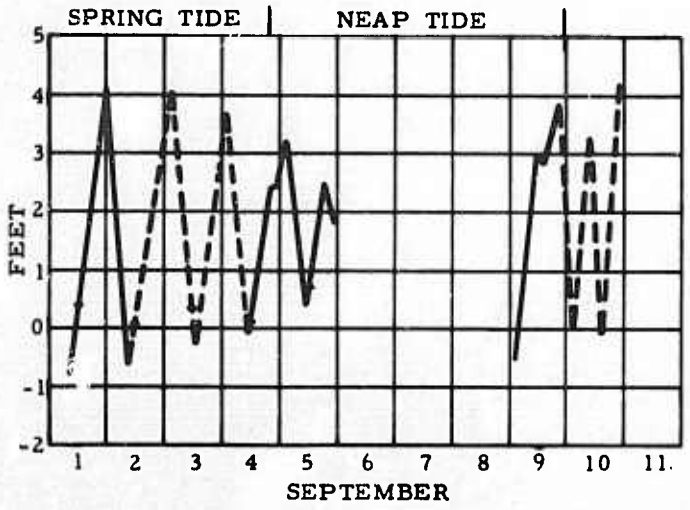

PHASE II

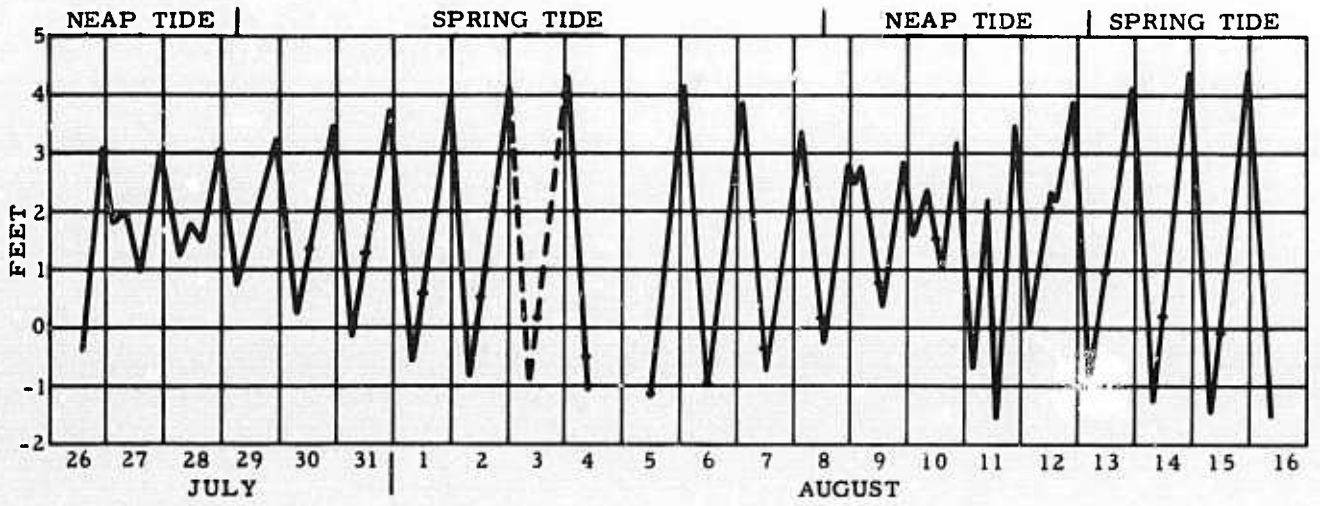

PHASE III

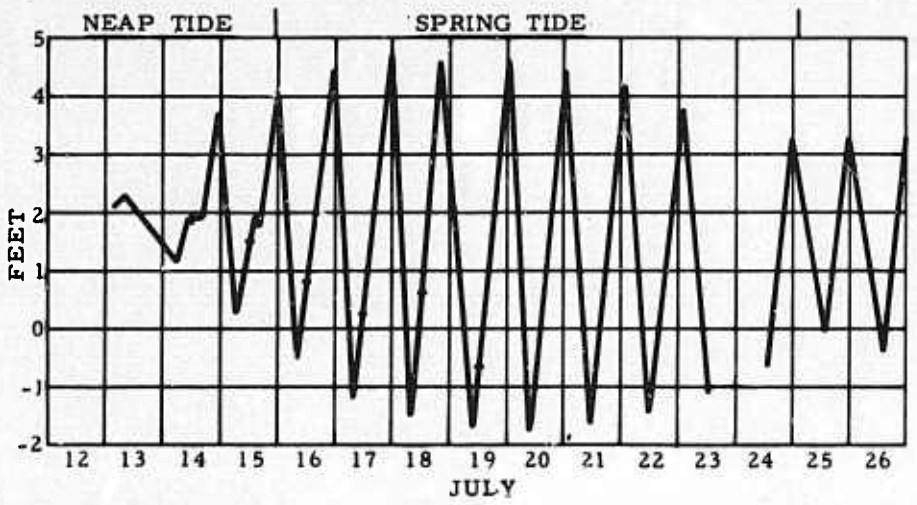

Figure II-6. Tide Curves for Phases I, II, and III

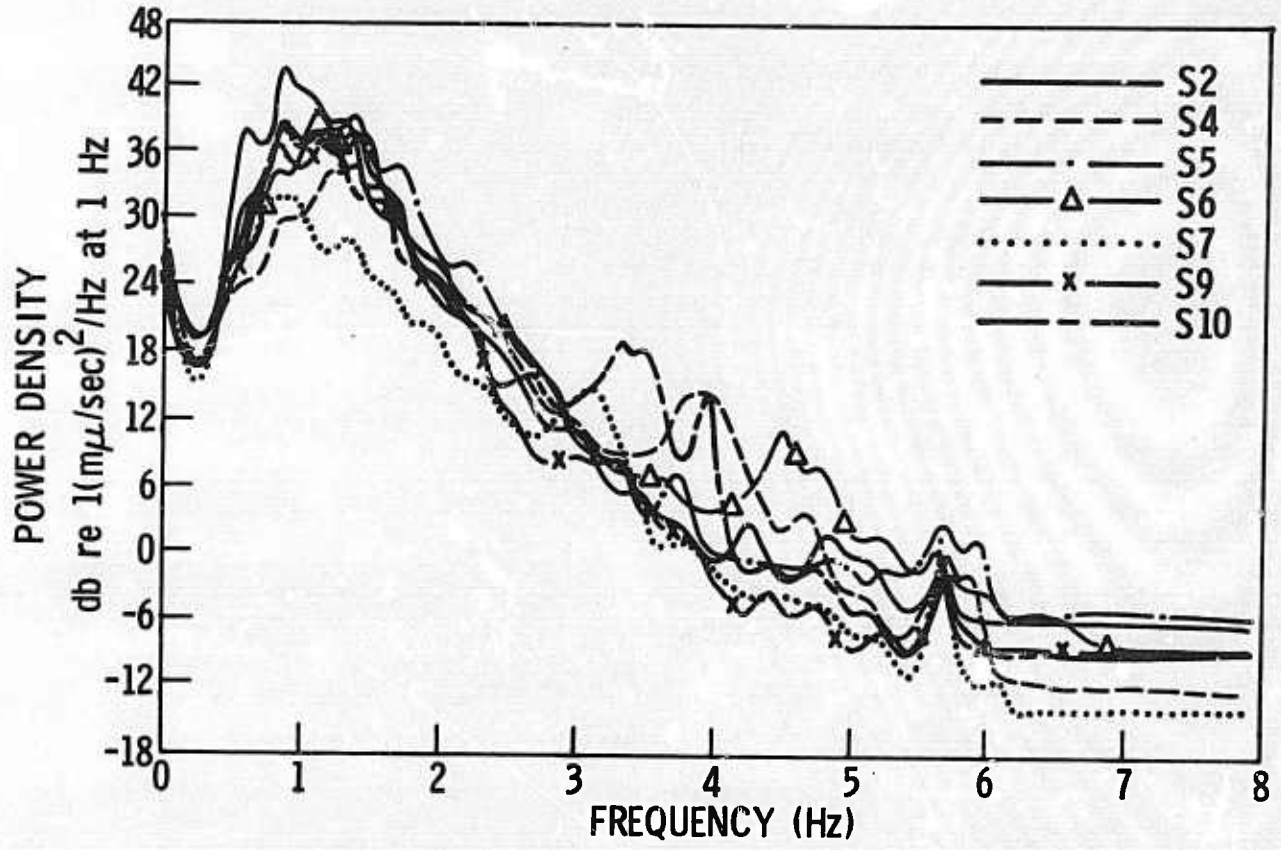

Figure II-7. Power-Density Spectra for Phase I, 7 September 1967

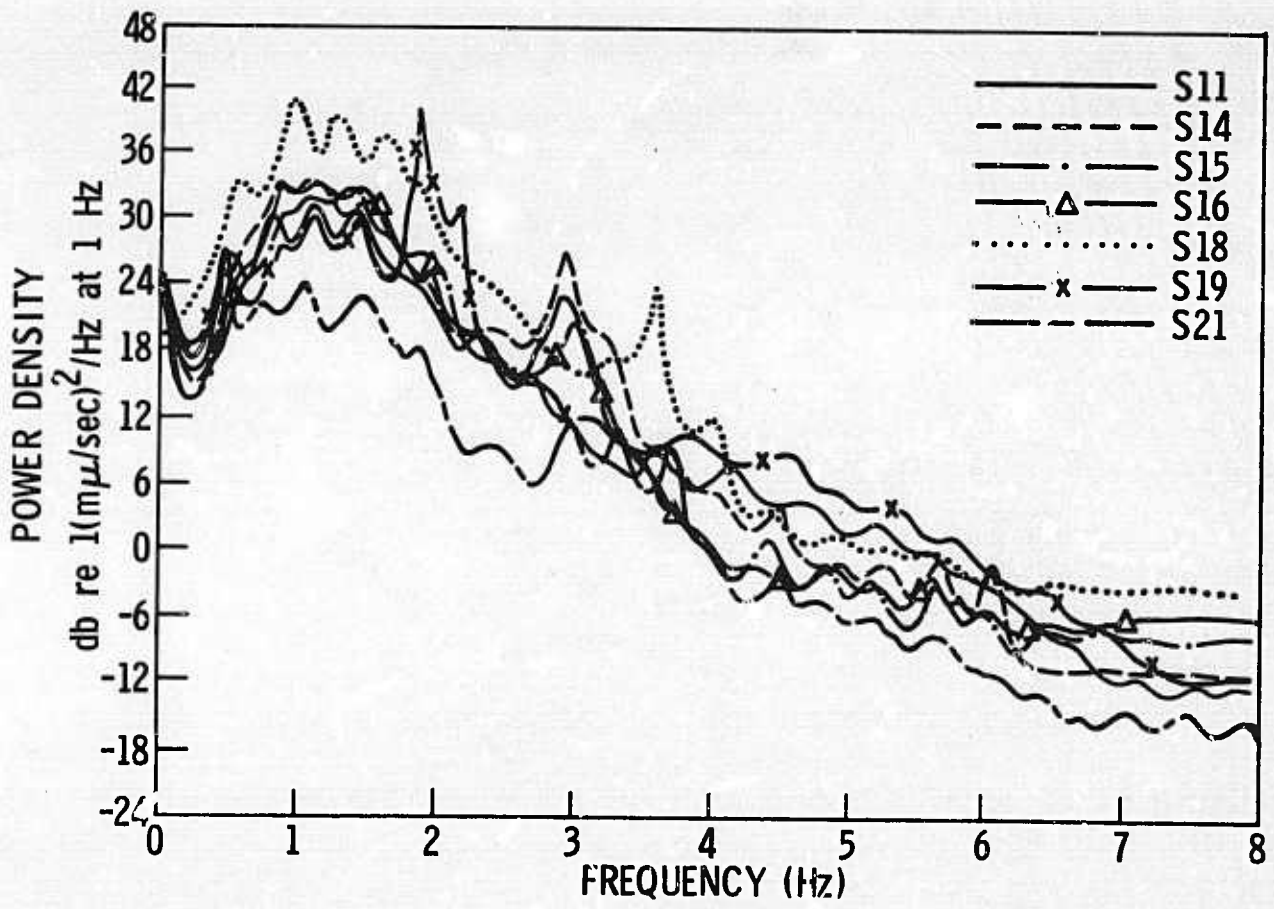

Figure II-8. Power-Density Spectra for Phase II, 11 August 1967

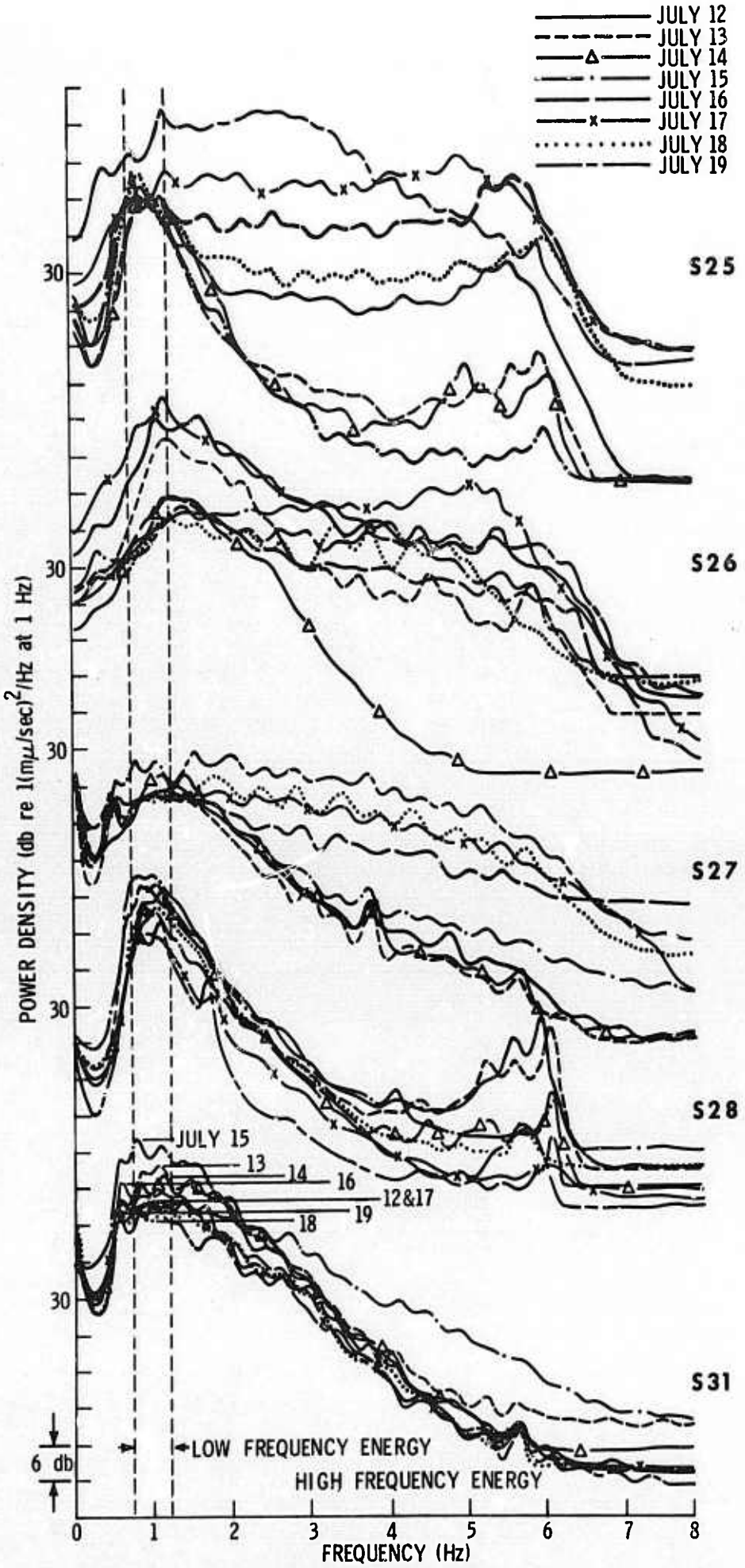

Figure II-9. Sample Power-Density Spectra for Phase III, 12 to 19 July 1967 (vertical component x10)

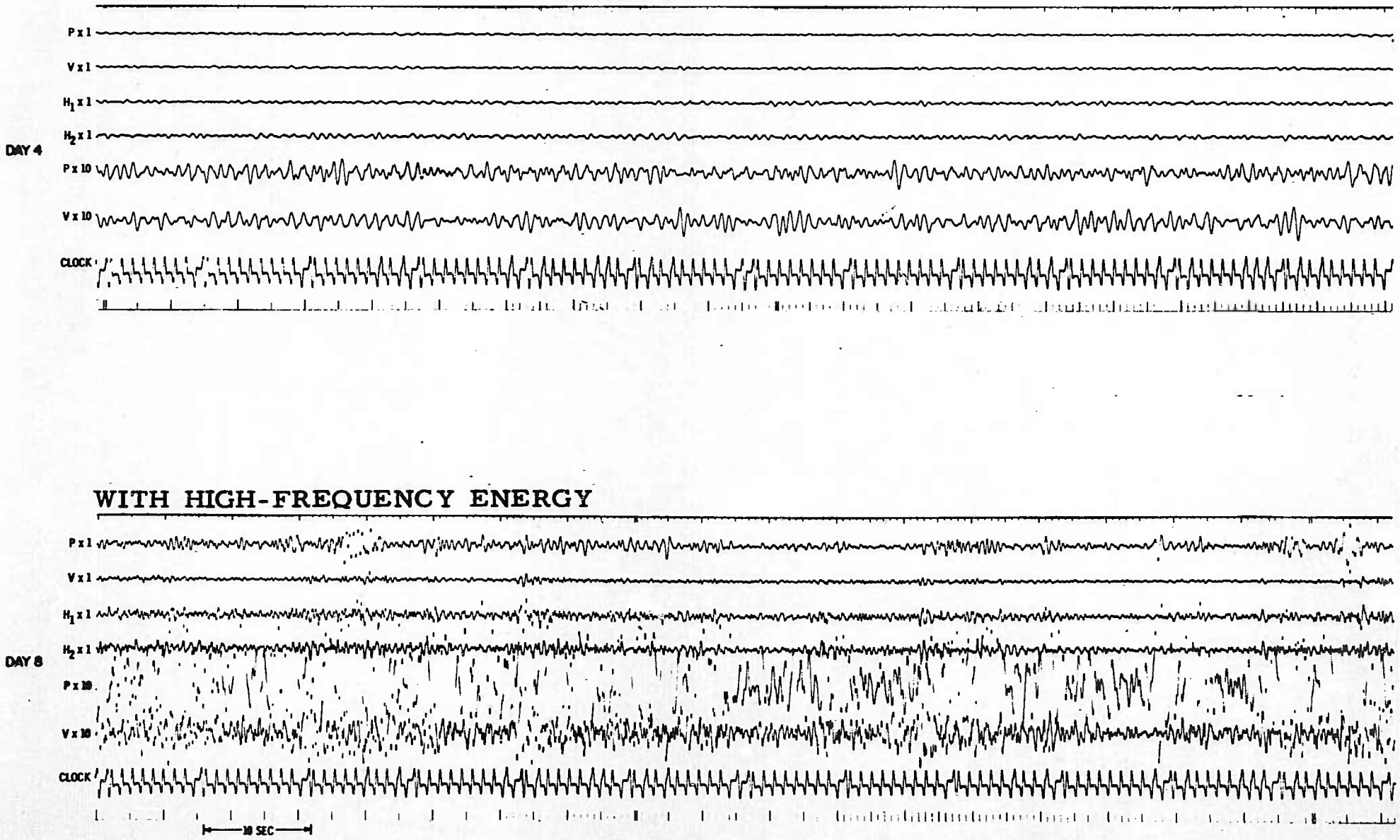

Figure II-10. Field Data Sample from Station 11, With and Without High-Frequency Energy

An attempt was made to explain the high-frequency energy on the basis of tidal phenomena, as suggested by Defant.[3] High and low tide values, listed on daily weather charts, were plotted against time for the period spanned by this experiment (Figure II-6). The RMS plots for shallow Phase III stations (shown later in Figure II-12) rise significantly during the later portion of the recording period. (Tick marks on the curves of Figure II-6 correspond to the time at which the data samples shown in Figures II-12 and II-13 were taken.) This rise corresponds with a spring-tide cycle (period of maximum tidal range) which begins about 15-16 July. In Phase II, large increases in the high-frequency energy component (reflected by the sharp increases in RMS levels) at S11 (Figure II-12) correlate with the early portion of the spring-tide cycles beginning 29-30 July and 12-13 August. As in Phase III, data samples are representative of flood tide. The other Phase II station (S19) recording high-frequency energy was approximately 1030 km southwest of S11, and the validity of Adak Island tide data for such a remote location is questionable. However, the trend of the S19 RMS plot is in general agreement with the respective portion of the tide curve (high RMS value corresponding to the latter portion of the spring-tide interval and a relative low amplitude during neap tide). Thus, it appears that the high-frequency energy which is present intermittently at shallow-water sites can be related to tidal activity.

In general, noise-level variations correlated well with weather for all three phases of the experiment and agree with past observations. Figure II-11 plots daily peak power levels in the 0.75- to 1.25-Hz band for each station, along with daily barometric pressure estimates for the area. The effect of poor weather on noise levels is quite clear for Phases I and III, where the pressure lows and noise-level highs correlate very well. The Phase II north sites (S11, S14, S15, and S16) also correlate with the weather; however, the Phase II south sites do not, probably because they are very far from Amchitka where the pressure readings were taken.

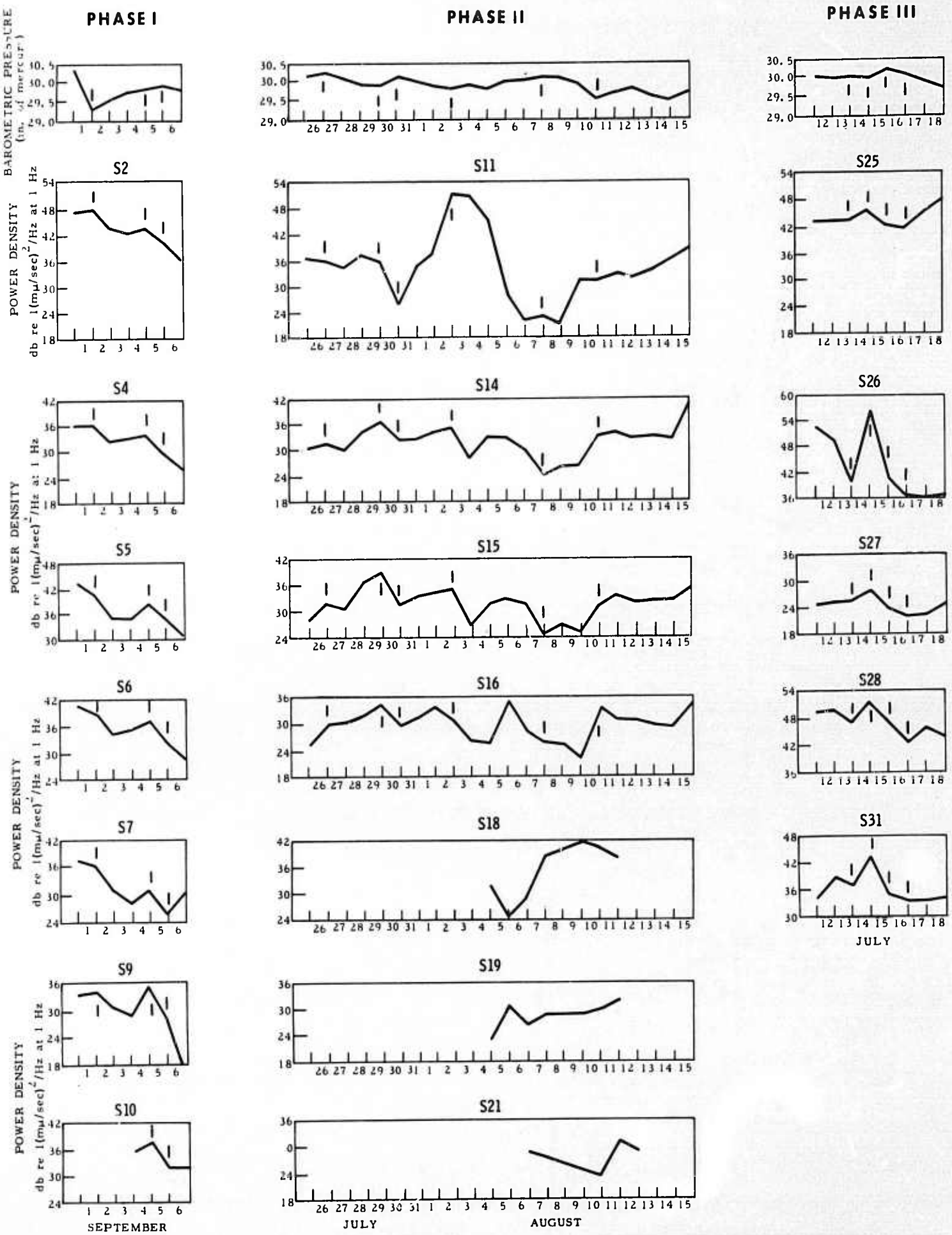

Figure II-11. Low-Frequency Peak-Amplitude Plots for Phases I, II, and III (vertical component x10)

Typical noise-level variations over the time span of several days are 12 db (0.6 magnitude units), with up to 18 db (0.9 magnitude units) observed at some sites.

Figures II-12 and II-13 plot the RMS levels as a function of time at each site for the vertical and pressure traces, respectively. At the deeper Phase I and Phase II sites, the plots are similar to those of Figure II-11 and have a similar shape for the several instruments of the phases. Phase III average power plots reflect the high-frequency energy present at some sites and are more variable.

Phase I stations illustrate the relationship of noise levels to water depth and proximity to land. Water depth increases from S1 to S7 then decreases slightly from S7 to S10. The stations, of course, become progressively farther from land. Noise levels generally decrease with increasing water depth and distance from land. Vertical data from station S4 appear to be anomalously low; however, this probably is due to instrumental gain problems because energy on the pressure component has the expected level. Pressure data from station S2 also appear low, but pressure data from this unit historically have been low, probably due to its somewhat low sensitivity. Vertical data from station S9 are more variable than data from other stations. Both the pressure and vertical components of S10 apparently were dead (amplifier malfunction) until 6 September, when they appear to have become operative, although some problem may still exist because the vertical and pressure plots do not have the same position relative to the plots from other sites.

Visual amplitude-period measurements from selected data samples representing maximum and minimum 1-Hz energy levels at each station were converted to millimicrons of ground motion and are displayed relative to water depth and distance from land in Figure II-14.

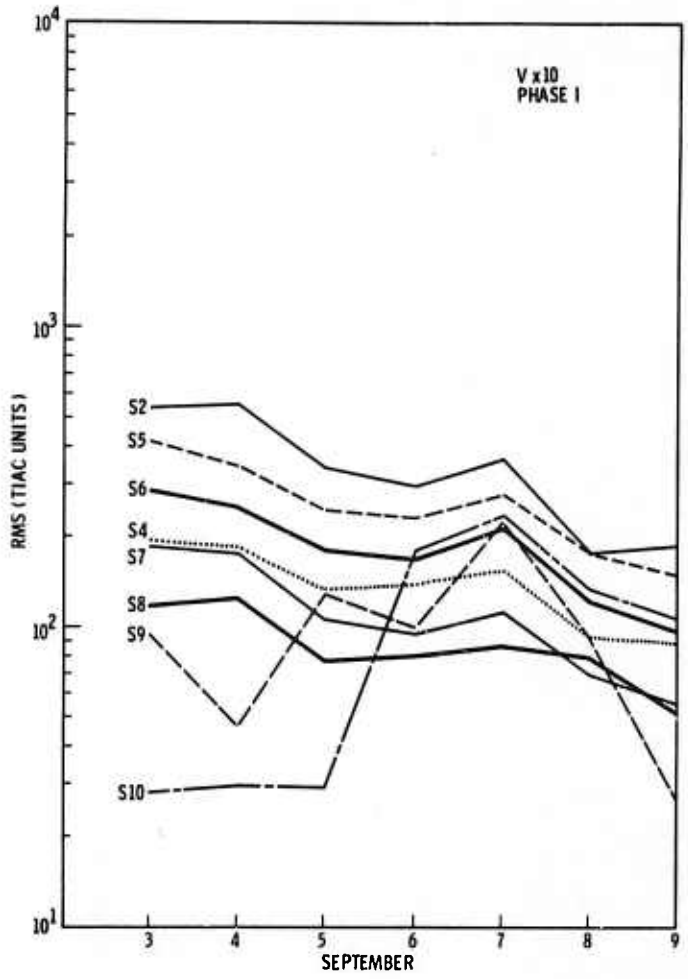

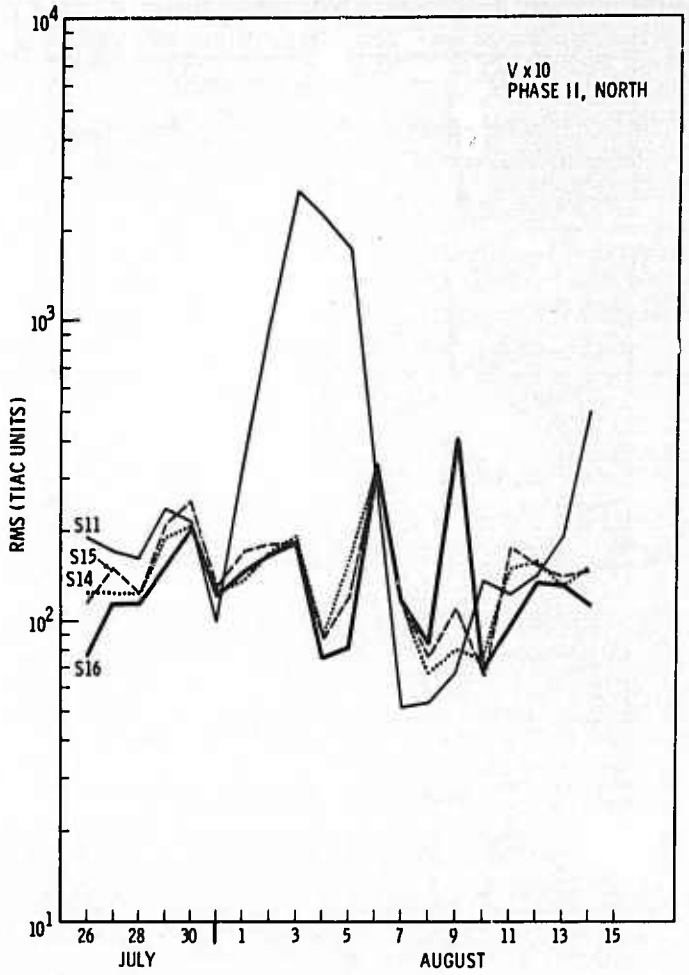

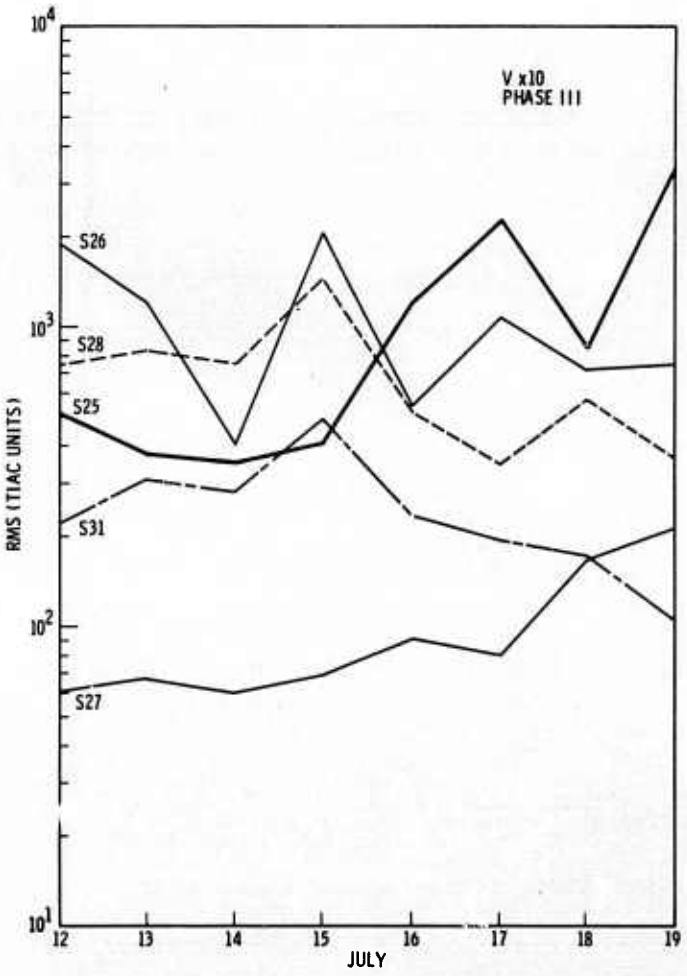

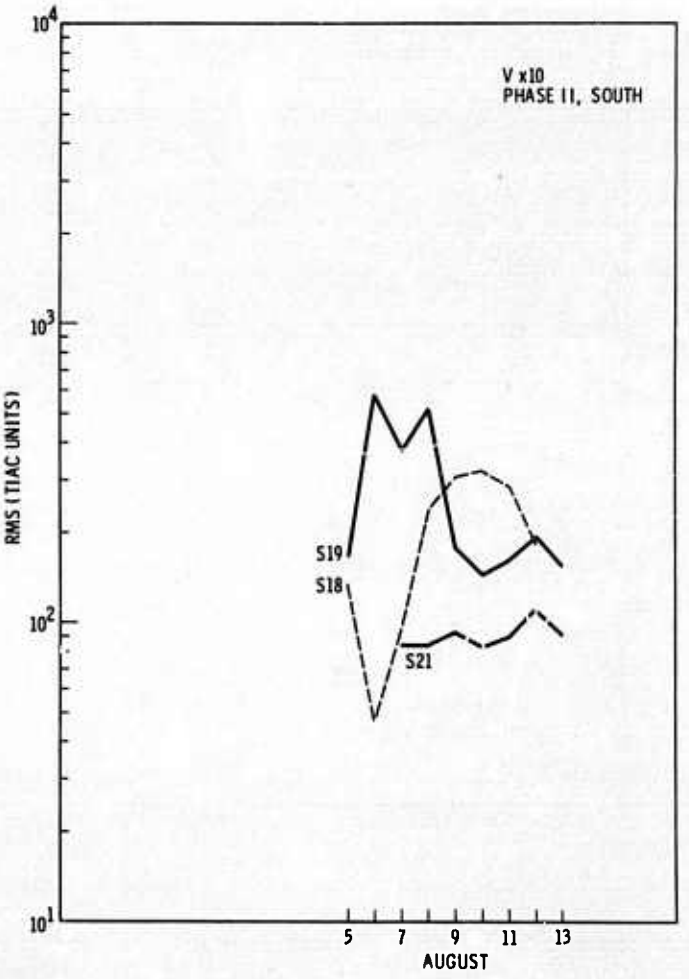

Figure II-12. Daily Variation in Root-Mean-Square for Various Units During Phases I, II, and III, Vertical Channels

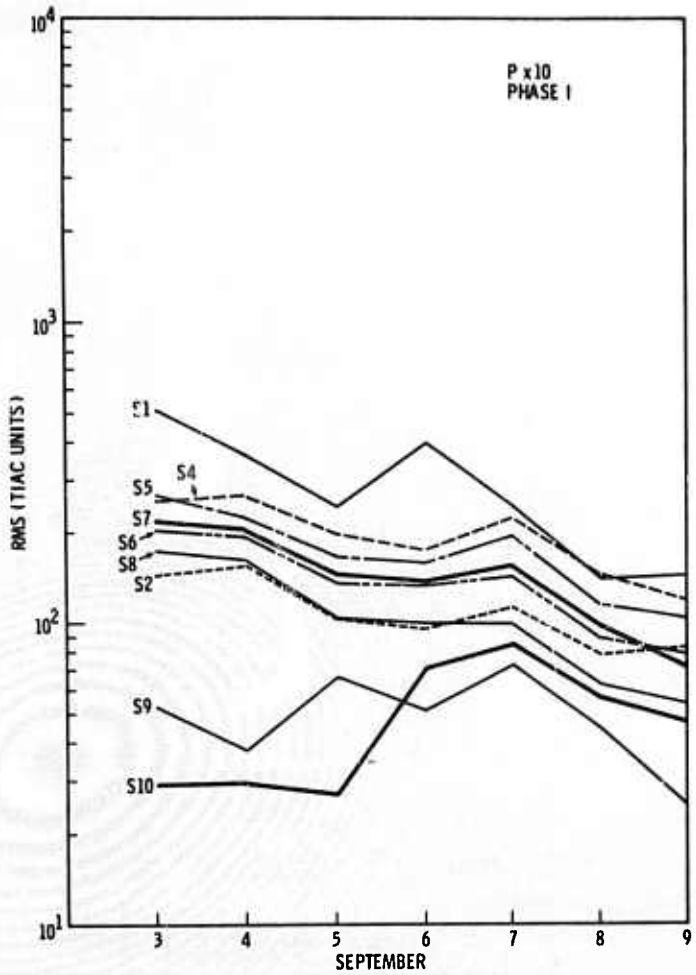

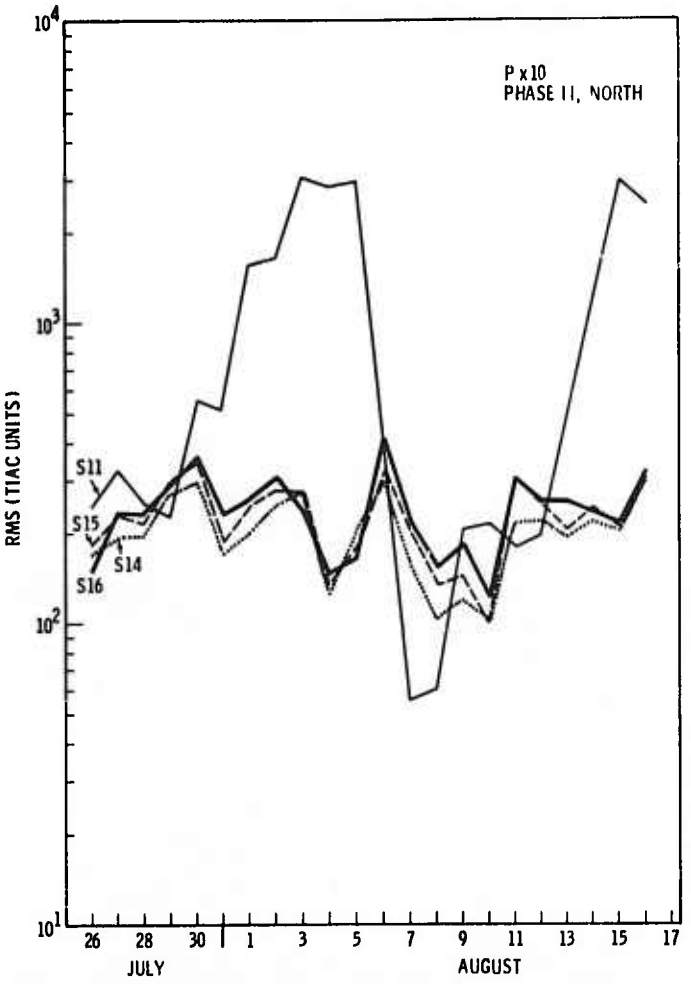

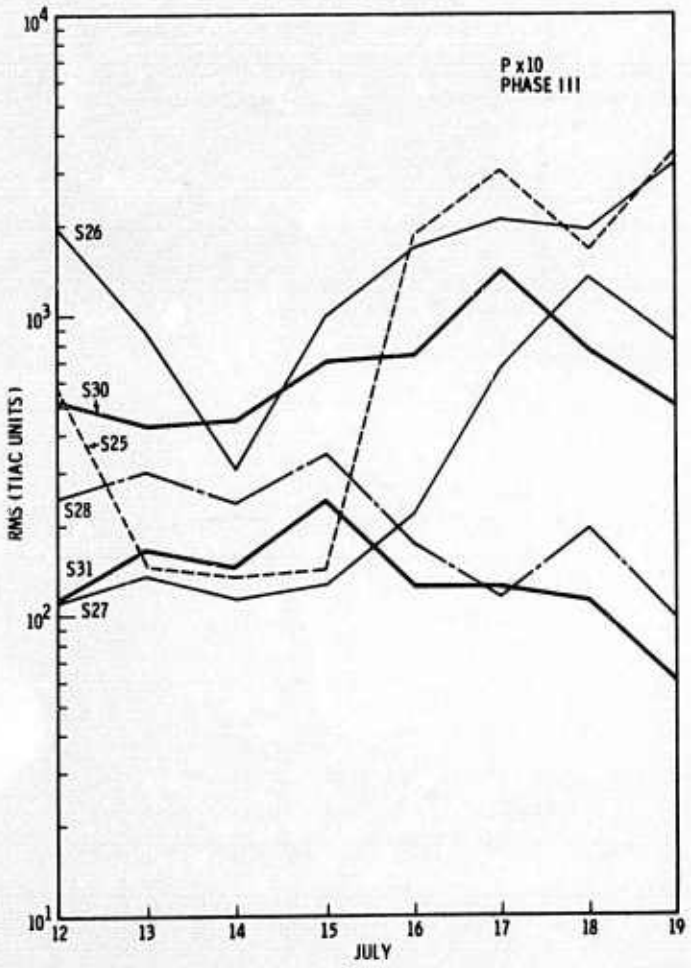

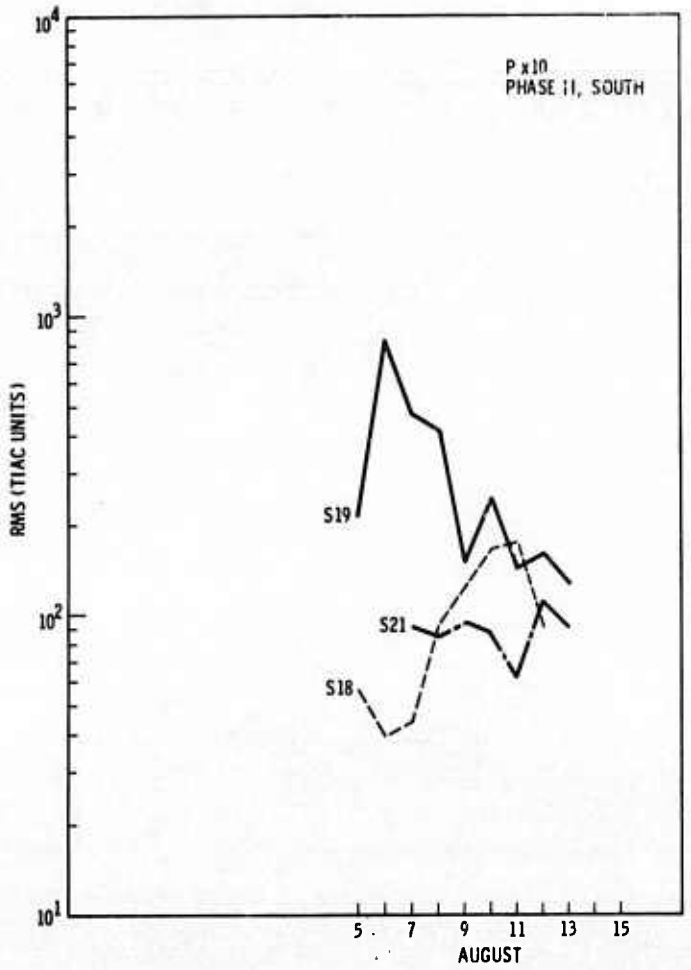

Figure II-13. Daily Variation in Root-Mean-Square for Various Units During Phases I, II, and III, Pressure Channels

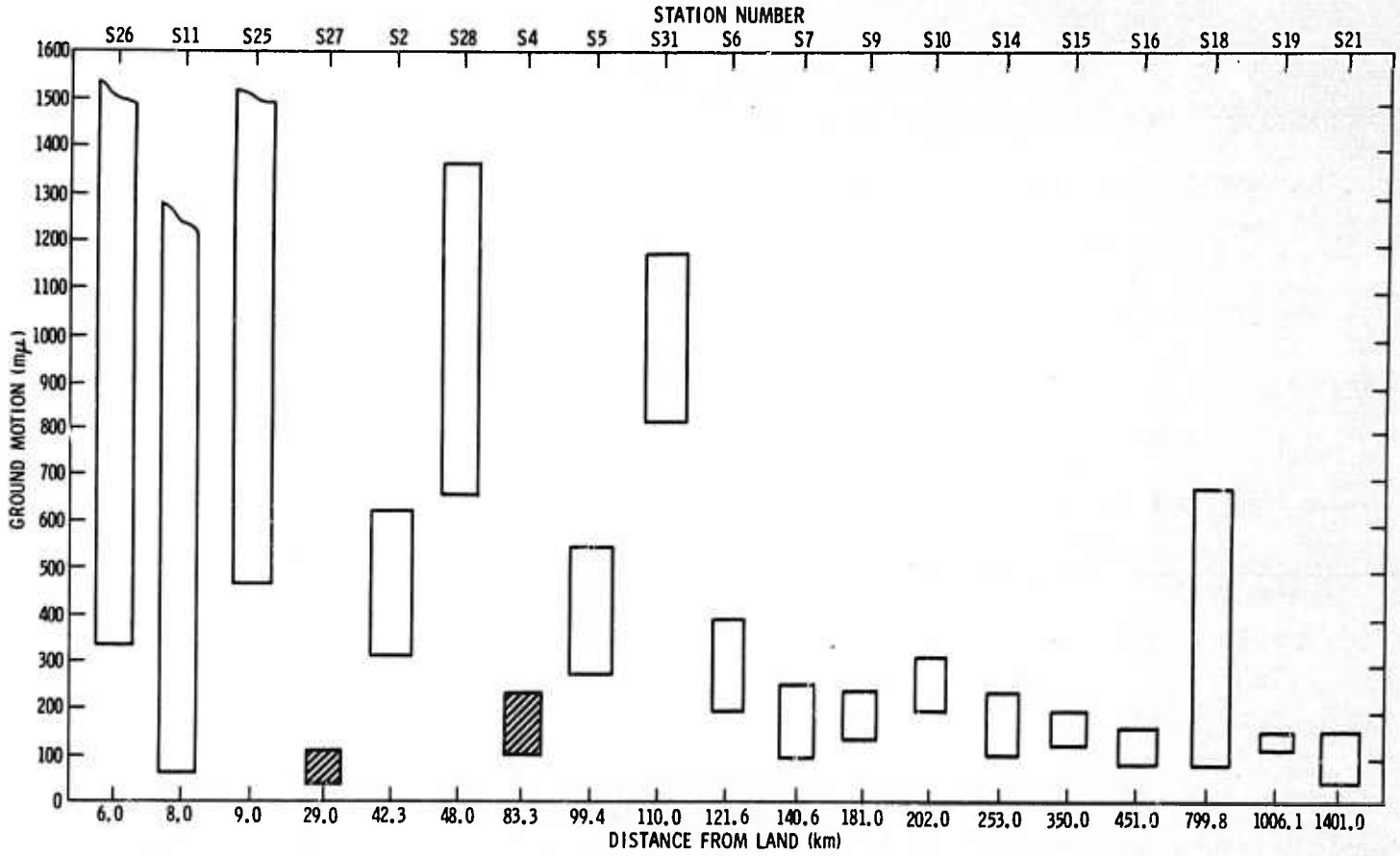

Figure II-14. Station Ground-Motion Range at 1 Hz Relative to Water Depth and Distance from Land

Stations exhibiting an undefined maximum limit had a large high-frequency energy component during most of the recording period (S26, S25, S11) which obscured the low-frequency energy. Stations S28 and S31 — having a similar environment and being relatively free of high-frequency energy — had large 1-Hz energy levels (0.65 to 1.30μ), so it is assumed that this also holds true for the stations displaying high-frequency energy. The high-frequency energy at S19 was low enough to allow identification of the 1-Hz energy, with the resulting measurement indicating low energy levels (137-mμ average noise amplitude) for the 1-Hz ambient noise. Ground-motion average values, with the exception of shallow-water near-shore observations, were usually 100 to 200 mμ which is comparable to those observed from 1966 Kurile Islands data (Table II-2).[4]

A detailed examination of RMS noise variations with time for shallow- and deep-water environments was provided by 2-hr samples from S2 and S10 data, respectively. The RMS values of these samples (Figure II-15) agree with the daily samples (tick marks), but they indicate that the daily samples do not necessarily represent maximum and minimum noise levels for a given day. Variations at S2 were 12 to 15 db over the time period (0.6 to 0.7 magnitude units); S10 covered a shorter time, but similar variations would seem likely, based on the agreement between the curves. Station S10 led station S2 by 2 to 3 hr, which suggests that the weather approached the array from the southwest at approximately 25 to 50 knots during this time period. This observation is consistent with the characteristic weather patterns in the area, as obtained from weather maps.

D. COHERENCE STUDY

Stations S4, S5, S16, and S21 were used to check the noise coherence between components. Vertical/pressure coherences were computed for all sites; vertical/horizontal coherences were computed for S16 and S21. Vertical/pressure noise coherences were very low for the Aleutian data over the entire frequency band (Figure II-16). This result contrasts sharply with the high vertical/pressure coherences observed in the Gulf data

but agrees with the results of Schneider et al[5] for Pacific ocean-bottom seismic data collected during 1963 in the Aleutian Islands area. Vertical/horizontal coherences were also low, which is characteristic of ocean-bottom noise data. Thus, it appears that the noise field in the Aleutian area is not only isotropic but also is composed of several modes.

Table II-2

ALEUTIAN ISLANDS — KURILE ISLANDS
NOISE-AMPLITUDE COMPARISON

Aleutian Islands			Kurile Islands		
Station	Depth (fm)	Average Amp (mμ)	Station	Depth (fm)	Average Amp (mμ)
26	32	366			
27*	36	65			
28	95	1045	4	230	136
25	101	780	4A	230	102
11	320	229	7A	330	273
19	720	137	1	400	174
2	785	470	3A	600	102
31	862	352	1A	900	162
4*	1784	163	13	1320	92
16	2000	117	7	1500	129
15	2025	169	11	1650	238
14	2030	156	12	2850	95
5	2580	402	10	3000	152
10	2690	169	5A	3100	288
21	2840	91			
9	2850	188	9	3200	68
6	2980	299			
18	3020	156			
7	3840	188			

*Instrument malfunction

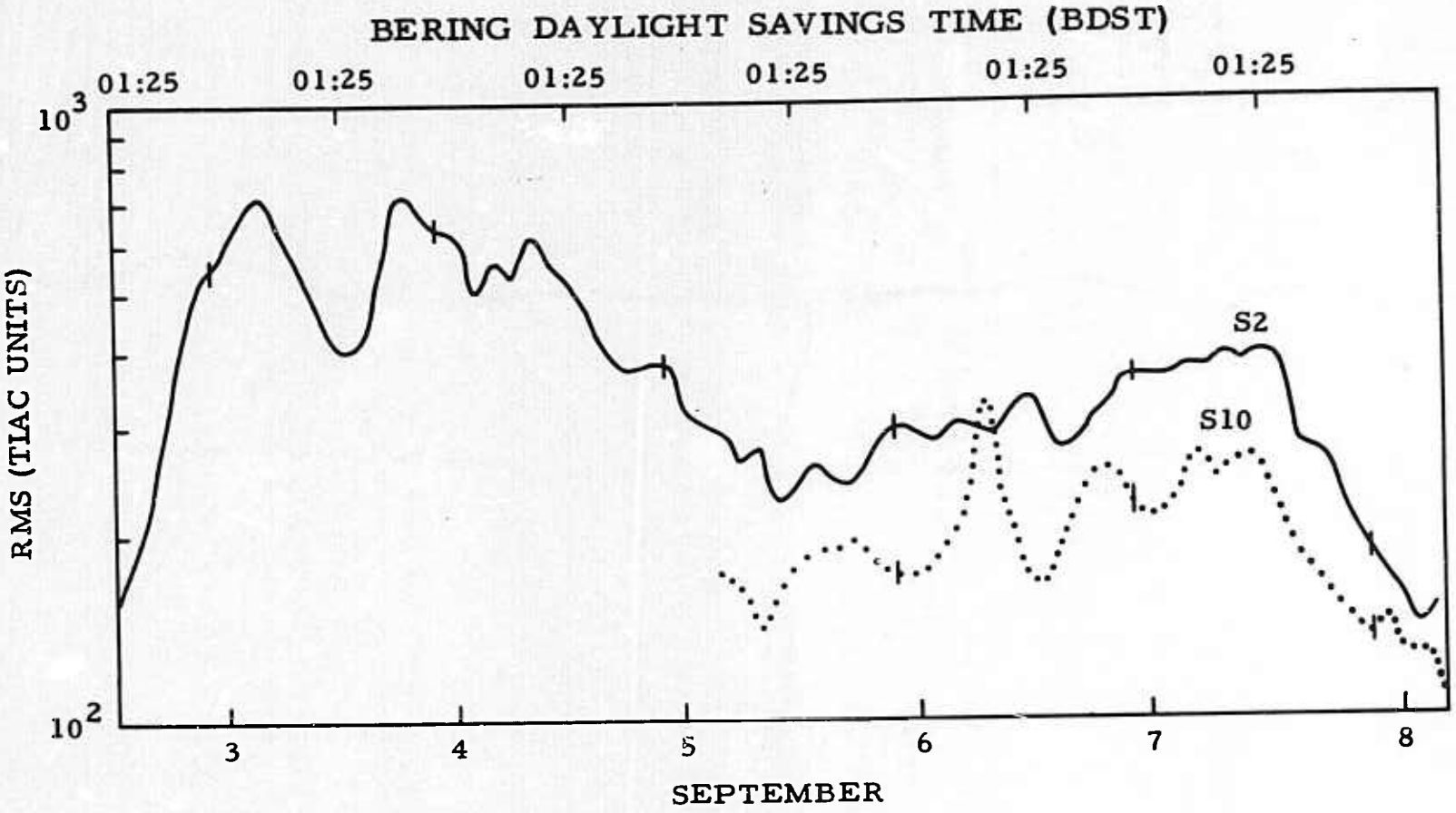

Figure II-15. RMS Plot of 2-Hr Data Samples for Stations S2 and S10

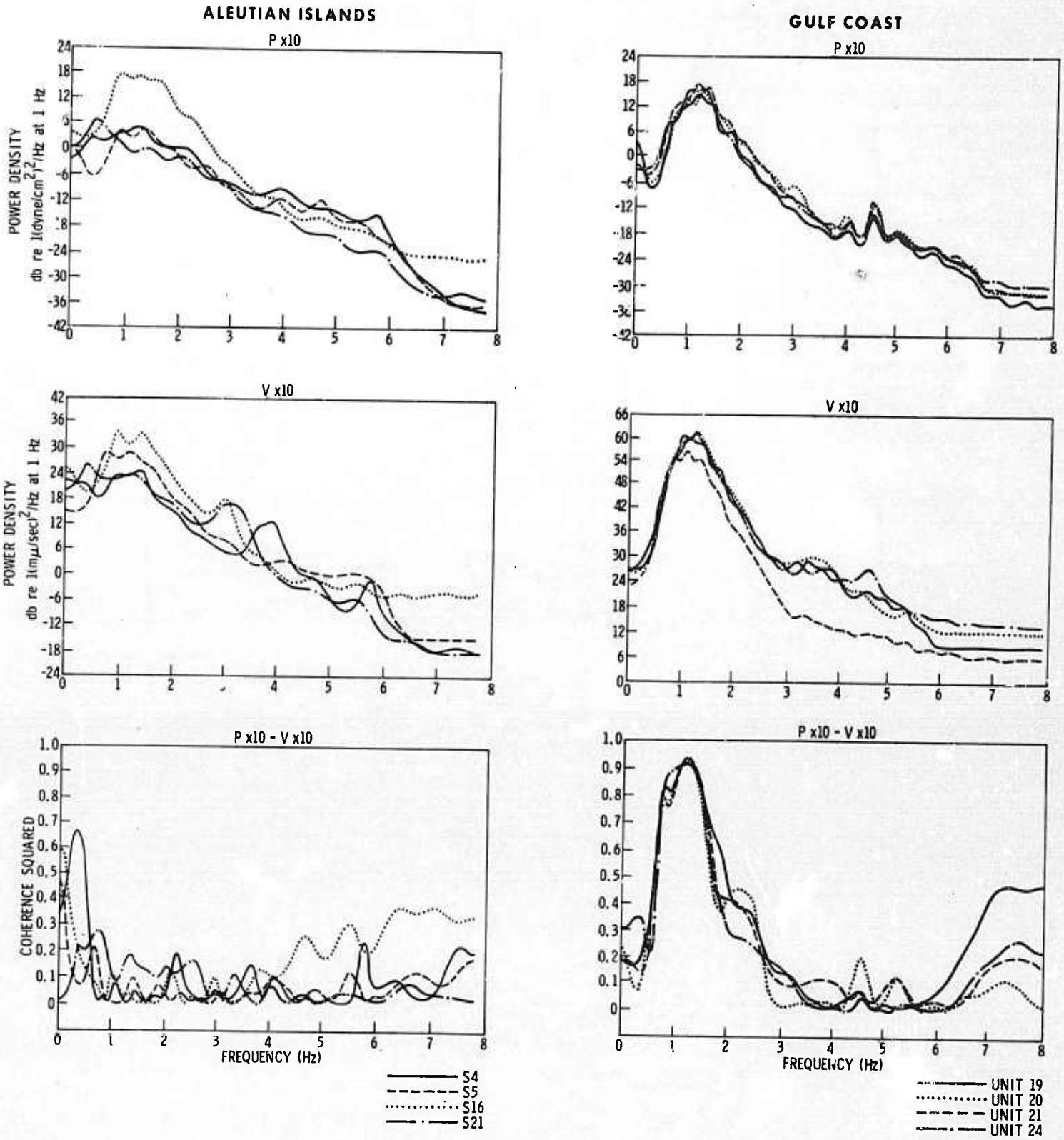

Figure II-16. Comparison of Aleutian Islands and Gulf Coast Power-Density Spectra and Coherence Using the Vertical and Pressure Components

BLANK PAGE

SECTION III

EARTHQUAKE SIGNAL ANALYSIS

A. DESCRIPTION OF THE DATA

To investigate the utility of certain signal-enhancement techniques, representative samples of teleseismic P-wave arrivals at several Phase I instruments were digitized in TIAC format from the OBS field tapes. These tapes were then converted to a format compatible with the IBM System 360 for processing. The instruments selected were S2, S4, S5, S6, S7, S8, S9, and S10. Table III-1 shows the eight earthquakes studied (designated earthquake 1 through earthquake 8), their magnitudes and locations, and the delta and azimuth from each earthquake to each station. The earthquakes span a time period of about 3 days.

A visual analysis of the earthquake recordings shows that signal characteristics vary across the array. Large variations in signal amplitude (for a given earthquake) are noted between stations separated by as little as 20 km (Table III-2). Station S5 tended to have the largest amplitudes and S7 the smallest, but the pattern varied from event to event. This can be seen by comparing signal amplitudes across the array for earthquakes 3 and 7 (Figures III-1 and III-2). The P-wave angle of incidence and the azimuth for these two events are quite different, suggesting that lateral changes in crustal and upper-mantle structure in the area also affect the observed variations.

Table III-3 compares the pressure/vertical (P/V) amplitude ratios of the noise and the amplitude ratios of the direct-to-reflected (water-bounce) signals on the vertical seismometer. Theory predicts that an unconsolidated bottom will give a noise P/V ratio of less than unity.[6] For this type of bottom, the acoustic impedance contrast between the water layer and the ocean bottom would be small, and essentially all energy would be transmitted through the interface. Under these conditions, the reflected arrival is larger than the initial arrival on the vertical seismometer.

Table III-1

EARTHQUAKES EMPLOYED IN EARTHQUAKE SIGNAL ANALYSIS

Earthquake	Earthquake Parameters						Deltas and Azimuths from OBS Sites to Earthquake Epicenters (°)													
	Location		Date (1967)	Origin Time (h, m, s)	Magnitude (m_b)	Depth (km)	S2		S4		S5		S6		S7		S8		S9		S10	
	Lat (°)	Long (°)					Δ	Az	Δ	Az	Δ	Az	Δ	Az	Δ	Az	Δ	Az	Δ	Az	Δ	Az
1	38.6N	144.0E	Sept 6	08:01:31.5	4.5	66	29.1	259.0	28.8	259.0	28.7	259.1	A		28.4	259.2	28.2	259.3	28.1	259.3	28.0	259.4
2	2.7N	124.3E	Sept 7	07:12:36.6	5.8	274	66.2	242.4	65.9	242.1	65.7	242.0	65.6	241.9	65.4	241.8	65.2	241.6	65.1	241.6	64.9	241.4
3	31.3S	179.6E	Sept 7	11:08:13.2	5.1	430	82.2	179.1	82.0	178.8	81.8	178.6	81.7	178.4	81.6	178.3	81.4	178.1	81.3	178.0	81.2	177.8
4	21.5N	144.0E	Sept 7	14:07:50.3	4.5	126	40.1	235.1	39.7	234.9	39.6	234.8	A		B		39.0	234.5	38.8	234.4	38.7	234.4
5	12.2N	140.8E	Sept 8	22:37:39.5	5.3	27	49.5	231.9	49.2	231.6	49.0	231.5	A		48.7	231.3	48.4	231.2	48.3	231.1	48.1	231.0
6	18.0N	145.5E	Sept 9	08:37:50.4	5.2	241	42.3	230.5	41.9	230.3	41.7	230.2	A		41.4	230.0	41.2	229.8	C		D	
7	27.7S	63.1W	Sept 9	10:06:44.1	5.8	578	128.6	87.3	128.9	87.2	129.0	87.2	129.1	87.1	129.2	87.1	129.4	87.0	D		D	
8	12.3N	140.7E	Sept 9	14:43:57.7	5.4	33	49.5	232.1	49.0	231.8	49.0	231.7	48.8	231.6	D		D		D		D	

A - Tape drive stopped
B - Data not digitized
C - Unit not operating
D - Unit not down

Table III-2

SIGNAL-AMPLITUDE VARIATION

Station	Relative Amplitude for Earthquake				
	2	3	5	6	7
S2	39	A	19	16	22
S4	32	13	16	15	27
S5	34	26	28	30	33
S6	29	19	B	B	33
S7	19	11	10	15	9
S8	28	22	23	19	15
S9	25	A	14	C	C
S10	28	22	A	C	C
Maximum Variation	2.1	2.4	2.8	2.0	3.7

A – Amplitude too small to measure

B – Event not analyzed because the tape stopped

C – Event not analyzed because the seismometer was not on on the bottom

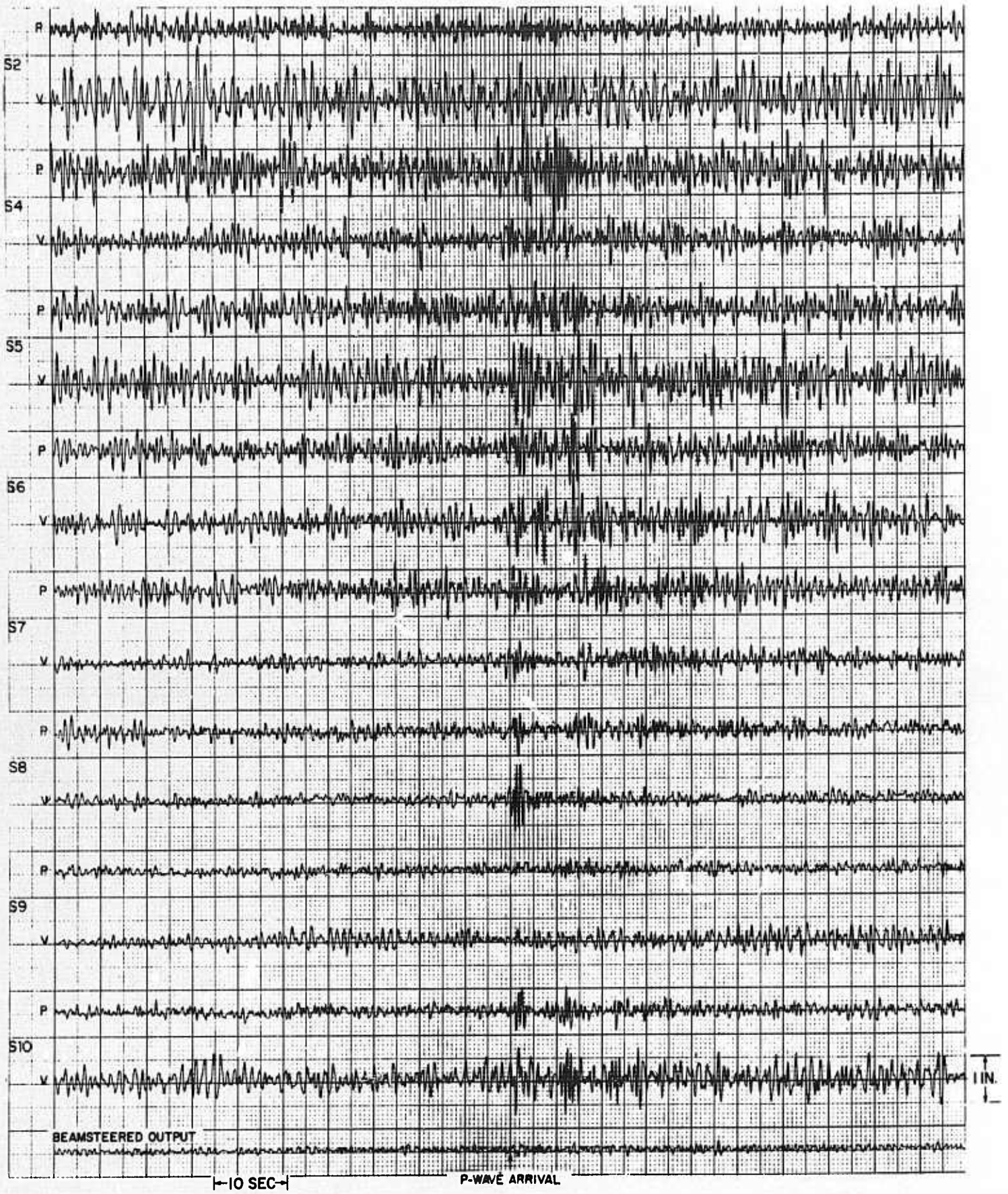

Figure III-1. Beamsteer Technique Applied to Earthquake 3, Averaged Time Differences Employed (scale: 1000 TIAC units/in.)

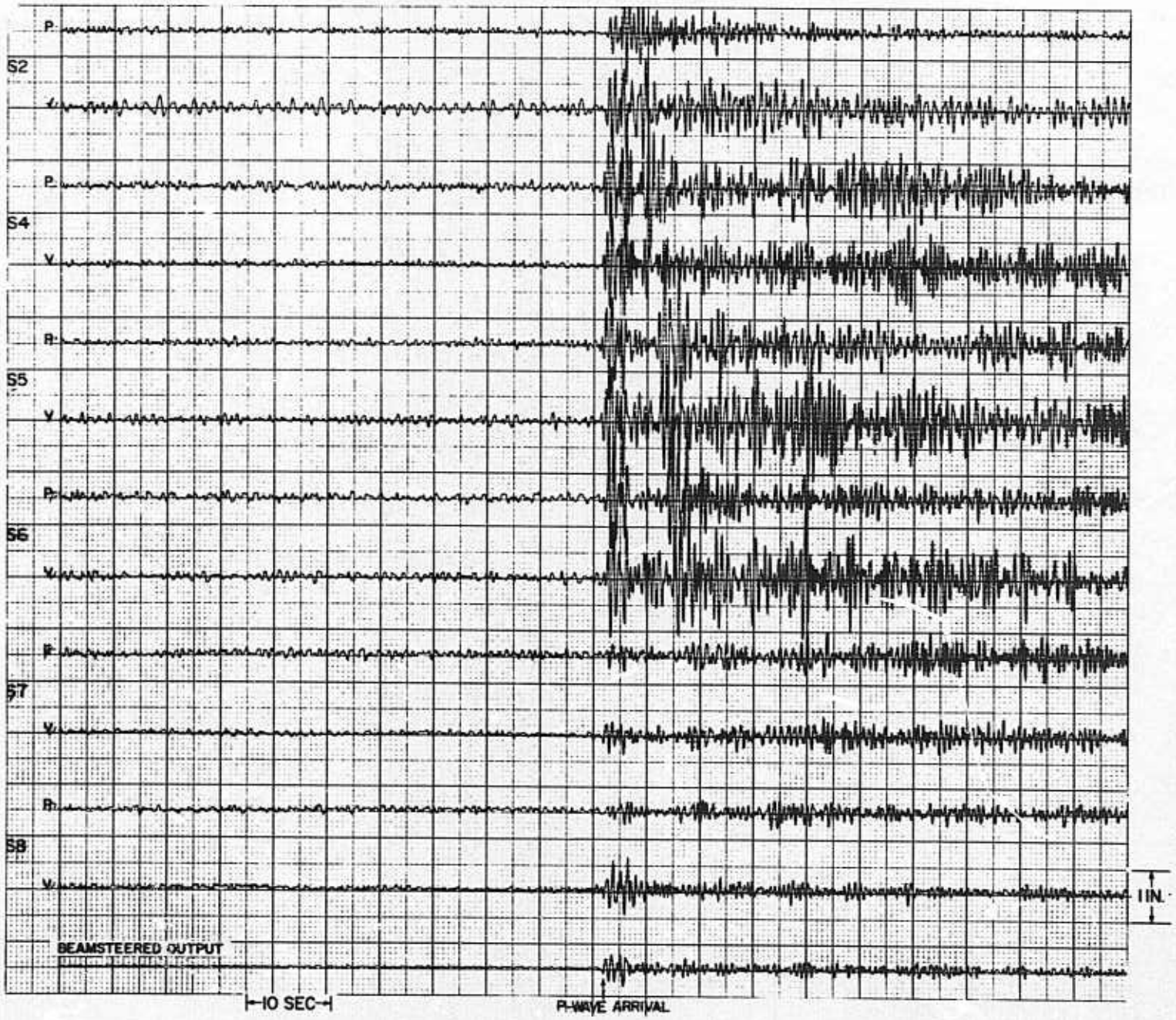

Figure III-2. Beamsteer Technique Applied to Earthquake 7, Averaged Time Differences Employed (scale: 2000 TIAC units/in.)

Table III-3

COMPARISON OF P/V NOISE RATIOS AND DIRECT-TO-REFLECTED SIGNAL-AMPLITUDE RATIOS ON THE VERTICAL SEISMOMETER

Station	P/V Noise Ratio	D/R Signal-Amplitude Ratio
S2	< 1	< 1
S4	> 1	> 1
S5	~ 1	~ 1
S6	~ 1	~ 1
S7	> 1	> 1
S8	>1	> 1
S9	< 1	< 1
S10	< 1	< 1

In all cases where P/V < 1, the direct-to-reflected (D/R) amplitude ratio is also less than unity. Conversely, when P/V > 1, D/R is also > 1. Figure III-2 best illustrates this: S2 has higher amplitude vertical noise and a significantly larger amplitude reflected arrival; S8 shows the opposite effect. From Table III-3, it therefore appears that the bottom was unconsolidated at S2, S9, and S10 and relatively consolidated at S4, S7, and S8. Stations S5 and S6 appear to fall between these two sets. Note also that, for all events, the stations with a low P/V noise ratio tended to have the best signal-to-noise ratio (especially S8).

Table III-4 compares USC&GS magnitudes with the average magnitudes computed using the OBS data. All events are in the 20° to 70° distance range and were recorded at more than a single station. The OBS magnitudes averaged 0.2 magnitude units higher. Data from events less than 20° were excluded because they showed considerably more scatter (in both directions), probably because the phase being observed (i.e., travelpath of the first arrival) varied from event to event. This small sample suggests that teleseismic signal amplitudes on the ocean bottom are about equal to or slightly higher than those at land stations.

Table III-4

COMPARISON OF OBS AND USC&GS MAGNITUDES

Event	Date (1967)	Time (h, m, s)	OBS Station	Magnitude		
				OBS	Average OBS	USC&GS
Fiji Islands	Aug 12	09:39:44.3	S21	5.9	6.0	5.8
			S19	5.7		
			S18	5.7		
			S11	6.5		
			S12	6.2		
			S14	6.6		
			S15	5.7		
Honshu Island	Aug 13	20:06:50.6	S21	5.9	6.4	6.0
			S19	6.5		
			S18	6.6		
			S14	6.1		
			S15	6.7		
Kurile Islands	Sept 1	22:42:01.8	S5	5.4	5.5	5.4
			S2	5.6		
Kermadec Islands	Sept 7	11:08:13.2	S10	5.5	5.3	5.1
			S8	5.3		
			S7	5.2		
Mariana Islands	Sept 9	08:37:50.4	S8	5.3	5.3	5.2
			S7	5.2		
			S4	5.1		
			S5	5.5		

B. DETECTION RESULTS

Table III-5 is a histogram which shows the number of reported events detected by the OBS arrays during each phase as a function of epicentral distance. Between 0° and 10°, all reported events were included; beyond 10°, those events with magnitude 5.0 and larger were included. (All but four events were between magnitudes 5.0 and 6.0). Detections were obtained from the Preliminary Analysis Report.[1] Also, since there may be some reported events which were not positively associated, actual detectability may be slightly better than indicated.

Between 0° and 10°, all but one reported event was detected; between 10° and 40°, 14 of 15 events were detected. (These events generally have shorter periods than events from longer ranges.) Beyond 40°, a few scattered events (generally those deep events with shorter periods) were detected. Thus, it appears that, out to about 40°, events of magnitude 5.0 and greater would be detected by at least some of an OBS array; beyond 40°, only very large events or events with relatively short periods would be detected.

C. SUM AND DIFFERENCE AND TIME-SHIFTED SUM TECHNIQUE

An earlier investigation of pressure/vertical velocity relationships for the OBS established that formation of sum and difference traces from the pressure and vertical velocity seismograms should permit the separation of direct-arrival energy from that reflected from the water surface.[6] The pressure and vertical velocity traces are out of phase for the direct P-wave arrival and in phase after reflection from the water surface. Therefore, subtracting the pressure trace from the vertical trace should enhance the direct arrival and suppress the reflected arrival; adding the pressure and vertical traces should suppress the direct arrival and enhance the reflected arrival. Also, the signal-to-noise ratio for each resultant trace should be improved by 3 db (i.e., $\sqrt{2}$) if the noise is incoherent between the two input channels.

Table III-5

NUMBER OF REPORTED EVENTS DETECTED BY OBS ARRAYS

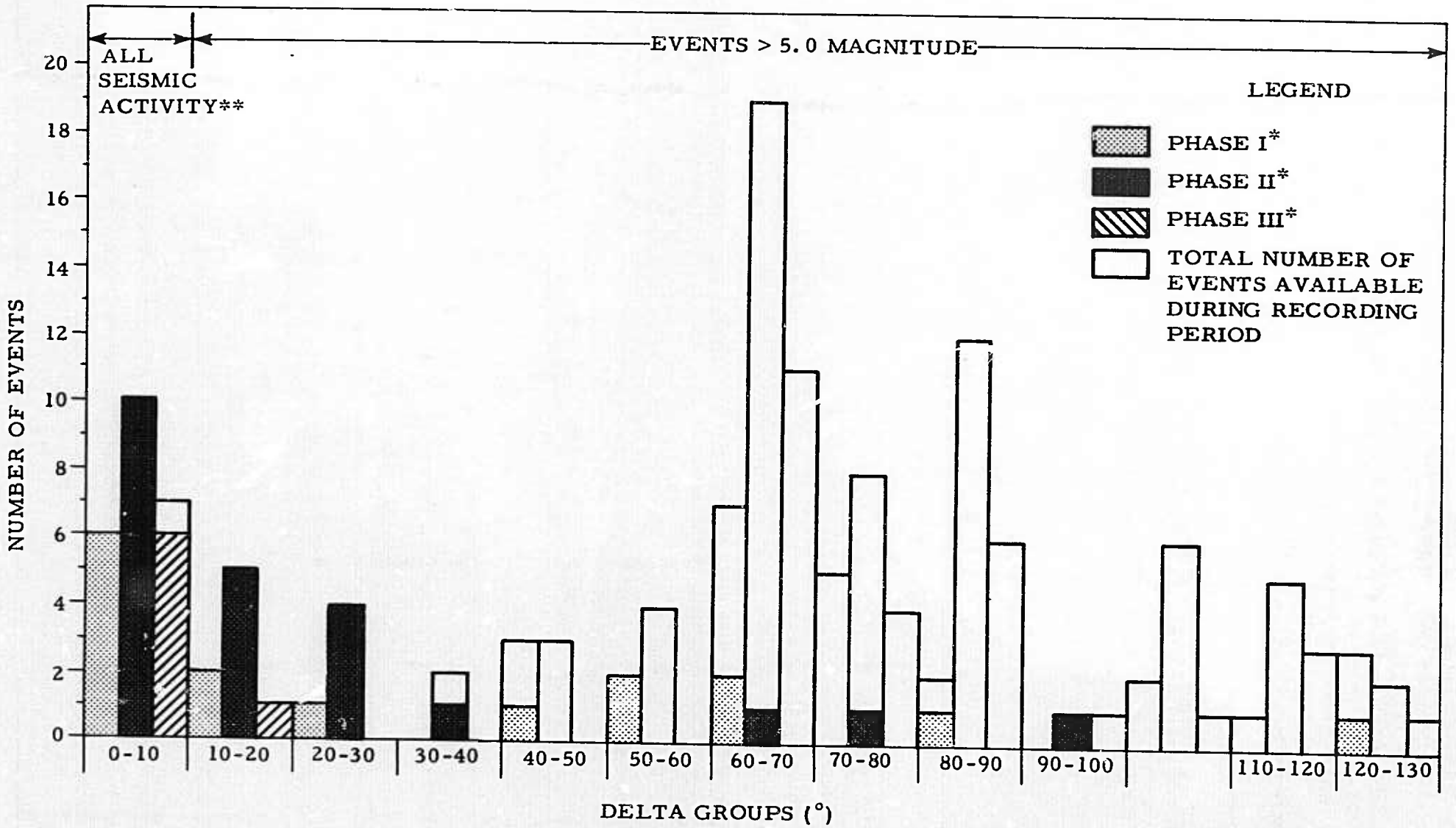

* Epicentral distance measured from center of array

** All seismic activity was < 5.0 magnitude

The sum and difference traces should be nearly identical; the sum trace, however, will be delayed with respect to the difference trace by an amount equal to the 2-way traveltime in the water layer. If the sum trace is shifted forward by an amount equal to this time delay and added to the difference trace, the result should be approximately a fourfold increase in the amplitude of the resultant signal over the original incoming signal.

A program was written for the IBM System 360 computer to form the difference, sum, and time-shifted sum traces for input pairs of pressure/vertical traces and to display the result by means of a computer-generated plot. The amplitude of the time-shifted and summed trace is divided by four before plotting so that it may be compared more readily with the input traces.

Figures III-3 and III-4 show two such plots for earthquake 7, recorded at stations S5 and S6. There is a significant improvement in the signal-to-noise ratio for each of the three output traces over the two input traces. However, summing the input traces does not completely cancel the portion of the incoming signal ahead of the water-surface reflection. When the sum trace is shifted and added to the difference trace, the incompletely cancelled portion shows up as a precursor to the incoming signal, making the exact point of signal onset less distinct than it is on the difference trace. Similar comments apply to Figures III-5 and III-6 which show arrivals from earthquake 5 at stations S5 and S9.

Figures III-7 and III-8 show the technique applied to signal arrivals from earthquake 3 at stations S7 and S10. In this instance, little improvement in signal-to-noise ratio of the output traces over the better of the two input traces is achieved because, in each case, one of the input traces has a significantly higher noise level than the other and a relatively low signal level.

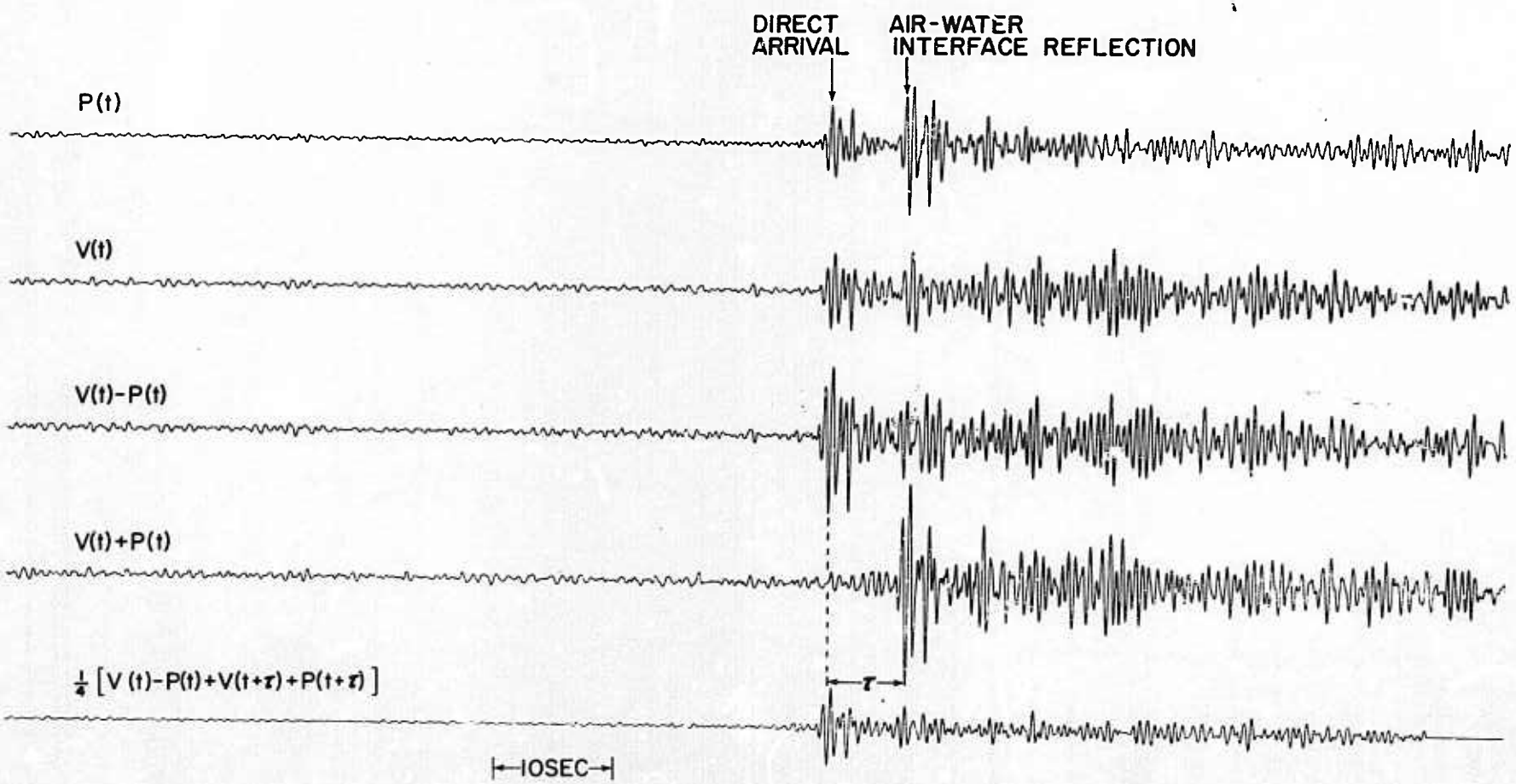

Figure III-3. Sum and Difference Technique Applied to Arrivals from Earthquake 7 at Station S5

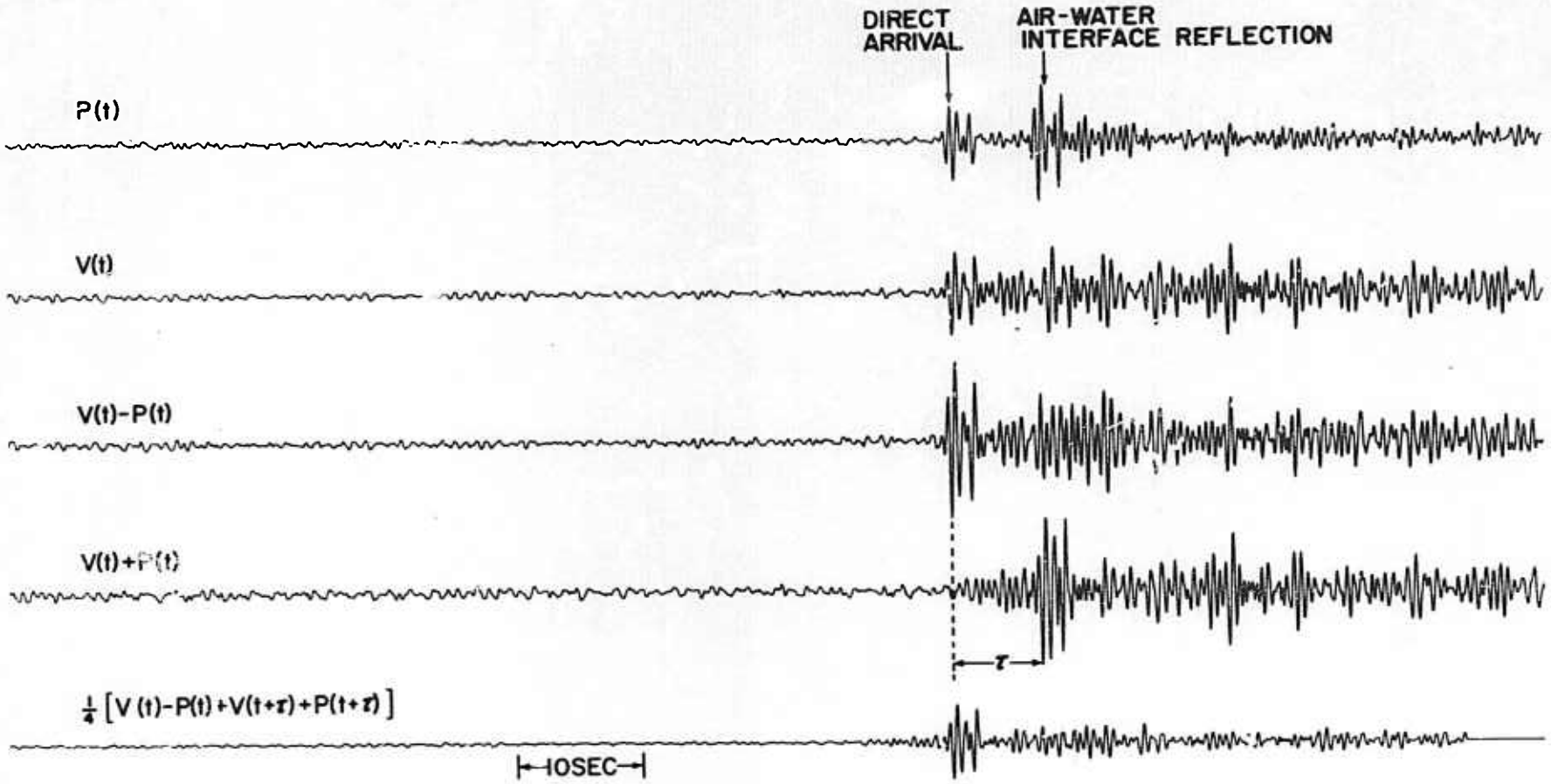

Figure III-4. Sum and Difference Technique Applied to Arrivals from Earthquake 7 at Station S6

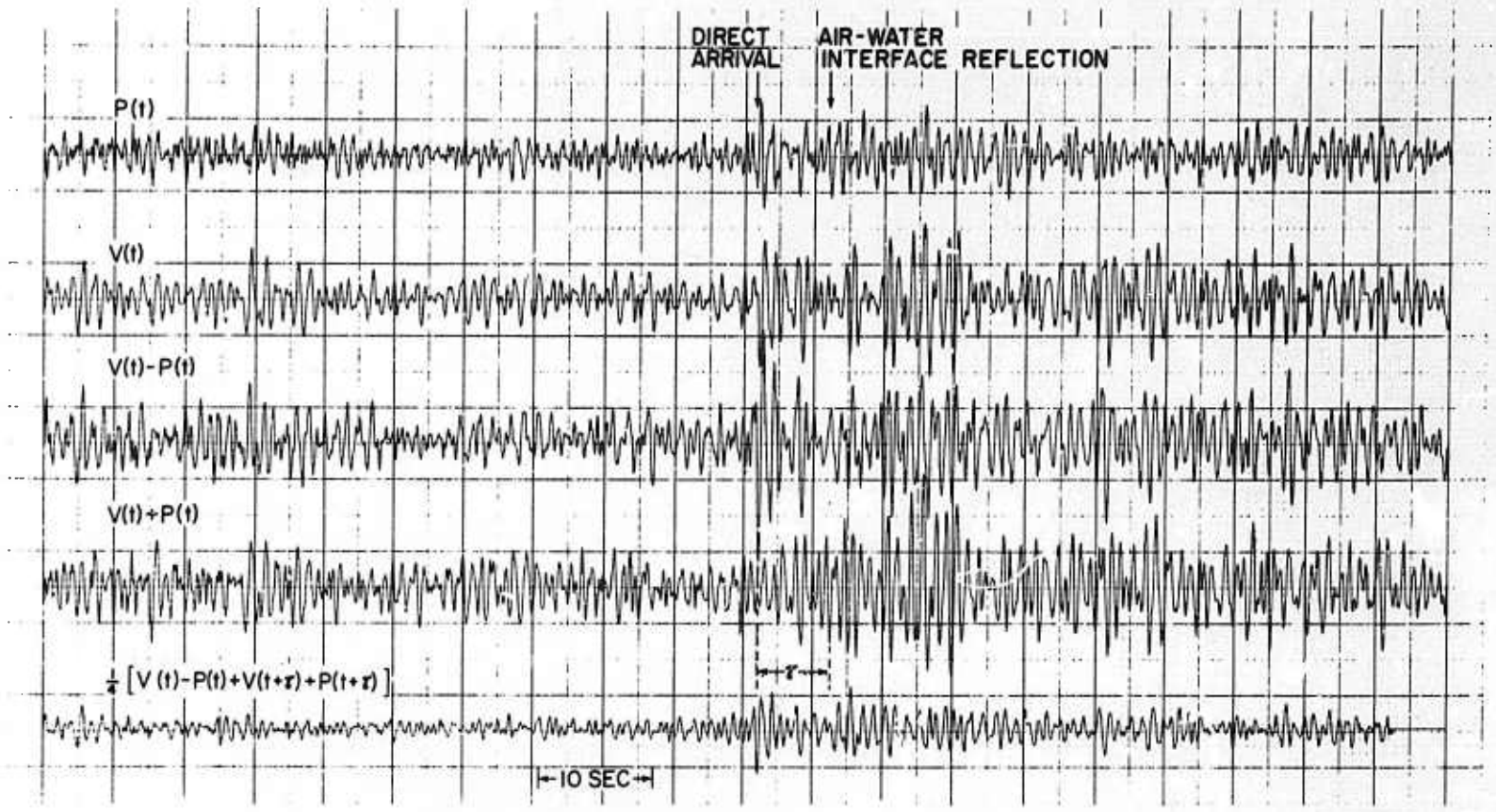

Figure III-5. Sum and Difference Technique Applied to Arrivals from Earthquake 5 at Station S5

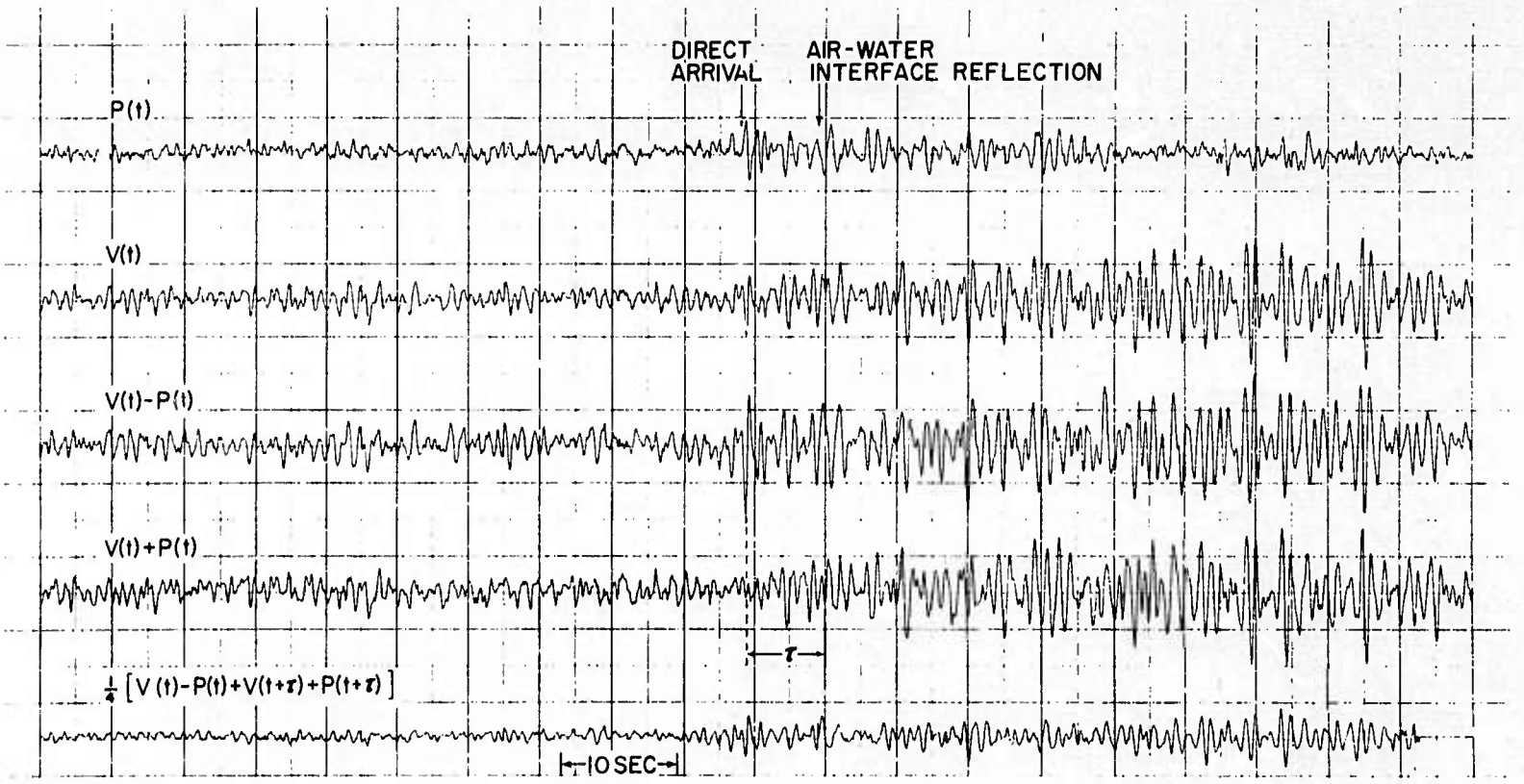

Figure III-6. Sum and Difference Technique Applied to Arrivals from Earthquake 5 at Station S9

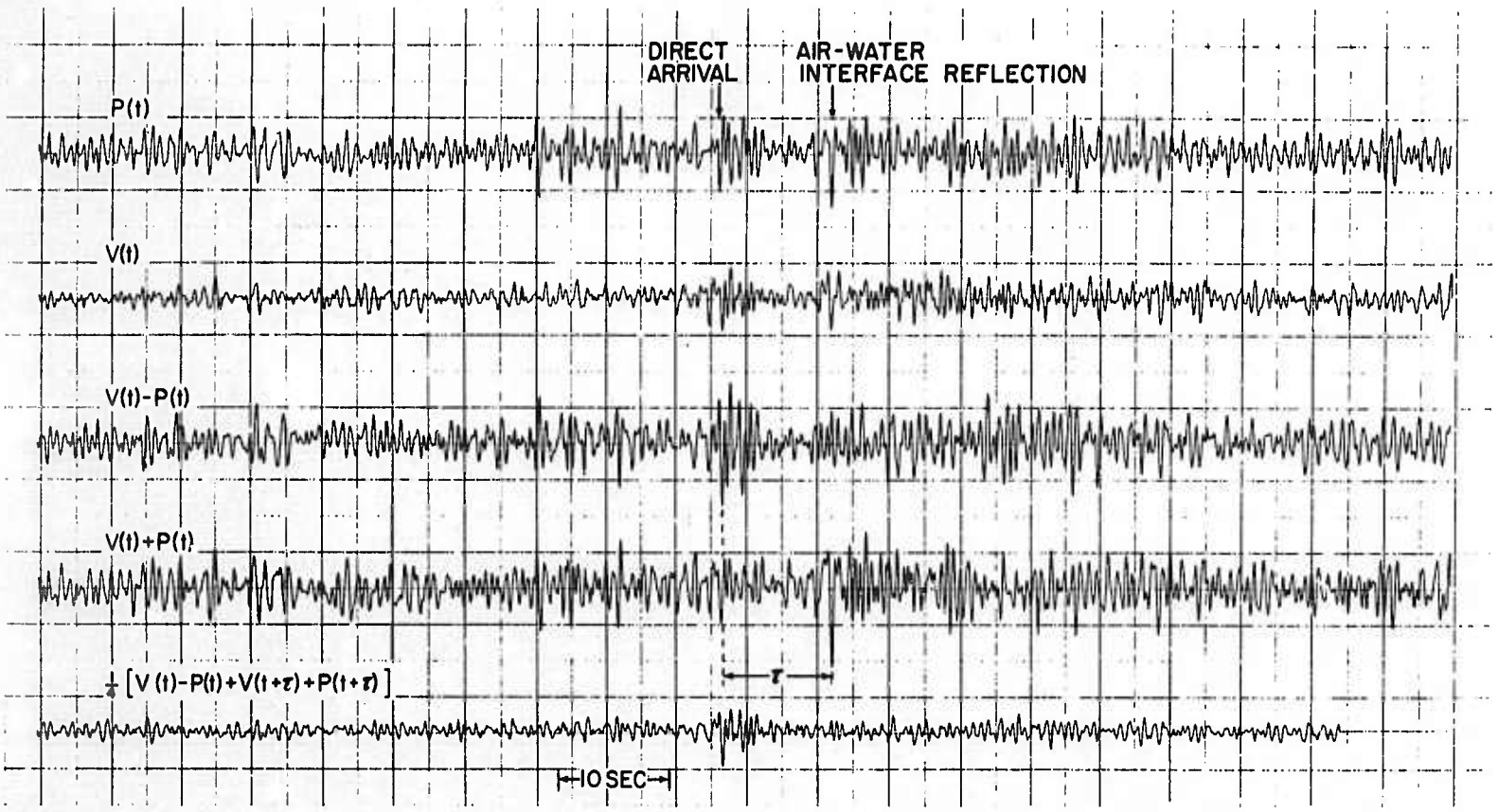

Figure III-7. Sum and Difference Technique Applied to Arrivals from Earthquake 3 at Station S7

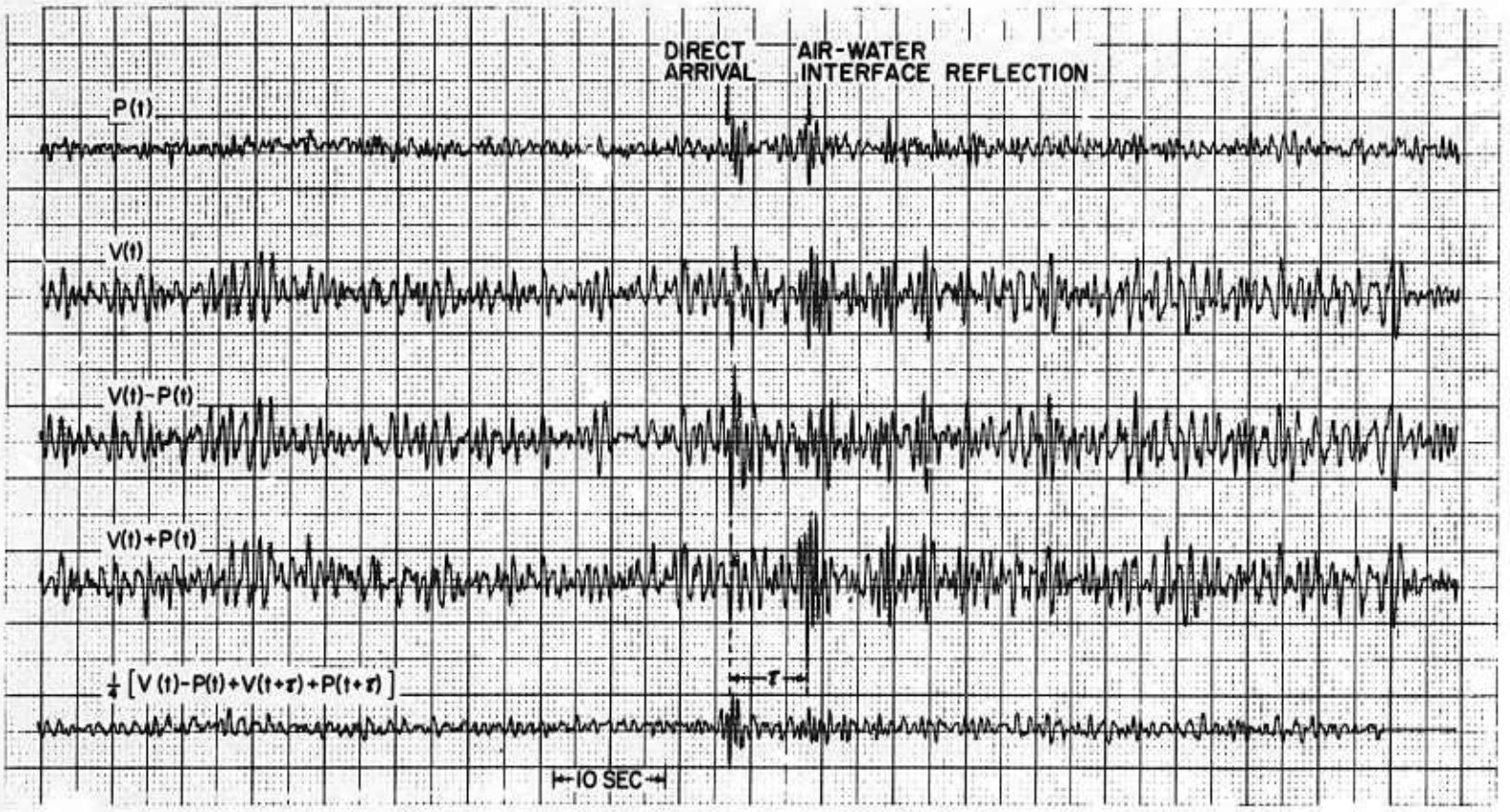

Figure III-8. Sum and Difference Technique Applied to Arrivals from Earthquake 3 at Station S10

The method was unsuccessfully applied to earthquake 1, a relatively weak event which was not detected on any of the selected instruments.

Figure III-9 shows the method applied to the signal arrival from earthquake 6 at station S7. In this case, the input data better satisfy the theoretical assumptions of the method; the input traces have approximately the same amplitude and signal-to-noise ratio, and the initial arrival is almost completely cancelled in the difference trace. The signal arrival on the final output trace shows a sharp onset, and the signal-to-noise ratio for this trace is between 3 and 6 db higher than it is on either input trace.

In summary, this technique will give at least 3-db signal-to-noise improvement if the signal-to-noise ratio on the pressure and vertical components are similar and the noise is uncorrelated between the two channels. In most cases, the difference trace is better than the other combinations because no precursor is introduced to the output trace (which is caused by imperfect cancellation of the energy between the initial arrival and water bounce). Occasionally, however, the sum of the difference trace and time-shifted sum trace can be used.

D. BEAMSTEERING

The beamsteer technique is a method of aligning and summing the seismograms from an array of seismographs to increase event-detection capability. If the noise is incoherent between the input traces and the waveform is preserved across the array, the method should result in $\sqrt{n}$ improvement of the signal-to-noise ratio of the output trace over the input traces, where n is the number of input traces summed. Because the data were readily available, the method was applied to the earthquake recordings even though it is known that array dimensions this large (160 km) can be expected to introduce critical signal-alignment problems, as well as degradation due to changes in signal character.

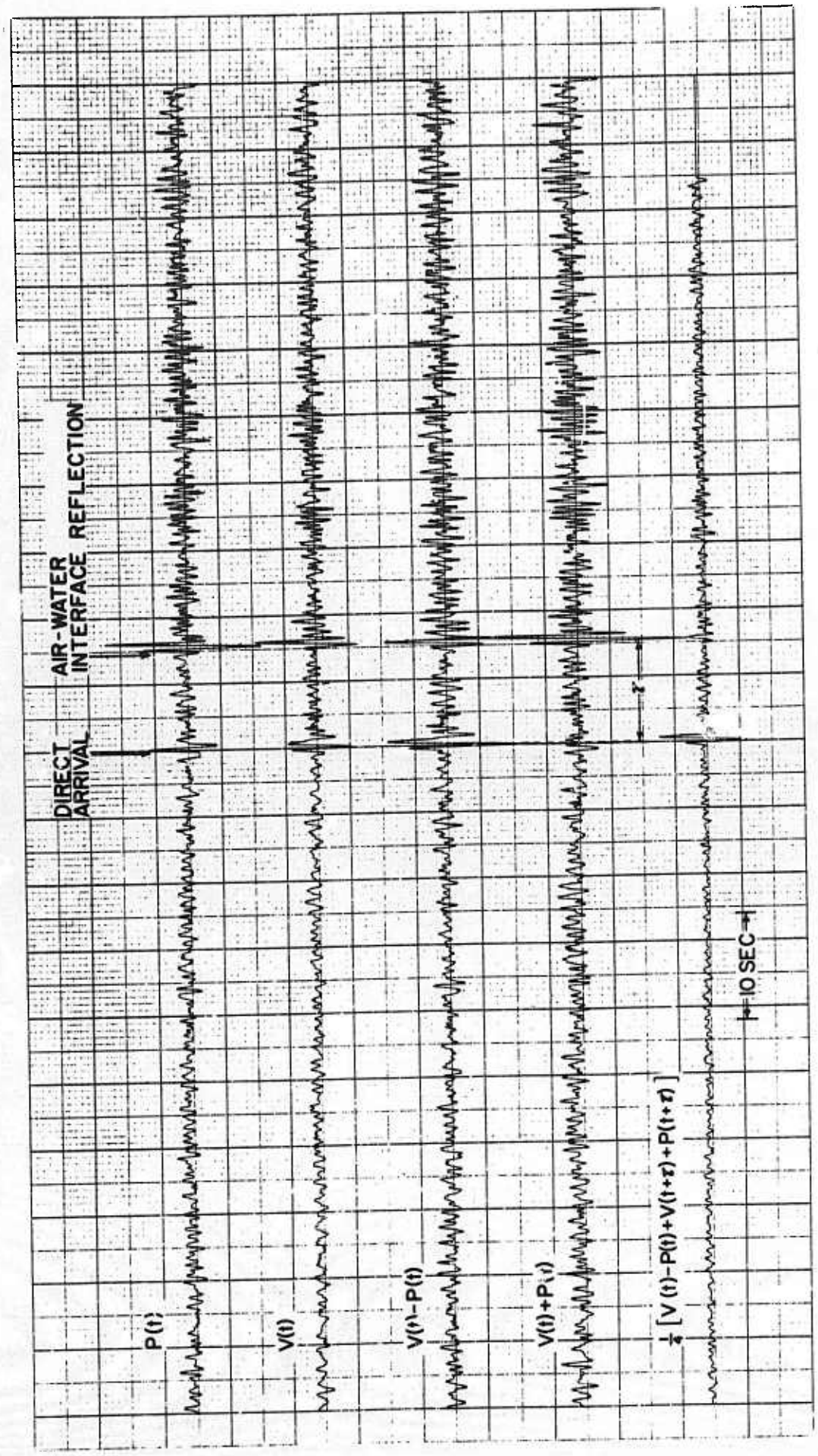

Figure III-9. Sum and Difference Technique Applied to Arrivals from Earthquake 6 at Station S7

The theoretical traveltimes from a strong earthquake to each array station were computed; from these, the theoretical arrival times of the signal at each unit were determined. The difference between the theoretical and true arrival time was noted for each station. Time differences are assumed to be due to crustal variations or other localized effects which are characteristic of the station and independent of the earthquake parameters.

In this investigation, the time differences at each station for all the visually detectable earthquakes — earthquakes 2, 3, 5, 6, 7, and 8 — were averaged to determine the time-difference (static-correction) characteristic of each station. Static-correction information is input to a computer program which shifts the traces, sums them, and plots the aligned input traces and the sum trace. The pressure and vertical velocity channels are used as dual inputs for each station, the pressure traces being inverted during summation to account for the 180° phase difference between the pressure and vertical traces. Also, to facilitate comparison with the input traces, the amplitude of the output trace is divided by the number of input traces before it is plotted.

Figures III-1 and III-2 and III-10 through III-15 show the individual seismometers and the beamsteered outputs of this program for earthquakes 1, 3, 4, 5, 6, 7, and 8 using the static correction just described. The method did not result in significant signal-to-noise-ratio improvement or onset-detection capability over the better input traces due to the following factors.

There is a substantial variation in signal strength and signal-to-noise ratio over the array, and the sum trace is degraded by the traces with poor signal-to-noise ratios. A technique of weighting the input traces based on their observed signal-to-noise-ratios (diversity stacking) might have improved results. For example, Figures III-12 and III-13 show the program output for earthquake 5 with and without the vertical trace of unit S8. In this case, the output trace is virtually unaltered when the S8 vertical trace is omitted, even though this trace has a significantly better signal-to-noise ratio than any of the others.

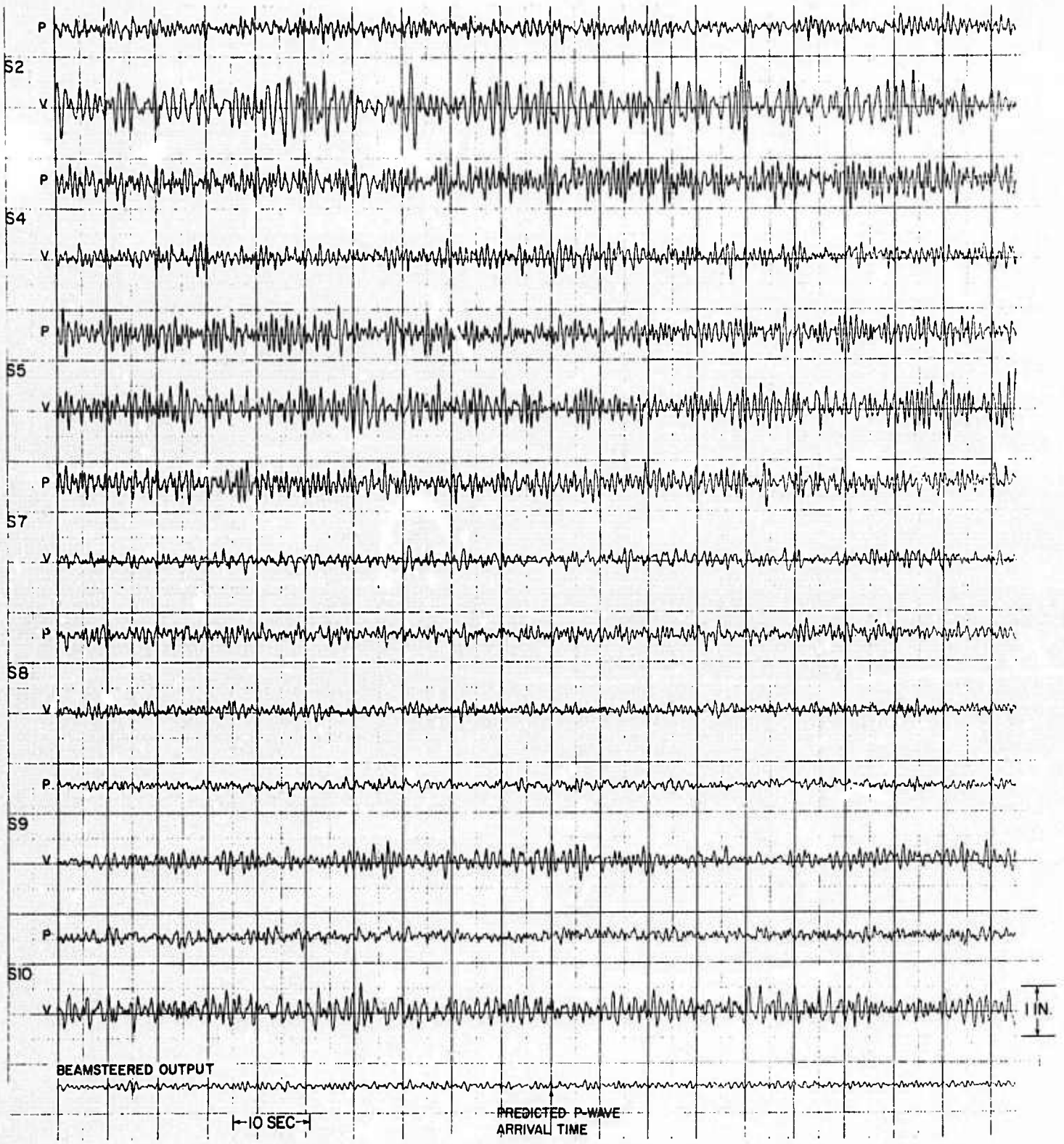

Figure III-10. Beamsteer Technique Applied to Earthquake 1, Averaged Time Differences Employed (scale: 1000 TIAC units/in.)

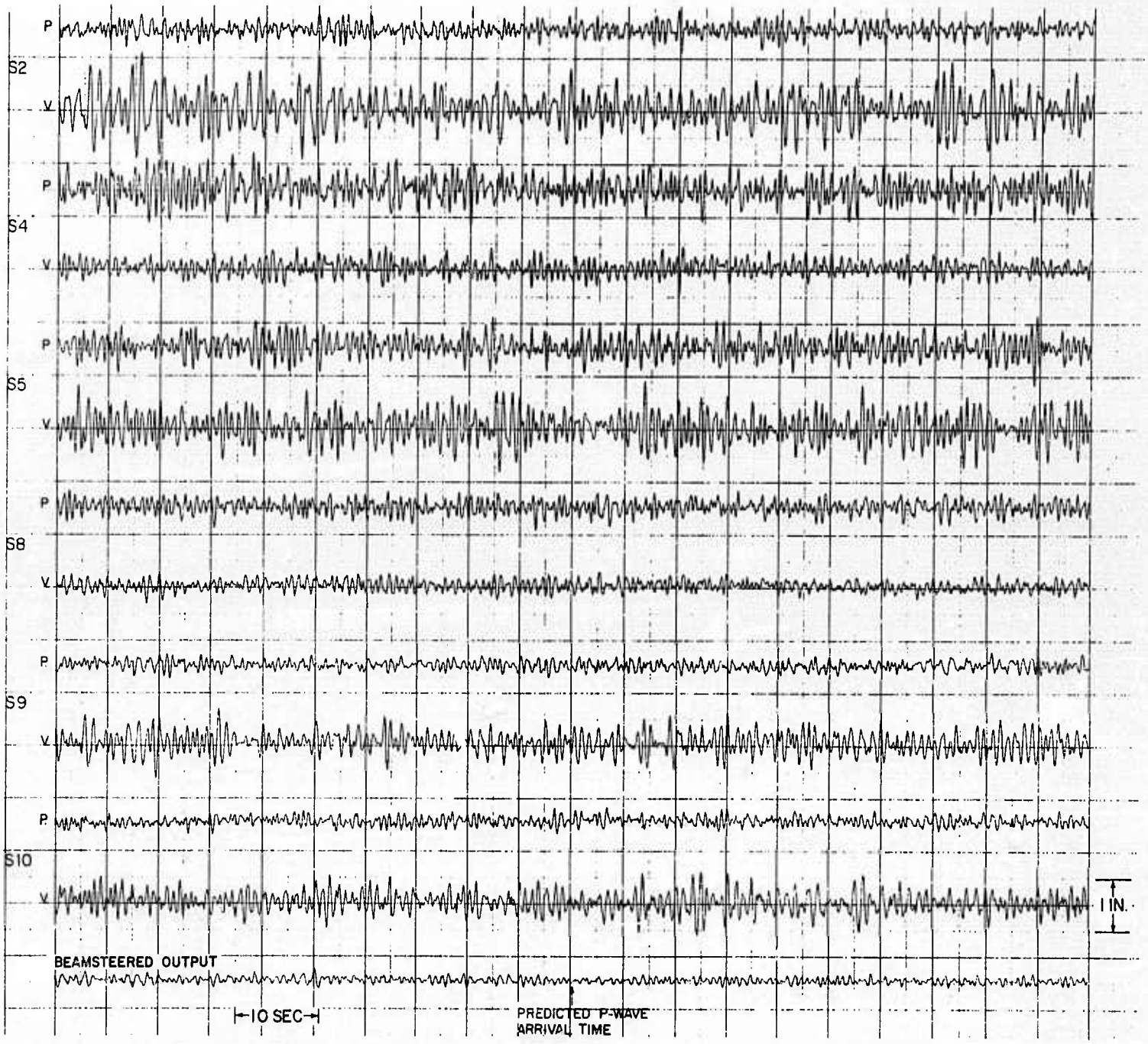

Figure III-11. Beamsteer Technique Applied to Earthquake 4, Averaged Time Differences Employed (scale: 1000 TIAC units/in.)

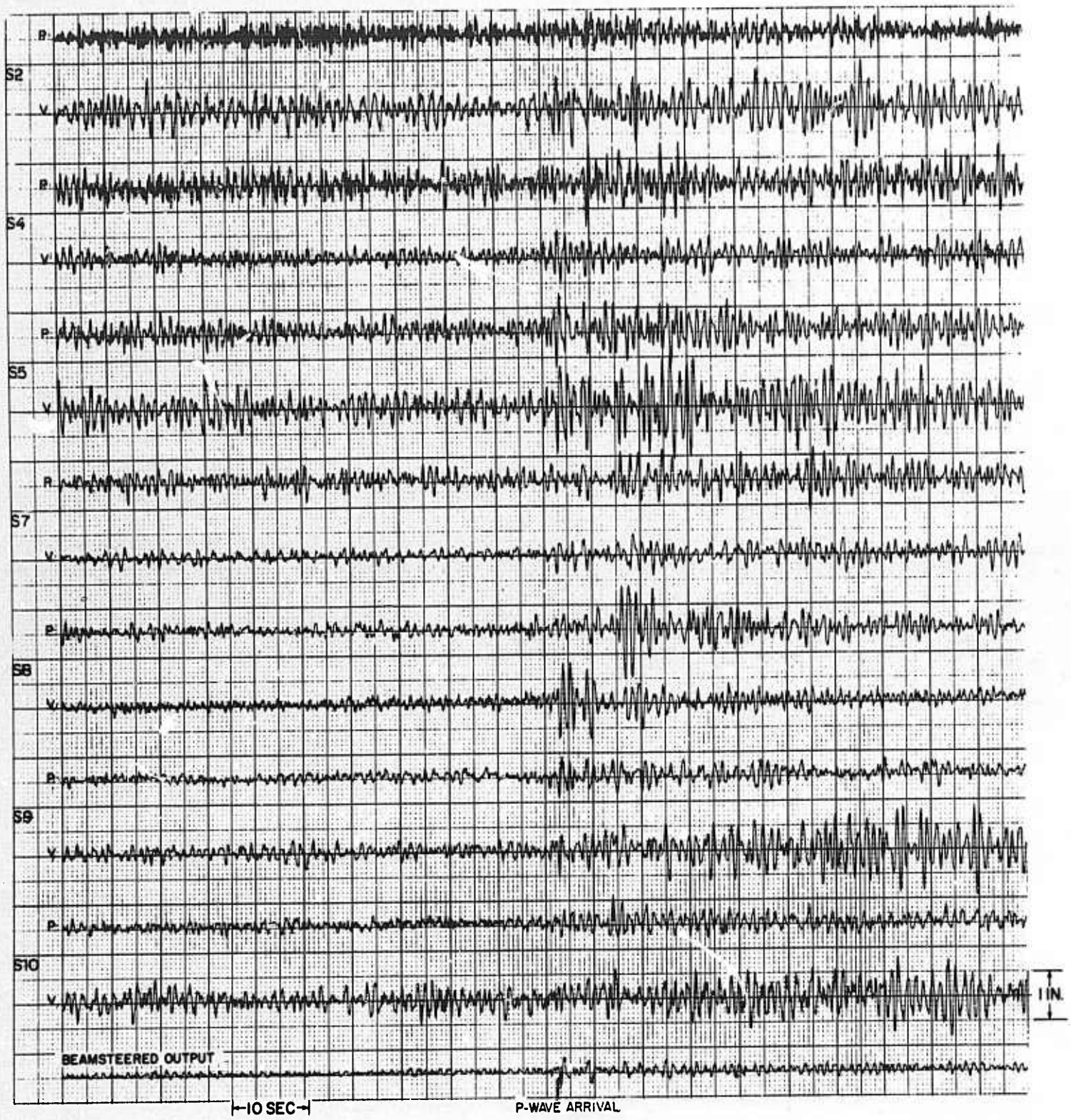

Figure III-12. Beamsteer Technique Applied to Earthquake 5, Averaged Time Differences Employed (scale: 1000 TIAC units/in.)

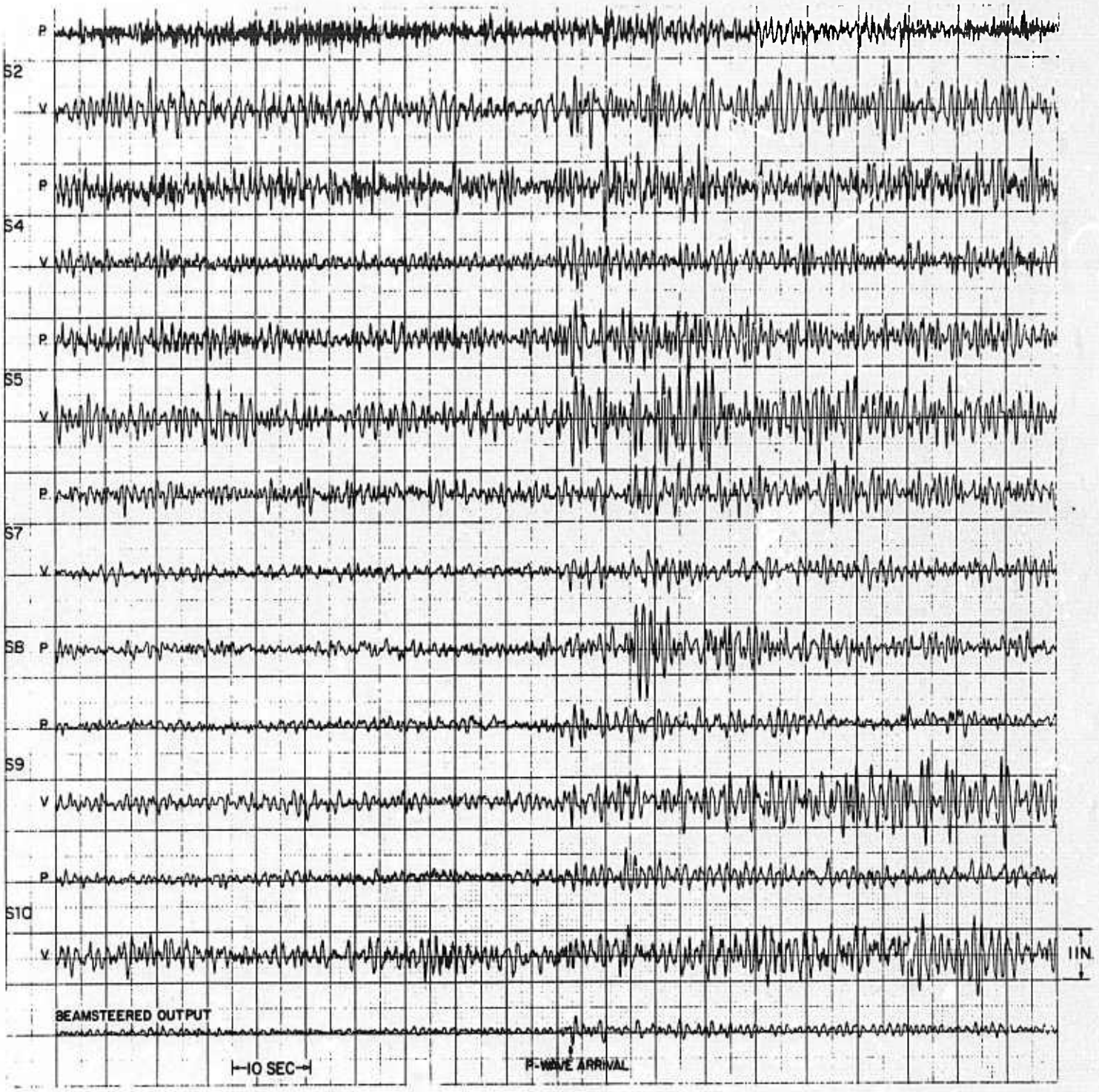

Figure III-13. Beamsteer Technique Applied to Earthquake 5, Averaged Time Differences Employed, Vertical Trace of Station S8 Omitted (scale: 1000 TIAC units/in.)

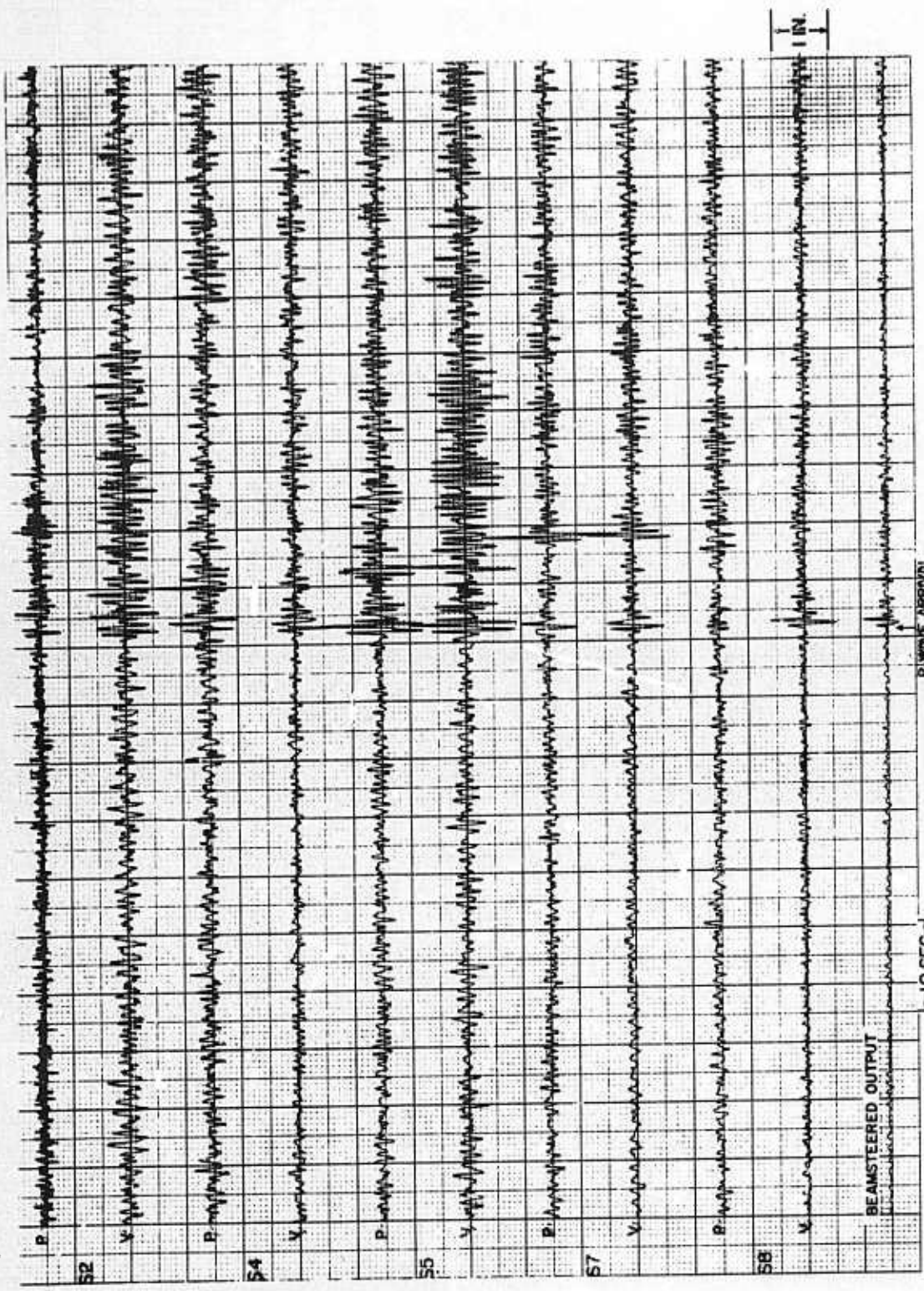

Figure III-14. Beamsteer Technique Applied to Earthquake 6, Averaged Time Differences Employed (scale: 1000 TIAC units/in.)

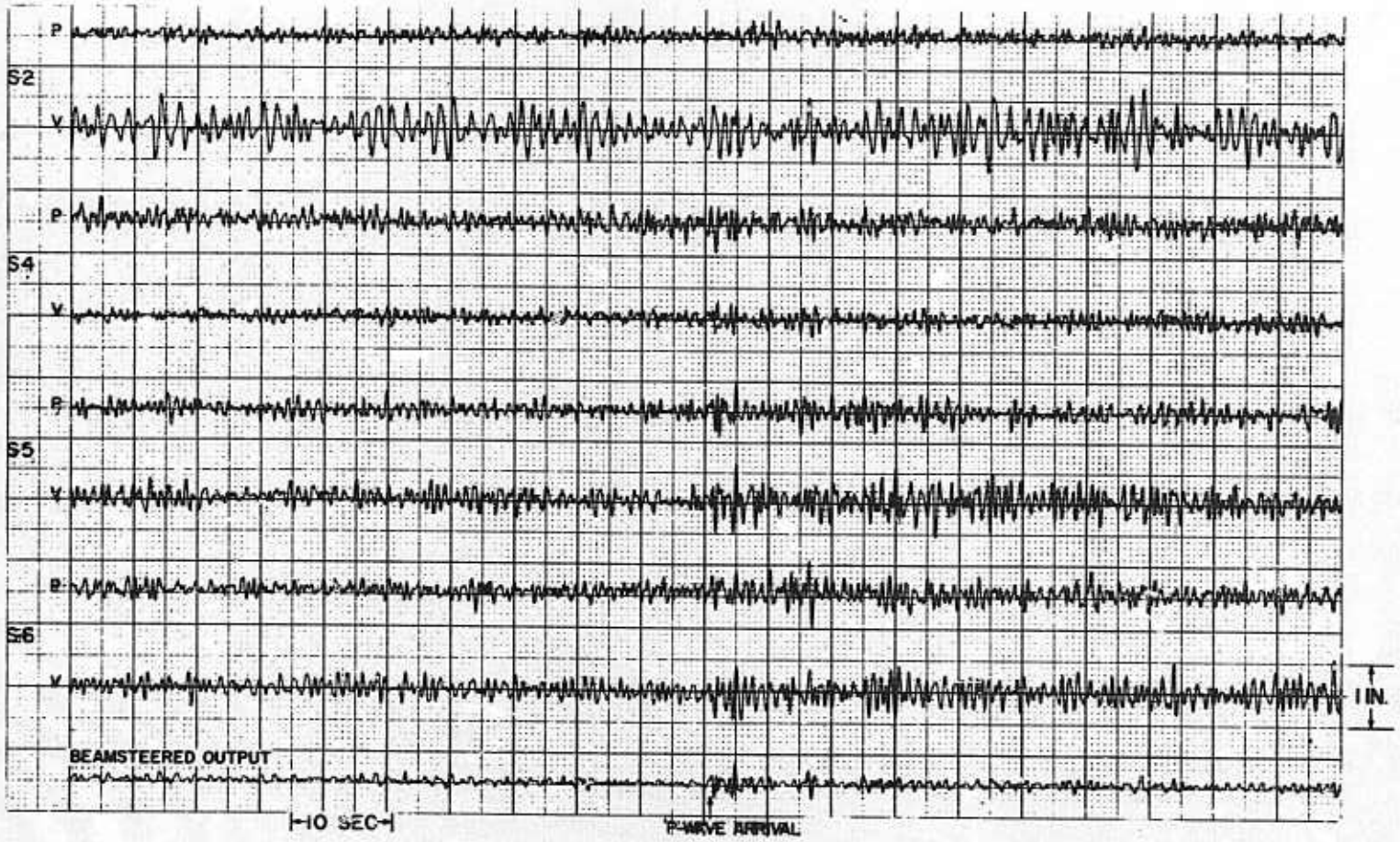

Figure III-15. Beamsteer Technique Applied to Earthquake 8, Averaged Time Differences Employed (scale: 1000 TIAC units/in.)

The sampling rate of the digitized data makes the amount of the time shifts critical. For the sample rate used, a difference of only eight data blocks is equivalent to a phase difference of 180° at 1 Hz.

The average static corrections were not sufficient. Figures III-16 and III-17 show the plotted program outputs for earthquakes 3 and 7, respectively; the traces are aligned and summed using the time shifts indicated by the individual earthquake rather than the averaged characteristic time difference. In each case, the sum trace using trace-alignment information from the individual earthquake shows a higher amplitude and signal-to-noise-ratio than the sum trace computed using the information averaged from several earthquakes. Thus, it appears that the static corrections are a function of earthquake location also (not a surprising result).

E. ZERO-PHASE BANDPASS FILTERING

Presented here are results of calculations aimed at improving signal-to-noise ratios by simple bandpass filtering. Instrument response can be changed to afford some noise rejection (thereby lowering the signal-detection threshold of the OBS), provided the signal and noise spectra peak at different frequencies. Change of the instrument response was simulated in the computer by applying zero-phase bandpass filters to the pressure and vertical velocity recordings of three earthquake events.

Power spectra were computed for signals on both the pressure and vertical channels of S4, S5, and S6 for earthquake 7 (magnitude 5.8). That event was chosen because its high signal-to-noise ratio allowed a good estimate of the signal spectra. In addition, noise power spectra were computed for noise samples immediately preceding each signal. Calculations were performed on the IBM System 360 computer using the Cooley-Tukey algorithm (fast Fourier transform), and CalComp plots of the power spectra were obtained. The number of points in each time trace was 1024 and the sample rate (Δt) was 0.0625 sec, giving a frequency increment (Δf) of 0.015625 Hz and a gate length of 64 sec.

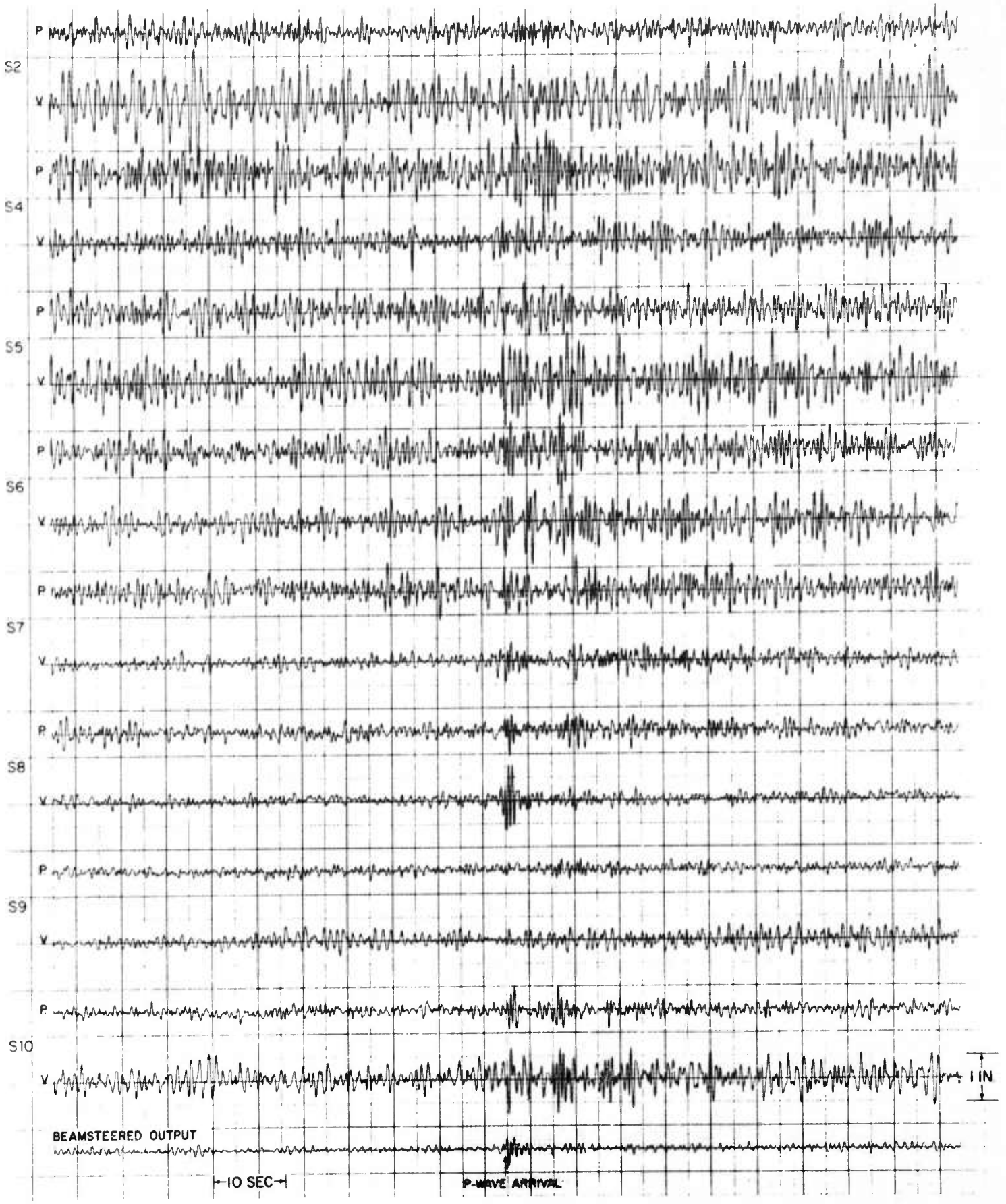

Figure III-16. Beamsteer Technique Applied to Earthquake 3, Optimum Visual Shift Employed (scale: 1000 TIAC units/in.)

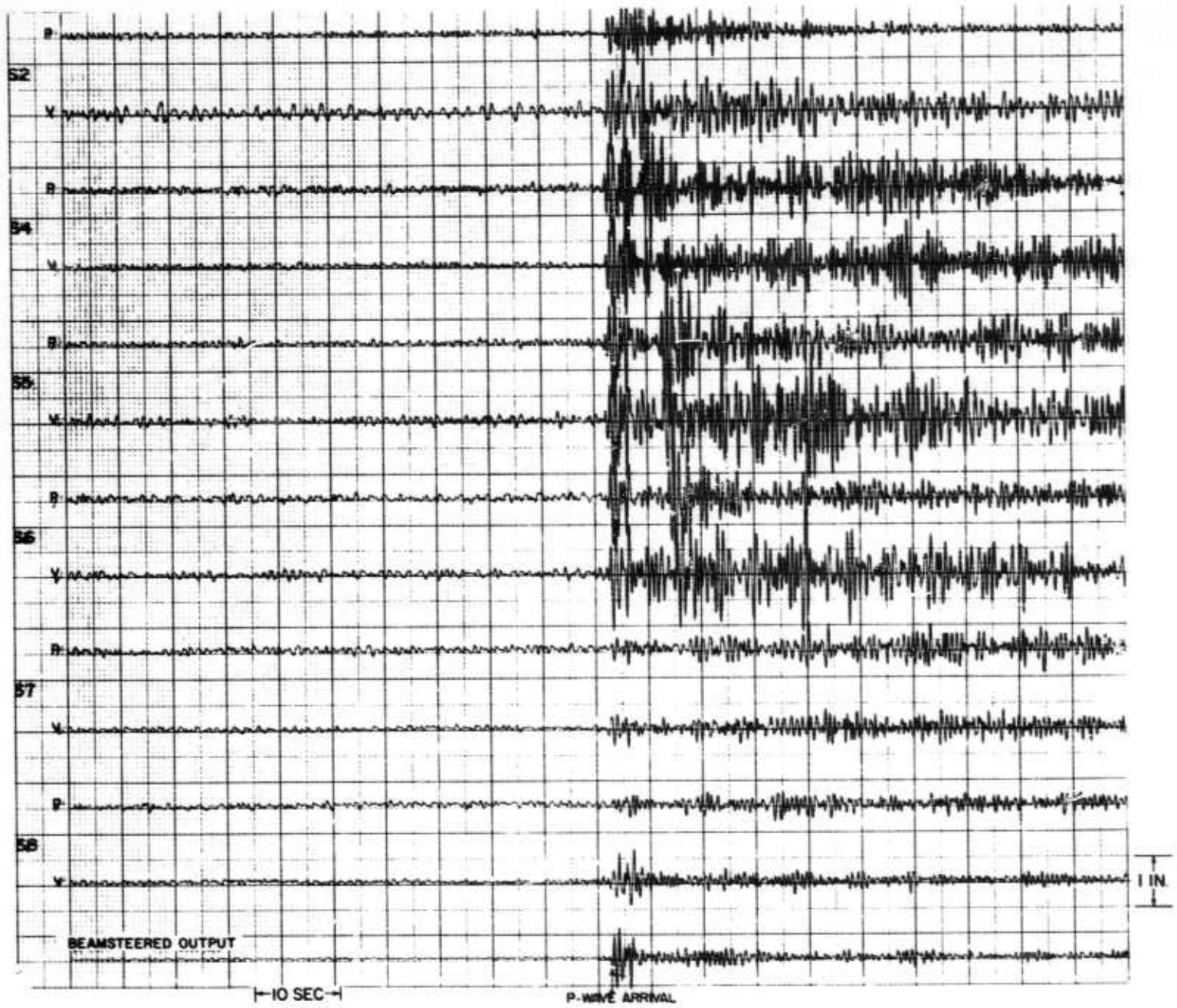

Figure III-17. Beamsteer Technique Applied to Earthquake 7, Optimum Visual Shift Employed (scale: 2000 TIAC units/in.)

The corresponding signal and noise spectra are plotted together in Figure III-18 to allow comparison of signal-to-noise ratios as a function of frequency. An inspection of the plots shows that the signal spectra for this earthquake peaked at about 1.8 Hz. At this frequency, the noise level on the vertical component is down between 10 and 15 db from the 1-Hz microseismic peak. If the earthquake had been a full magnitude unit lower (4.8) with the same spectrum, a signal-to-noise ratio of 10 db (3:1) at 1.8 Hz would still have existed.

Table III-6 shows that the average period of teleseismic arrivals was 0.6 sec (1.7 Hz). This relatively high frequency is probably the result of the lower frequency arrivals (around 1 Hz) being obscured by noise (considerably higher at 1 Hz) so that only the higher frequency events are observed. It should be pointed out that explosive sources generally have a spectrum which is relatively rich in high-frequency energy; therefore, the detection capability of the OBS would be significantly better for explosions than for earthquakes.

Table III-6

AVERAGE PERIOD OF TELESEISMIC ARRIVALS

Delta (°)	Number of Station Observations	Average Period (sec)
10-20	15	0.21
20-30	9	0.64
30-40	4	0.55
40-50	4	0.55
50-60	–	–
60-70	5	0.52
70-80	6	0.67
Total (20° to 80°)	28	0.60

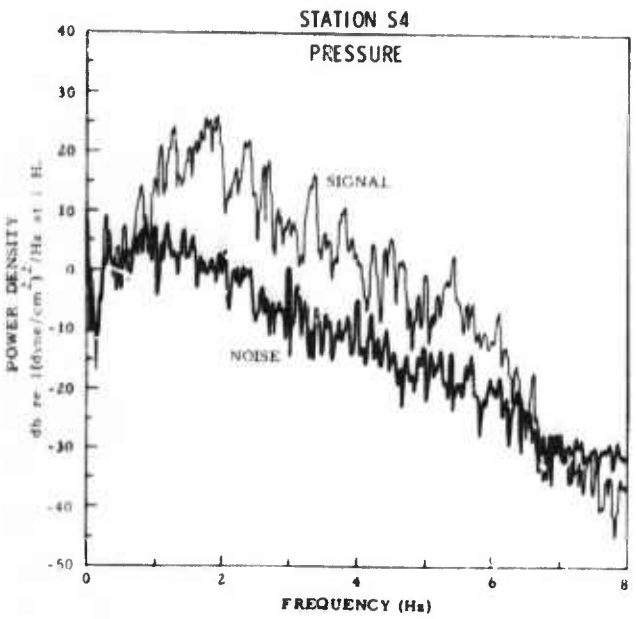

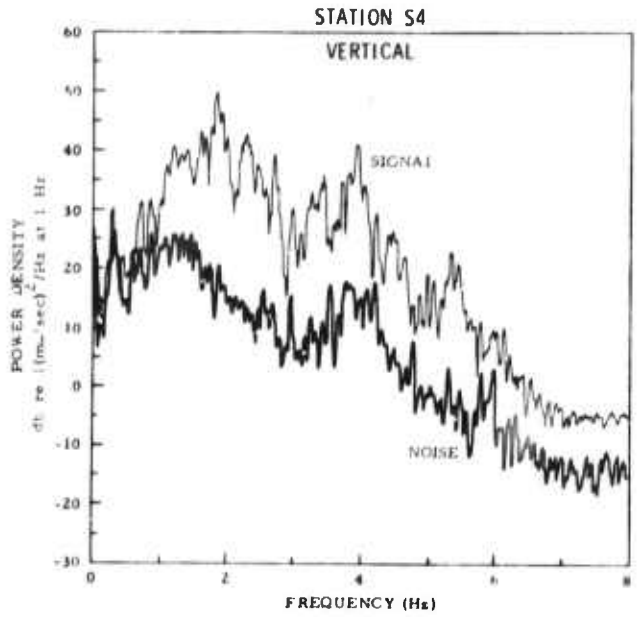

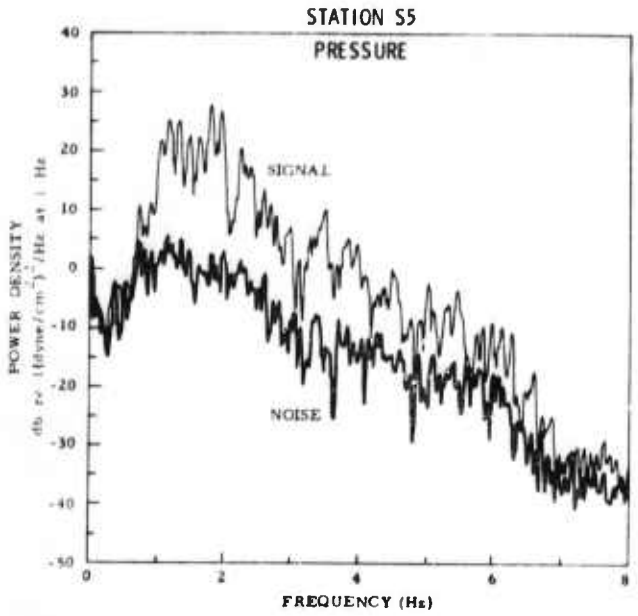

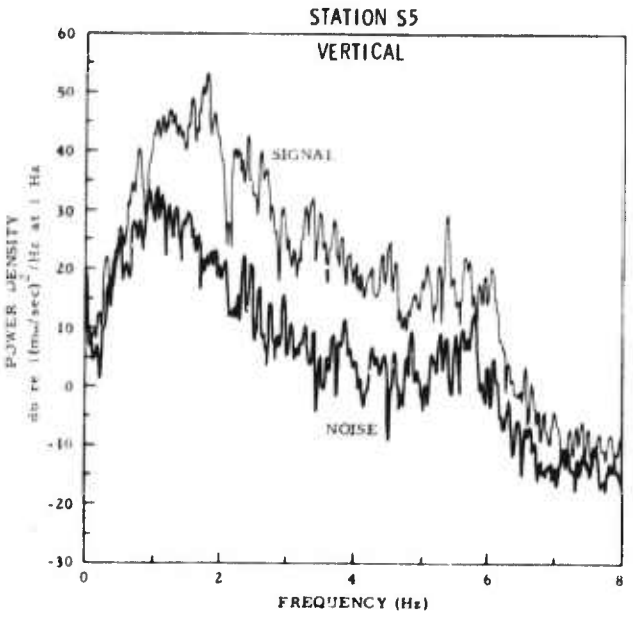

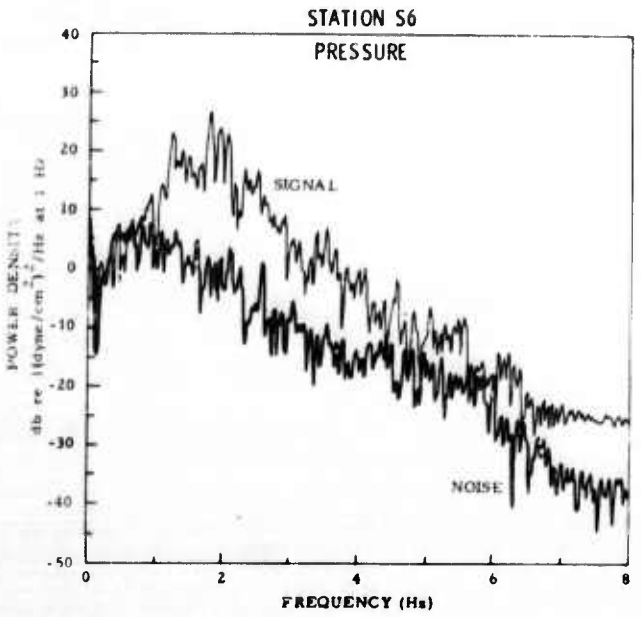

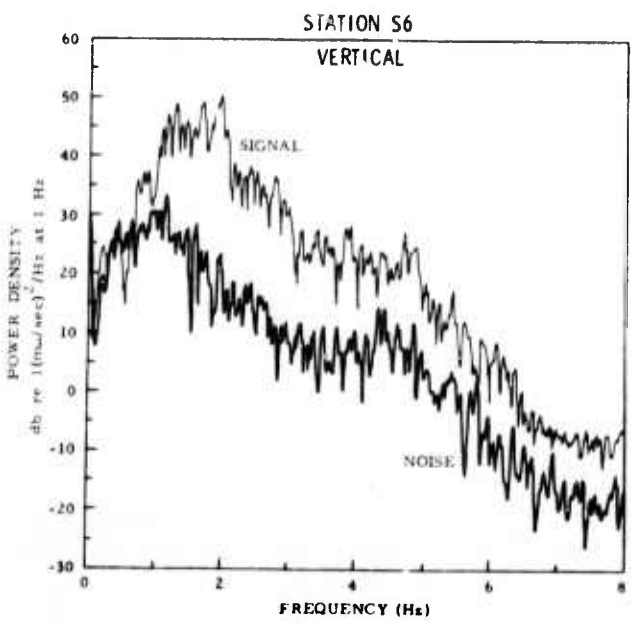

Figure III-18. Signal and Noise Spectra for Earthquake 7 Recorded at Stations S4, S5, and S6 (pressure x10, vertical x10)

Five zero-phase shift digital filter operators (2-sec in lenght) were designed. The response of each filter is described by the cutoff frequencies f_o, f_1, f_2, and f_3 given in Table III-7, where the desired frequency response H(f) is

$$H(f) = 0 \qquad \text{for } 0 \le f \le f_o$$

$$H(f) = \frac{1}{2} + \frac{1}{2} \cos \pi \frac{f - f_1}{f_o - f_1} \qquad \text{for } f_o \le f \le f_1$$

$$H(f) = 1 \qquad \text{for } f_1 \le f \le f_2$$

$$H(f) = \frac{1}{2} - \frac{1}{2} \cos \pi \frac{f - f_3}{f_2 - f_3} \qquad \text{for } f_2 \le f \le f_3$$

$$H(f) = 0 \qquad \text{for } f_3 \le f \le \frac{1}{2\Delta t}$$

Table III-7

FILTER CUTOFF FREQUENCIES

Filter	Frequency (Hz)			
	f_o	f_1	f_2	f_3
1	0.7	1.0	1.3	1.7
2	0.9	1.2	1.6	2.2
3	1.0	1.6	2.0	2.6
4	1.4	2.0	2.4	3.0
5	0.0	0.0	2.0	3.0

Filters 3 and 4 were applied by convolution to the digital recordings of earthquake 3. The input traces are shown in Figure III-19 (where the signals are vertically aligned); the filtered outputs of filters 3 and 4 are shown in Figures III-20 and III-21, respectively. Filter 4 gave noticeable signal-to-noise-ratio improvement on some of the noisier channels because the filter passband was centered near the signal frequency and the dominant noise frequency was outside the passband. The ringing appearance of the traces is due to the narrow passband specified in the filter response.

Filters 1 through 4 were applied to earthquake 5. The input traces are shown in Figure III-22, and the filtered outputs appear in Figures III-23 through III-26. For this earthquake filter 1 was centered near the signal frequency, which should give the best signal-to-noise improvement. However, the signal frequency was closer to the dominant noise frequency, so the improvement was less than that obtained for earthquake 3. This filter did reject a significant amount of the low- and high-frequency noise energy outside the passband. The low-amplitude levels seen in Figures III-25 and III-26 for filters 3 and 4 indicate low signal and noise energy in those frequency bands.

If the OBS were located in a highly seismic region, a large number of teleseismic events would be obscured by local and near-regional earthquake activity. For example, a total of 2230 unassociated station events were recorded during the 1967 Aleutian Islands Experiment. These local and near-regional events would be considered as undesirable noise in terms of the capability to record teleseisms. Generally, however (since their energy is predominately high frequency), events could be removed from the recordings by changing the instrument response.

Figure III-27 shows earthquake 2 masked by a near-regional event. The predicted arrival time for the teleseismic P-wave is indicated for each station, the traces are not aligned. The telesismic P-wave is obscured at most stations by the high-frequency near-regional event. Filter 5 was applied to the traces, and the output is shown in Figure III-28 where the teleseismic signal is aligned vertically. The high-cut filter adequately removed the near-regional event from the recordings, allowing the telesiesmic P-wave to be observed.

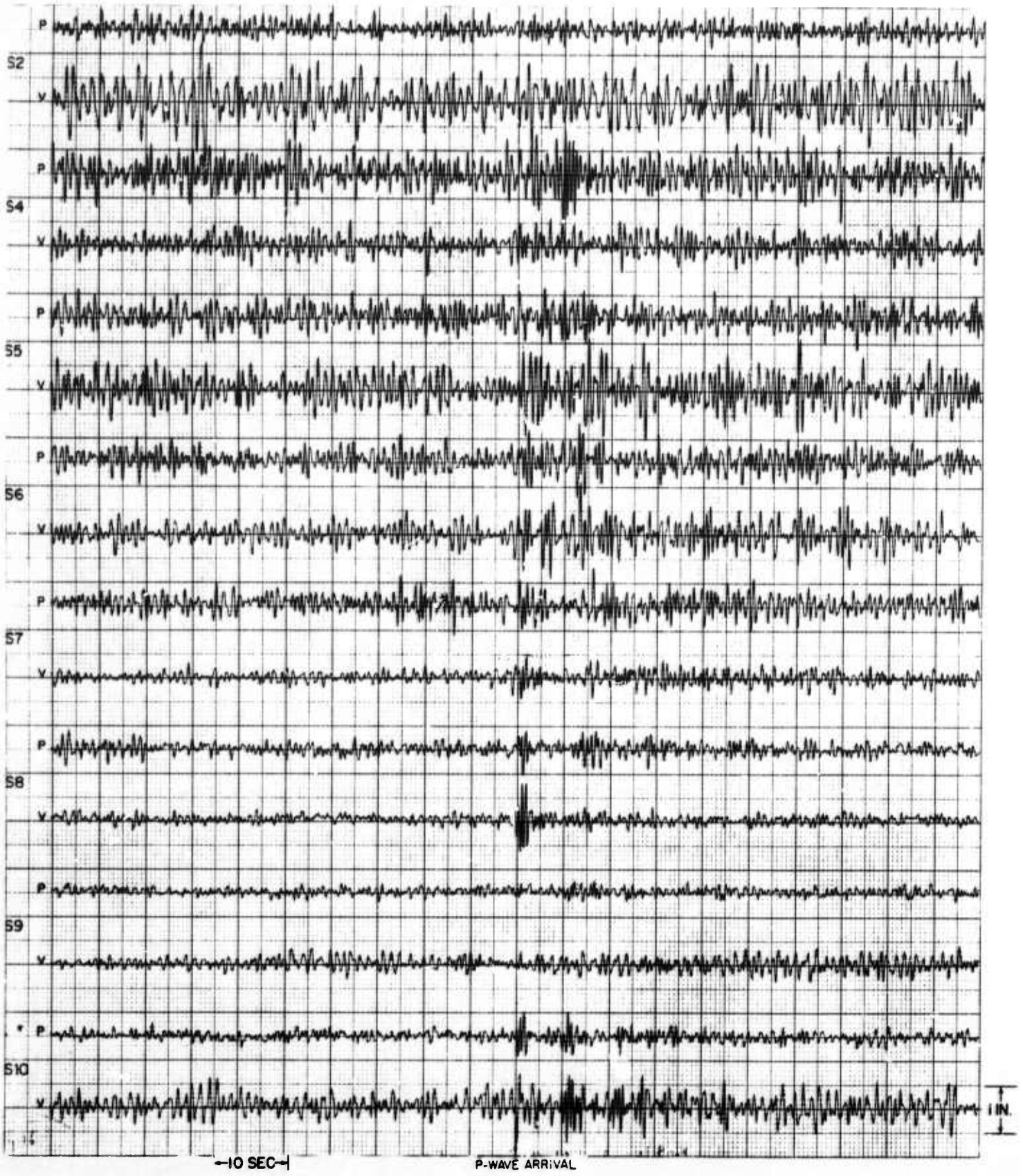

Figure III-19. Earthquake 3, No Filtering (scale: 1000 TIAC units/in.)

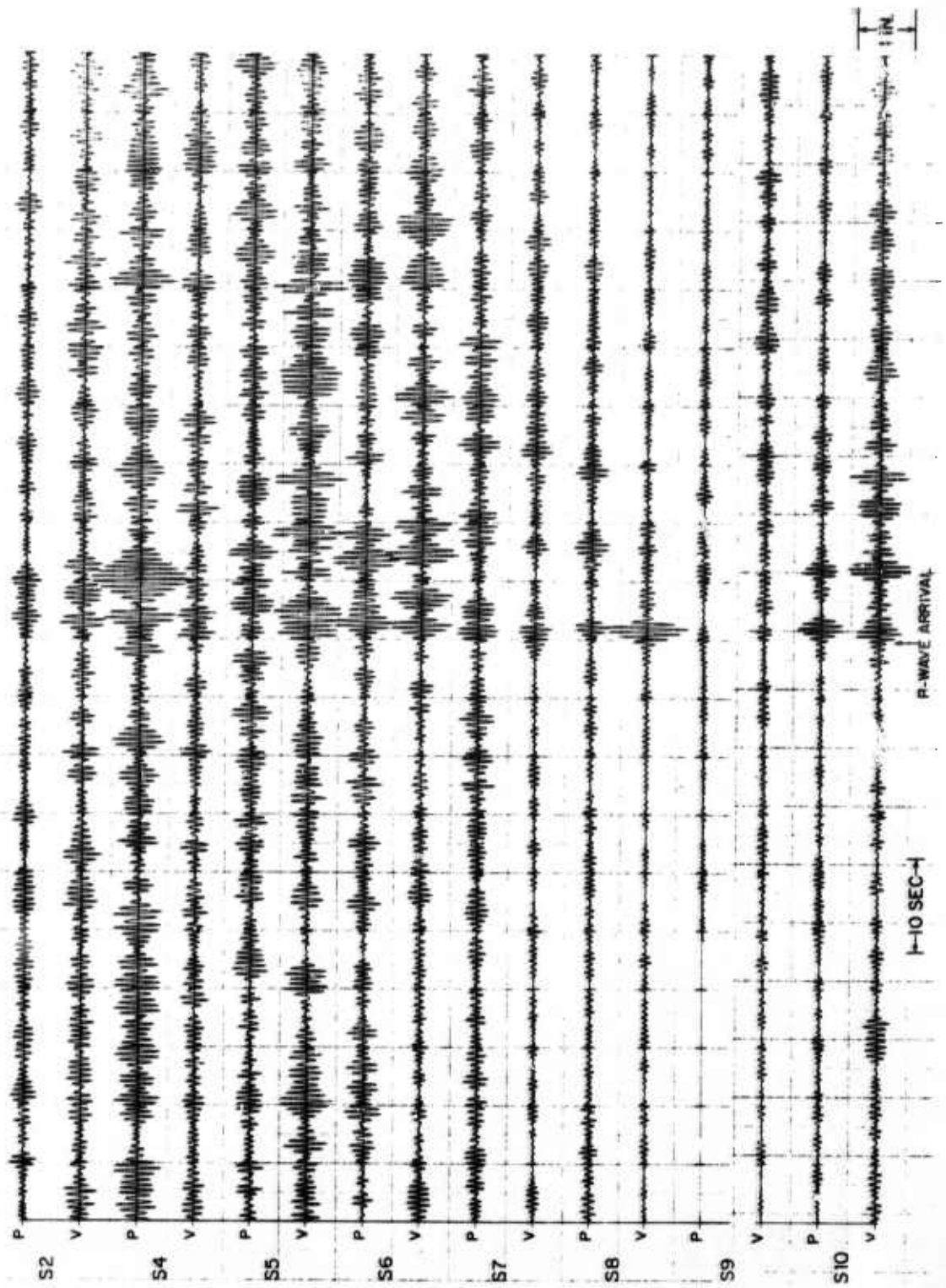

Figure III-20. Filtered Output of Earthquake 3, Filter 3 (scale: 1000 TIAC units/in.)

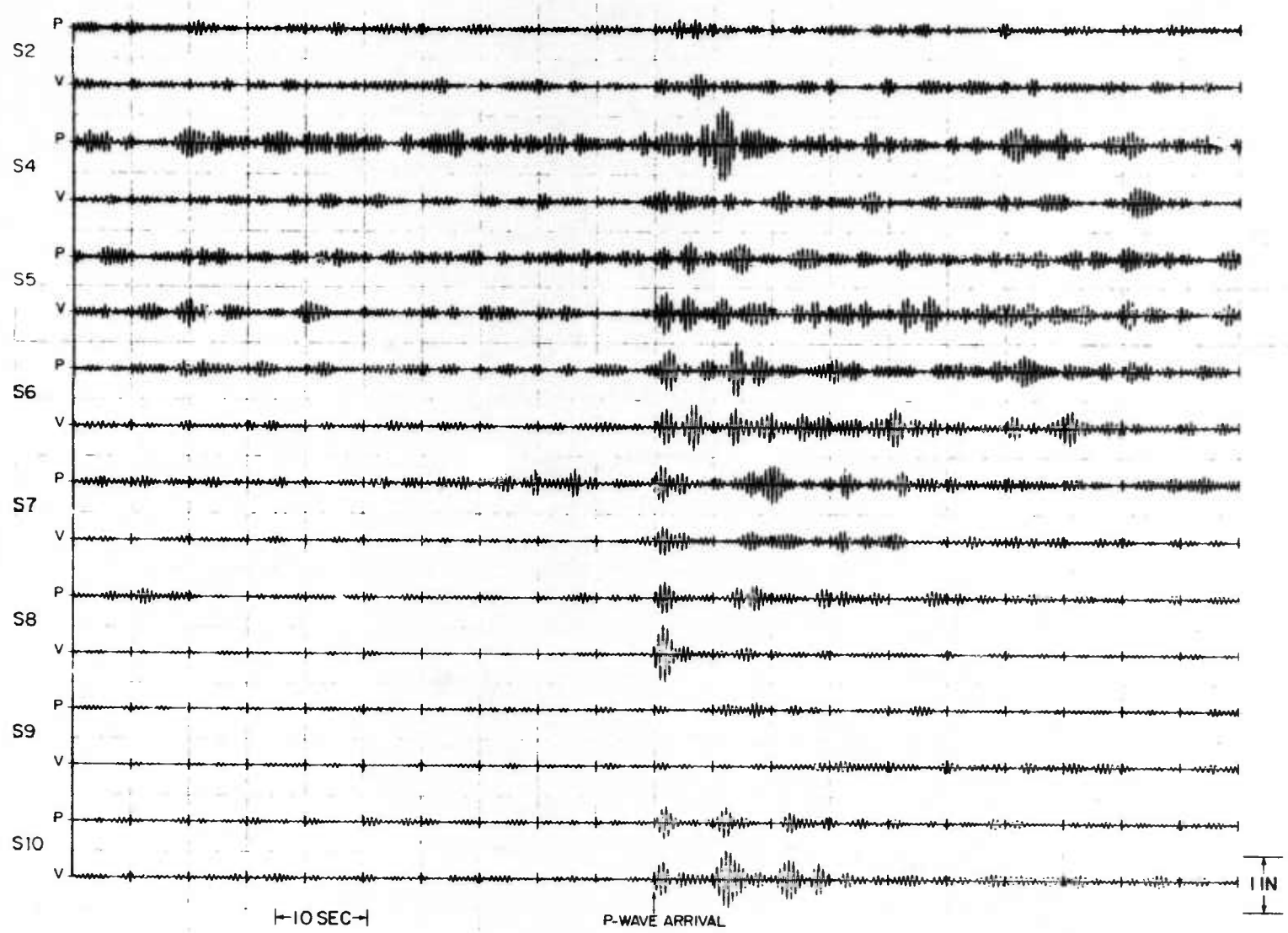

Figure III-21. Filtered Output of Earthquake 3, Filter 4 (scale: 1000 TIAC units/in.)

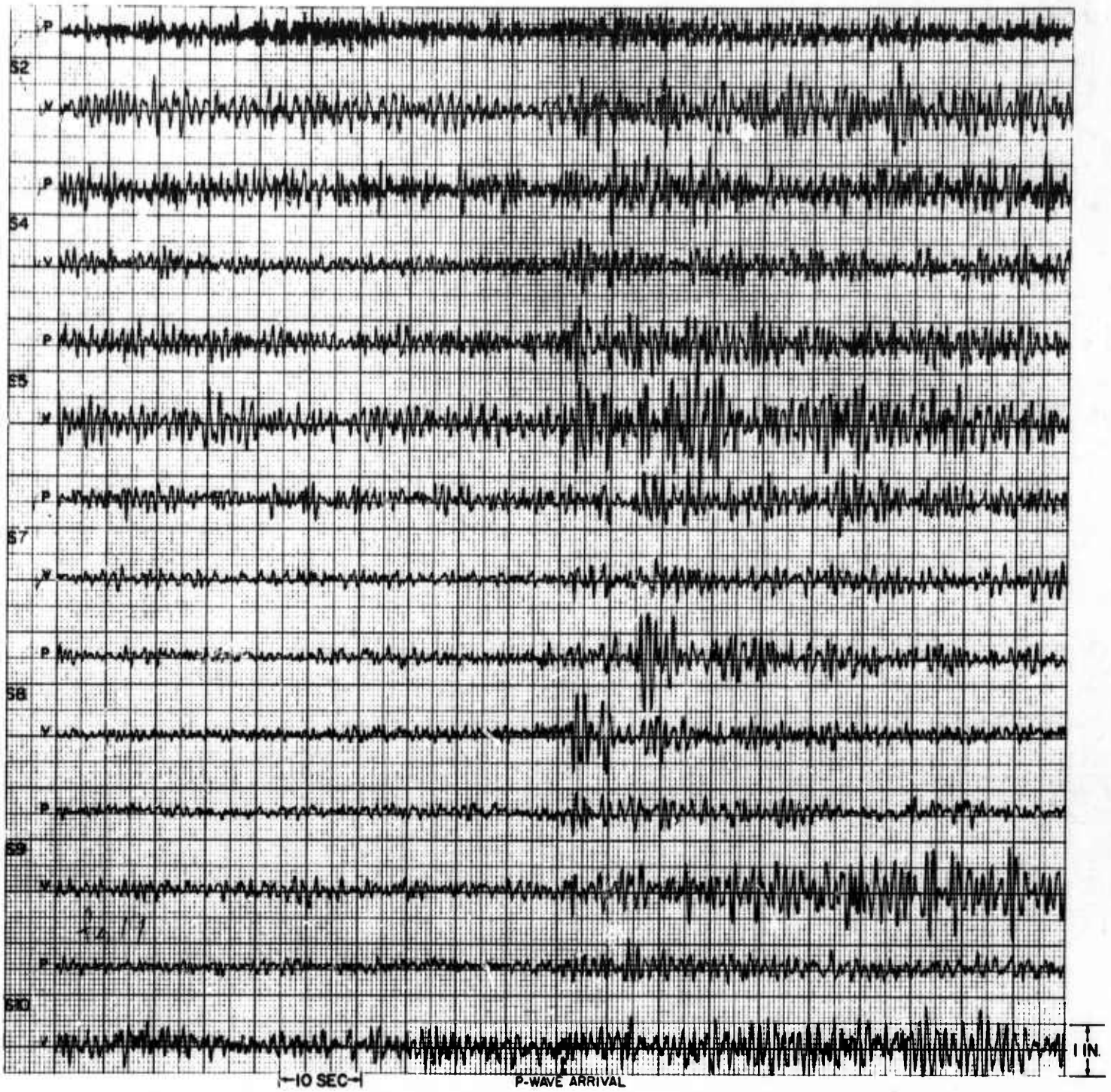

Figure III-22. Earthquake 5, No Filtering (scale: 1000 TIAC units/in.)

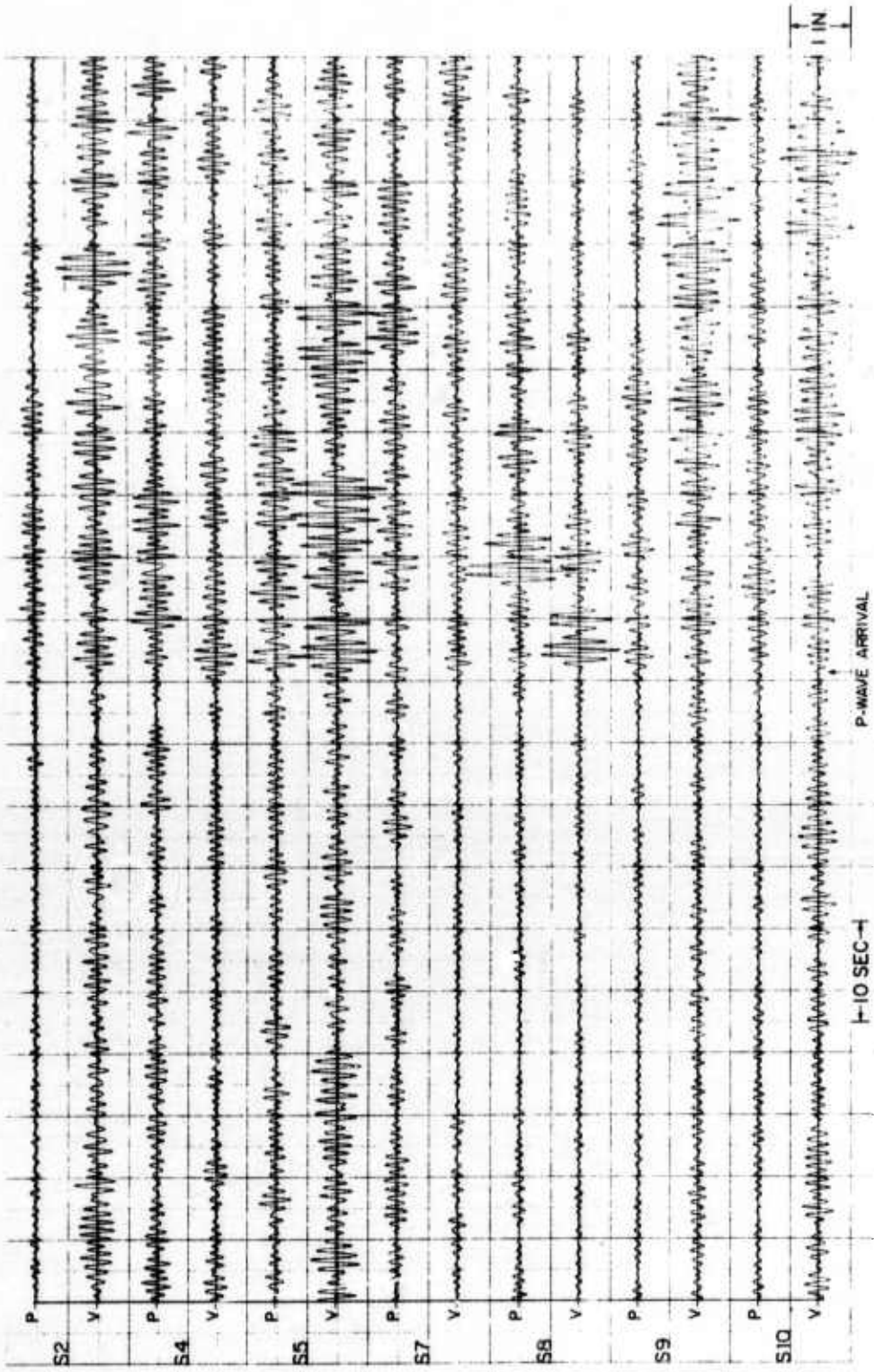

Figure III-23. Filtered Output of Earthquake 5, Filter 1 (scale: 1000 TIAC units/in.)

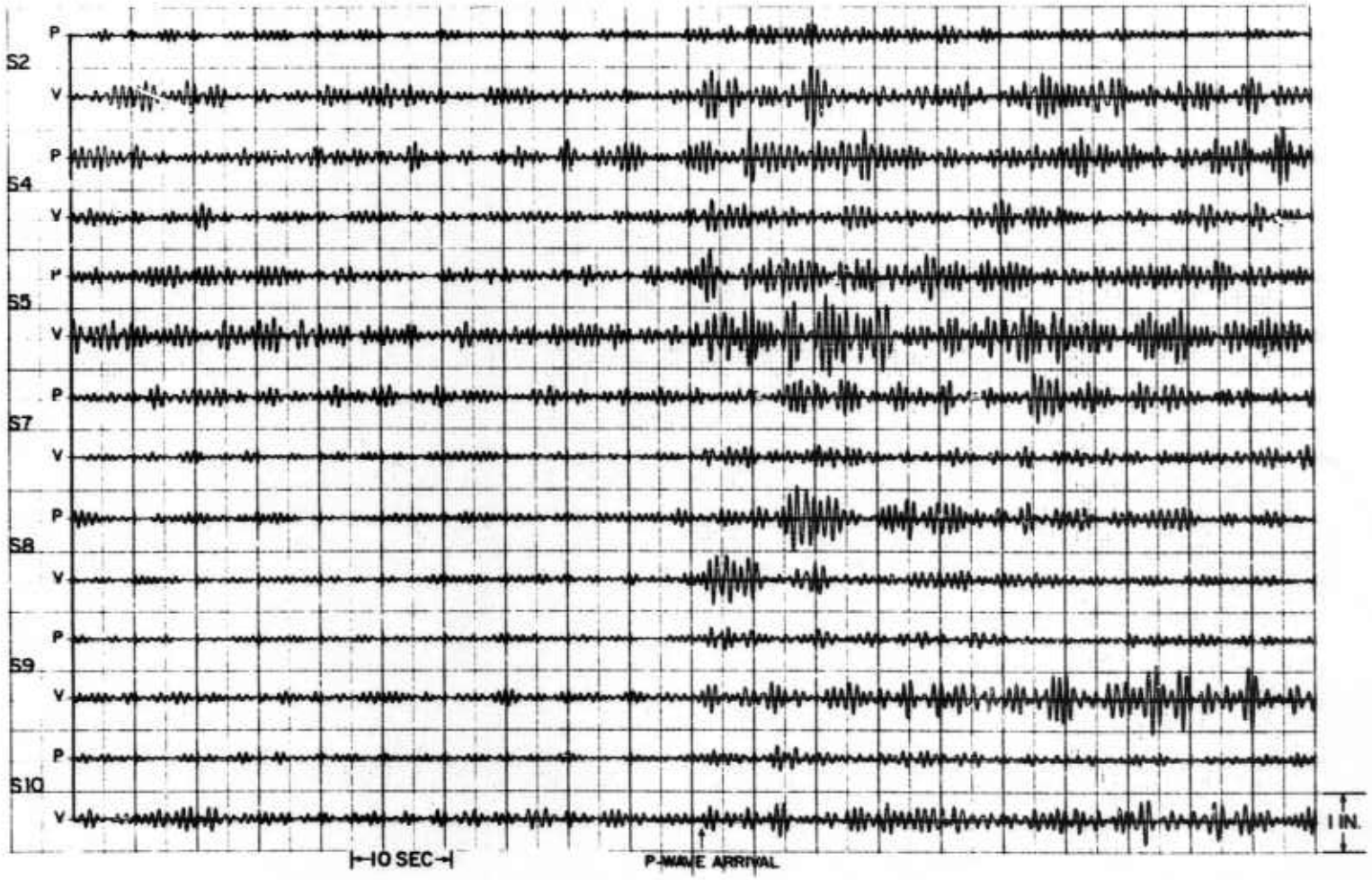

Figure III-24. Filtered Output of Earthquake 5, Filter 2 (scale: 1000 TIAC units/in.)

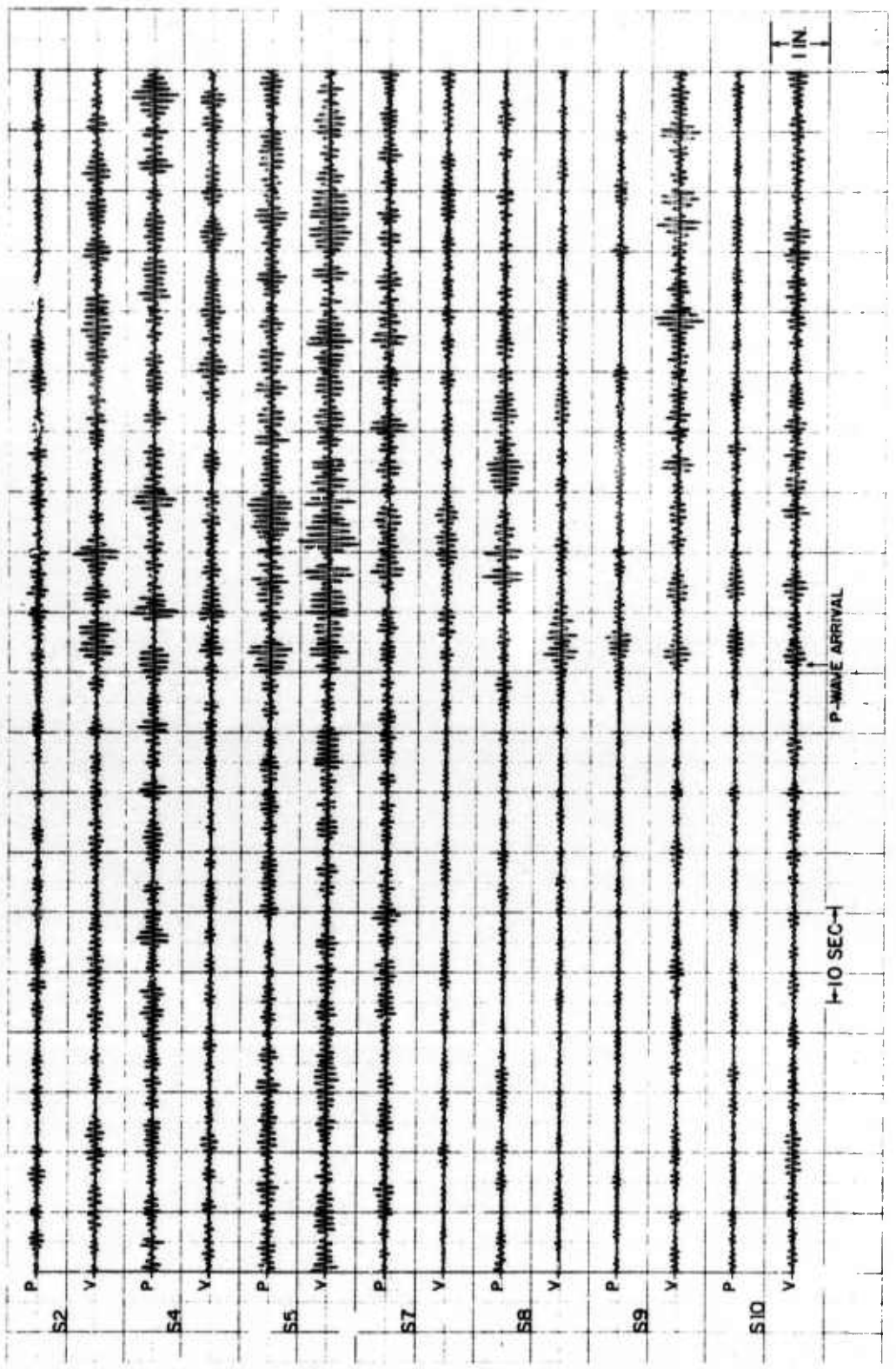

Figure III-25. Filtered Output of Earthquake 5, Filter 3 (scale: 1000 TIAC units/in.)

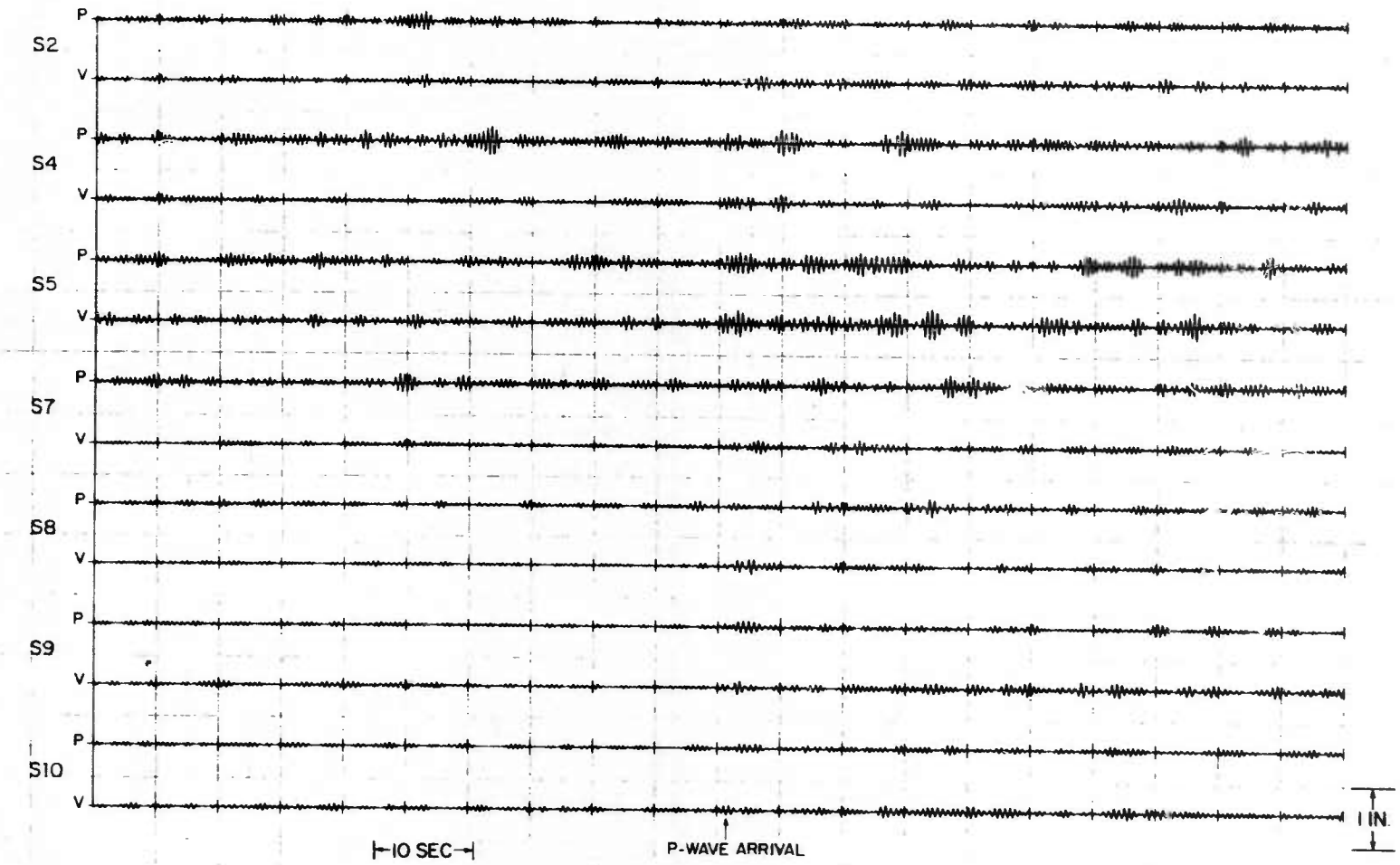

Figure III-26. Filtered Output of Earthquake 5, Filter 4 (scale: 1000 TIAC units/in.)

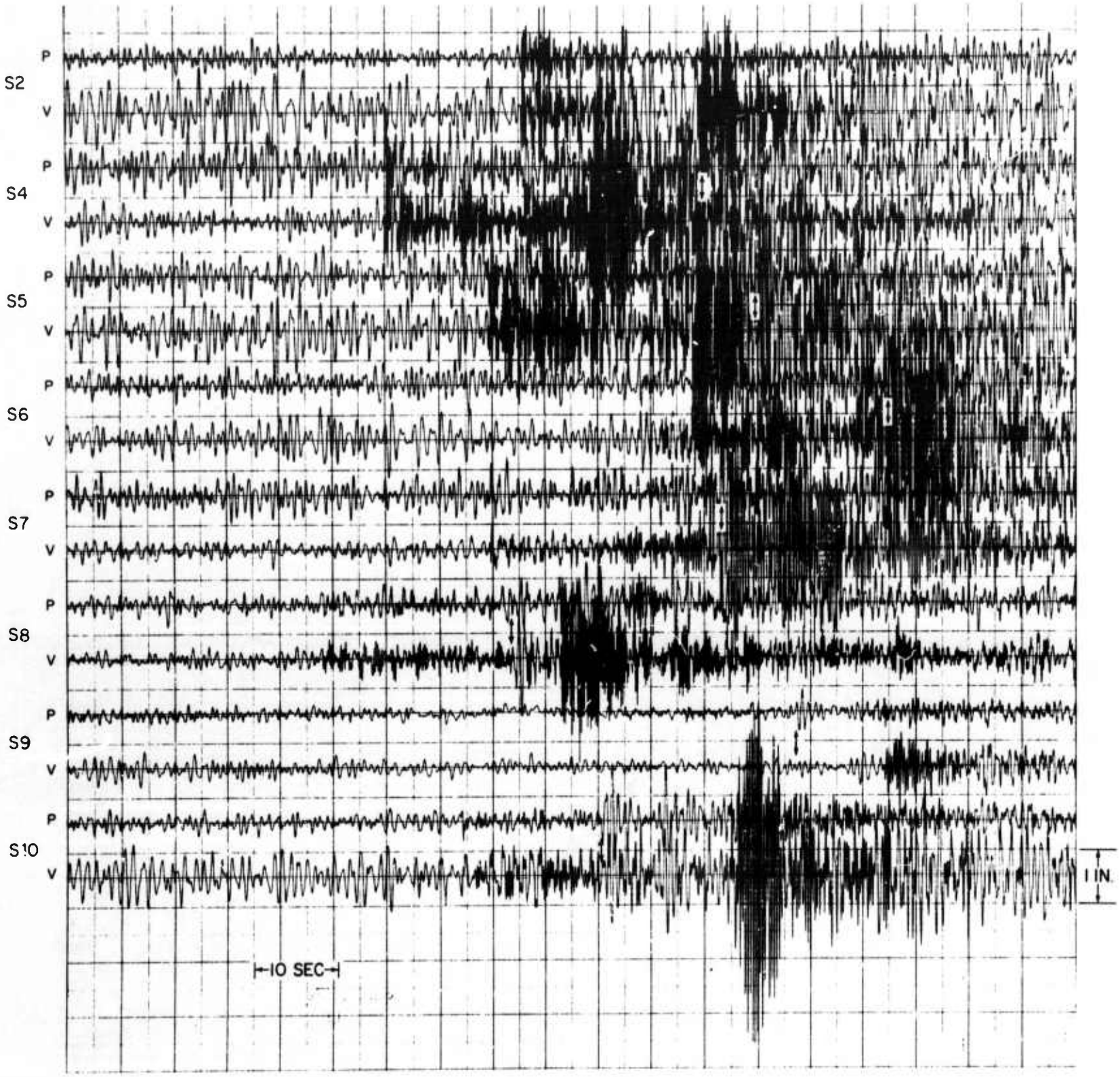

Figure III-27. Earthquake 2 and Near-Regional Event, No Filtering, Traces Not Aligned (scale: 1000 TIAC units/in.)

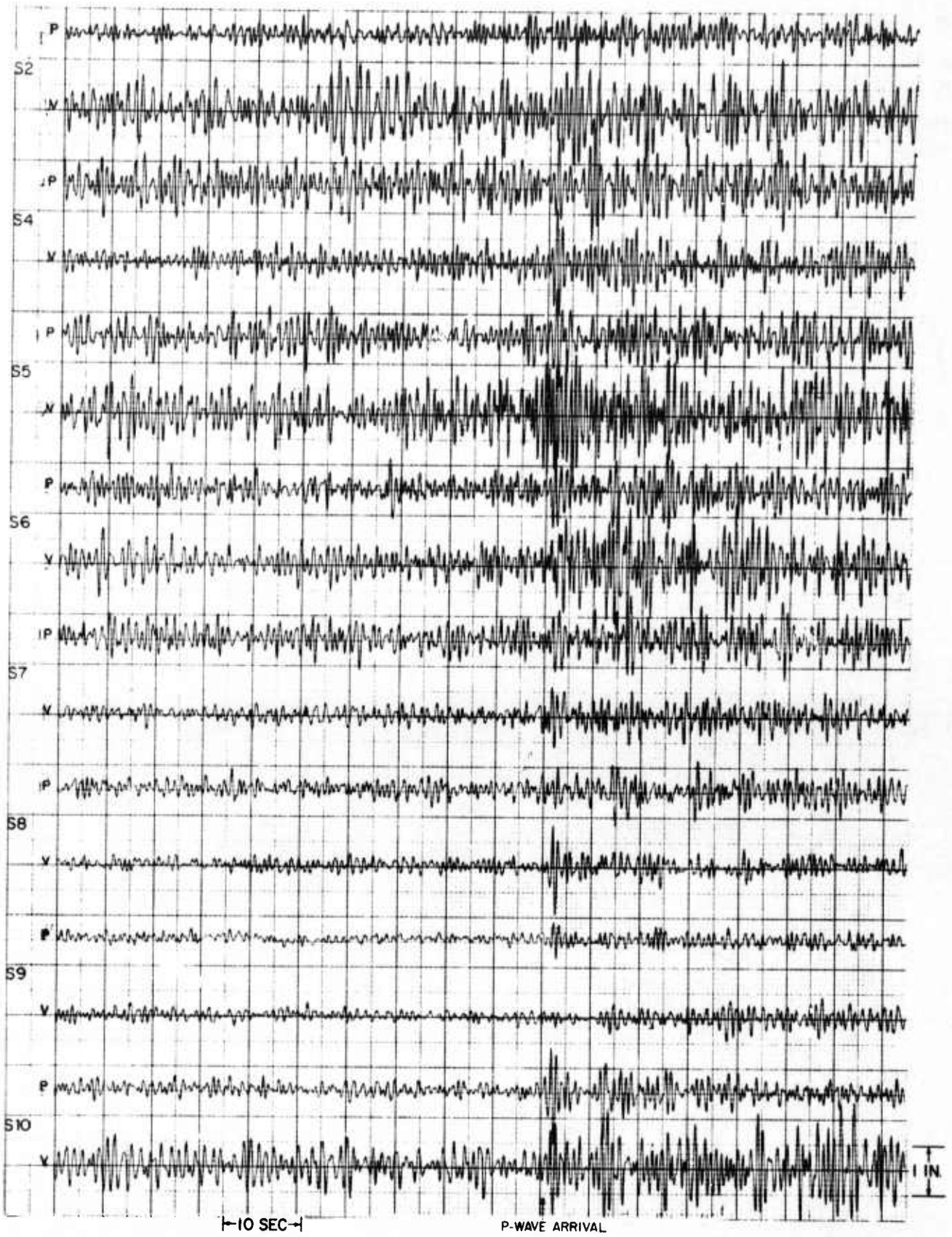

Figure III-23. Filtered Output of Earthquake 2, Filter 5, Traces Vertically Aligned (scale: 1000 TIAC units/in.)

SECTION IV

REFERENCES

1. Texas Instruments Incorporated, 1968: Aleutian Islands Experiment, Ocean-Bottom Seismographic Experiments, Prelim. Anal. Rpt., Contract F33657-67-C-1341, 31 Jan.

2. Texas Instruments Incorporated, 1968: Ocean-Bottom Seismograph Production and Gulf of Mexico Data Analysis, Final Rpt., Contract F33657-68-C-0242, 31 July.

3. Defant, Albert, 1961: Physical Oceanography, Volume II, Pergamon Press, New York.

4. Texas Instruments Incorporated, 1967: Kurile Islands Experiment, Ocean-Bottom Seismographic Experiments, Final Rpt., Contract F33657-67-C-0105, 30 Aug.

5. Schneider, William A., P.J. Farrell, and R.E. Brannian, 1964, Collection and analysis of Pacific ocean-bottom seismic data: Geophys., v. 29, p. 745-771.

6. Texas Instruments Incorporated, 1962: Ocean-Bottom Seismometer Data Analysis Program, Semiannual Tech. Rpt. 3, Contract AF 19(604)-8368, 15 Nov.

APPENDIX A

RELATIONSHIP BETWEEN OBS INSTRUMENT MAGNIFICATION AND TIAC UNITS

APPENDIX A

RELATIONSHIP BETWEEN OBS INSTRUMENT MAGNIFICATION AND TIAC UNITS

Recent ocean-bottom seismograph shaketable tests were used to relate film amplitudes to ground motion.* The shaketable data were used to derive a similar relationship for the digitized data (TIAC** units/mμ).

Unit 21 shaketable data from 0.6 to 12 Hz were selected and digitized using a 0.03125-sec sample rate. The data were demultiplexed and transcribed to the IBM System 360 for input to a program which determined

- Mean (which was removed)
- Peak amplitudes
- Average peak amplitude
- Average frequency

Amplitudes (Table A-1) were averaged over the 20 largest 0-to-peak values at a given frequency after removal of the mean. Using the known table amplitude, a conversion factor (TIAC units/mμ) was calculated and plotted (Figure A-1). The x1 and x10 channels are separated by the expected factor of about 10 from 1.5 to 8.5 Hz. However, outside this band, system noise masks the calibration signal on the x1 channel, so the x10 data were used to obtain the conversion.

Using the TIAC units/mμ ratio calculated at 1 Hz, the power spectra were converted to absolute units - db relative to $1(m\mu)^2/Hz$ at 1 Hz. The spectra shown throughout the report are in absolute units.

---

*Texas Instruments Incorporated, 1968: Ocean-Bottom Seismograph System Response Study, Aleutian Islands Experiment, Contract F33657-67-C-1341, 31 Jan.

**Trademark of Texas Instruments Incorporated

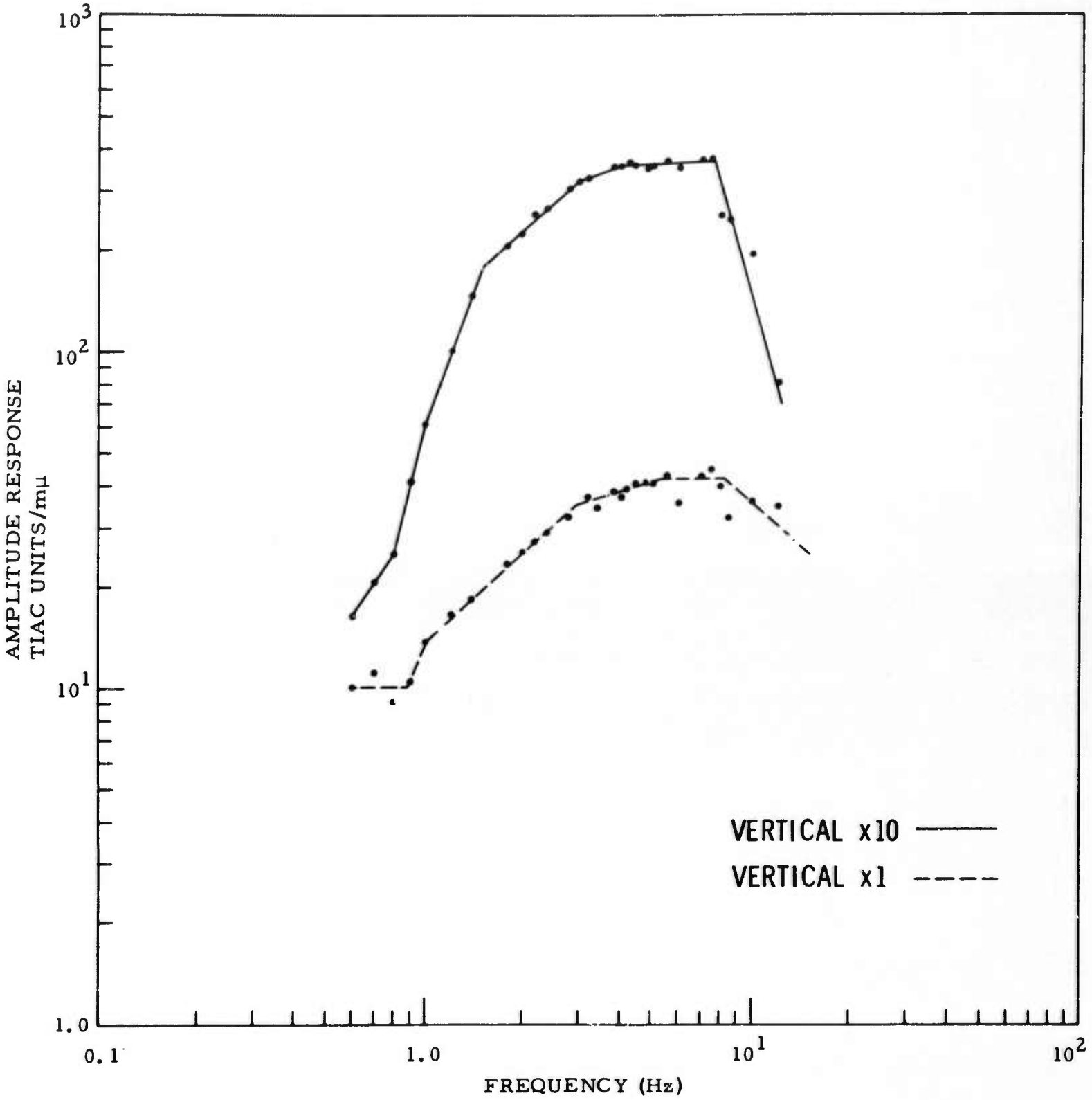

Figure A-1. Amplitude-Response Curve

Table A-1

UNIT 21 SHAKETABLE TESTS
(Vertical Component at -60 db)

Frequency (Hz)	Table Magnitude (μ)		Amplitude (0-p) of TIAC Units		Amplitude Normalized to 1 mμ and 0 db (units/mμ)	
	p-p	0-p	x1	x10	x1	x10
0.6	9.6	4.8	48.038	78.270	10.008	16.306
0.7	9.6	4.8	52.973	98.466	11.036	20.514
0.8	9.6	4.8	44.039	119.486	9.175	24.893
0.9	9.2	4.6	48.045	190.705	10.445	41.458
1.0	9.0	4.5	61.704	274.469	13.712	60.993
1.2	9.0	4.5	74.074	455.524	16.461	101.228
1.4	8.6	4.3	78.808	633.805	18.327	147.397
1.8	8.4	4.2	97.484	857.575	23.210	204.185
2.0	8.4	4.2	106.200	948.340	25.286	225.795
2.2	8.2	4.1	111.270	1037.794	27.139	253.120
2.4	8.0	4.0	116.511	1065.146	29.128	266.287
2.8	7.8	3.9	125.387	1179.009	32.151	302.310
3.0	7.6	3.8	135.379	1214.195	35.626	319.525
3.2	7.5	3.75	138.627	1233.574	36.967	328.953
3.4	7.2	3.6	122.720	1219.900	34.089	338.861
3.8	7.0	3.5	133.847	1235.298	38.242	352.942
4.0	7.0	3.5	130.324	1244.846	37.235	355.670
4.2	6.8	3.4	132.954	1235.414	39.104	363.357
4.4	6.7	3.35	135.418	1202.243	40.42	358.879
4.8	6.6	3.3	135.204	1152.118	40.971	349.127
5.0	6.4	3.2	130.300	1147.197	40.719	358.499
5.5	6.1	3.05	130.836	1127.754	42.897	369.755
6.0	5.8	2.9	103.250	1015.495	35.603	350.171
7.0	5.2	2.6	110.028	974.777	42.318	374.914
7.5	5.0	2.5	110.800	941.915	44.320	376.766
8.0	4.8	2.4	95.875	610.299	39.948	254.291
8.5	4.5	2.25	72.269	558.598	32.119	248.266
10.0	3.8	1.9	68.207	368.958	35.898	194.188
12.0	3.2	1.6	55.900	129.718	34.937	81.074

APPENDIX B

REPORTS PREPARED UNDER OCEAN-BOTTOM SEISMOGRAPHIC CONTRACTS

APPENDIX B

REPORTS PREPARED UNDER OCEAN-BOTTOM SEISMOGRAPHIC CONTRACTS

The following reports were written under Contract F33657-67-C-1341:

- Operations Report, Aleutian Islands Experiment, Ocean-Bottom Seismographic Experiments, 31 January 1968
- Ocean-Bottom Seismograph, System-Response Study, 31 January 1968
- Preliminary Analysis Report, Aleutian Islands Experiment, Ocean-Bottom Seismographic Experiments, 31 January 1968
- Final Analysis Report, Aleutian Islands Experiment, Ocean-Bottom Seismographic Experiments, 31 July 1968
- Aleutian Mantle Study, Aleutian Islands Experiment, Ocean-Bottom Seismographic Experiments, 31 July 1968
- Noise Analysis Report, Aleutian Islands Experiment, Ocean-Bottom Seismographic Experiments, 31 October 1968

Reports written under Contract F33657-68-C-0242 are as follows:

- Final Report, Ocean-Bottom Seismograph Production and Gulf of Mexico Data Analysis, 31 July 1968
- Operation Manual for 30-Day Ocean-Bottom Seismograph, August 1968

Written under Contract F33657-68-C-0875 was this report:

- Final Report, 1968 Aleutian Islands Experiment, Ocean-Bottom Seismographic Experiments, 23 August 1968

UNCLASSIFIED

Security Classification

DOCUMENT CONTROL DATA - R&D

(Security classification of title, body of abstract and indexing annotation must be entered when the overall report is classified)

1 ORIGINATING ACTIVITY *(Corporate author)*
Texas Instruments Incorporated
Science Services Division
P. O. Box 5621, Dallas, Texas 75222

2a. REPORT SECURITY CLASSIFICATION
Unclassified

2b GROUP
—

3. REPORT TITLE
SIGNAL AND NOISE ANALYSIS REPORT, ALEUTIAN ISLANDS EXPERIMENT, OCEAN-BOTTOM SEISMOGRAPHIC EXPERIMENTS

4. DESCRIPTIVE NOTES *(Type of report and inclusive dates)*
Special Report 31 October 1968

5. AUTHOR(S) *(Last name, first name, initial)*
Linville, A. Frank
Howard, R. Fred
McNeely, Gary D.
Harley, Terence W.

6. REPORT DATE	7a. TOTAL NO. OF PAGES	7b. NO. OF REFS
31 October 1968	80	7

8a. CONTRACT OR GRANT NO.
Contract F33657-67-C-1341

b. PROJECT NO.
AFTAC Project No. VELA T/7704

c.

d.

9a. ORIGINATOR'S REPORT NUMBER(S)
—

9b. OTHER REPORT NO(S) *(Any other numbers that may be assigned this report)*
—

10. AVAILABILITY/LIMITATION NOTICES
This document is subject to special export controls and each transmittal to foreign governments or foreign nationals may be made only with prior approval of Chief, AFTAC.

11. SUPPLEMENTARY NOTES
ARPA Order No. 624
ARPA Program Code No. 7F10

12. SPONSORING MILITARY ACTIVITY
Advanced Research Projects Agency
Department of Defense
The Pentagon, Washington, D.C. 20301

13. ABSTRACT

Aleutian Islands signal and noise data were analyzed to determine the teleseismic recording capability of the Ocean-Bottom Seismograph (OBS). From this analysis it was concluded that both noise and signal levels vary with OBS location, and the lowest noise sites are in deep water far from land. The noise spectrum is sharply peaked at 1 Hz; as the frequency increases to 2 Hz, the levels are down 10 to 20 db. Thus, ocean-bottom seismographs can perceive higher-frequency events up to a full magnitude better than they can perceive 1-Hz events (important in detecting explosive events at teleseismic distances). OBS perceptibility is quite variable at 1 Hz because of the variability of signal level with location and noise level with location and time. It appears that events of magnitude 5.0 or greater can be detected by at least some of the OBS stations, provided that the events are 40° or less from the array. Events of magnitude 6.0 or greater usually can be detected at all epicentral distances. The noise field determines the type of processing which can be used.

DD FORM 1 JAN 64 1473

UNCLASSIFIED

Security Classification

14 KEY WORDS	LINK A		LINK B		LINK C	
	ROLE	WT	ROLE	WT	ROLE	WT
Ocean-Bottom Seismographs						
Aleutian Islands Experiment						
Signal and Noise Analysis						
Recording of Teleseismic Events						

INSTRUCTIONS

1. ORIGINATING ACTIVITY: Enter the name and address of the contractor, subcontractor, grantee, Department of Defense activity or other organization *(corporate author)* issuing the report.

2a. REPORT SECURITY CLASSIFICATION: Enter the overall security classification of the report. Indicate whether "Restricted Data" is included. Marking is to be in accordance with appropriate security regulations.

2b. GROUP: Automatic downgrading is specified in DoD Directive 5200.10 and Armed Forces Industrial Manual. Enter the group number. Also, when applicable, show that optional markings have been used for Group 3 and Group 4 as authorized.

3. REPORT TITLE: Enter the complete report title in all capital letters. Titles in all cases should be unclassified. If a meaningful title cannot be selected without classification, show title classification in all capitals in parenthesis immediately following the title.

4. DESCRIPTIVE NOTES: If appropriate, enter the type of report, e.g., interim, progress, summary, annual, or final. Give the inclusive dates when a specific reporting period is covered.

5. AUTHOR(S): Enter the name(s) of author(s) as shown on or in the report. Enter last name, first name, middle initial. If military, show rank and branch of service. The name of the principal author is an absolute minimum requirement.

6. REPORT DATE: Enter the date of the report as day, month, year, or month, year. If more than one date appears on the report, use date of publication.

7a. TOTAL NUMBER OF PAGES: The total page count should follow normal pagination procedures, i.e., enter the number of pages containing information.

7b. NUMBER OF REFERENCES: Enter the total number of references cited in the report.

8a. CONTRACT OR GRANT NUMBER: If appropriate, enter the applicable number of the contract or grant under which the report was written.

8b, 8c, & 8d. PROJECT NUMBER: Enter the appropriate military department identification, such as project number, subproject number, system numbers, task number, etc.

9a. ORIGINATOR'S REPORT NUMBER(S): Enter the official report number by which the document will be identified and controlled by the originating activity. This number must be unique to this report.

9b. OTHER REPORT NUMBER(S): If the report has been assigned any other report numbers *(either by the originator or by the sponsor)*, also enter this number(s).

10. AVAILABILITY/LIMITATION NOTICES: Enter any limitations on further dissemination of the report, other than those imposed by security classification, using standard statements such as:

(1) "Qualified requesters may obtain copies of this report from DDC."

(2) "Foreign announcement and dissemination of this report by DDC is not authorized."

(3) "U. S. Government agencies may obtain copies of this report directly from DDC. Other qualified DDC users shall request through

_____."

(4) "U. S military agencies may obtain copies of this report directly from DDC. Other qualified users shall request through

_____."

(5) "All distribution of this report is controlled. Qualified DDC users shall request through

_____."

If the report has been furnished to the Office of Technical Services, Department of Commerce, for sale to the public, indicate this fact and enter the price, if known.

11. SUPPLEMENTARY NOTES: Use for additional explanatory notes.

12. SPONSORING MILITARY ACTIVITY: Enter the name of the departmental project office or laboratory sponsoring *(paying for)* the research and development. Include address.

13. ABSTRACT: Enter an abstract giving a brief and factual summary of the document indicative of the report, even though it may also appear elsewhere in the body of the technical report. If additional space is required, a continuation sheet shall be attached.

It is highly desirable that the abstract of classified reports be unclassified. Each paragraph of the abstract shall end with an indication of the military security classification of the information in the paragraph, represented as *(TS)*, *(S)*, *(C)*, or *(U)*

There is no limitation on the length of the abstract. However, the suggested length is from 150 to 225 words.

14. KEY WORDS: Key words are technically meaningful terms or short phrases that characterize a report and may be used as index entries for cataloging the report. Key words must be selected so that no security classification is required. Identifiers, such as equipment model designation, trade name, military project code name, geographic location, may be used as key words but will be followed by an indication of technical context. The assignment of links, rules, and weights is optional.